MAGNETIC STATES IN AMORPHOUS $Pd_{41}Ni_{41}B_{18}$ ALLOYS CONTAINING CHROMIUM AND IRON

Thesis by

Victor K. C. Liang

In Partial Fulfillment of the Requirements

For the Degree of

Doctor of Philosophy

California Institute of Technology

Pasadena, California

1971

(Submitted August 18, 1970)

To my parents and to my Hua-Shen

ACKNOWLEDGEMENT

The author wishes to express his deepest appreciation to Professor Pol Duwez and Dr. Chang-Chyi Tsuei for their highly inspirational advice and never ending understanding and encouragement throughout this work. He is also deeply grateful to Professor David Goodstein for numerous stimulating and highly rewarding discussions. Many useful discussions with Drs. R. Hasegawa and L. N. Newkirk, and their assistance in connection with the magnetic measurements are thankfully acknowledged. This work was made possible through the help of A. Lo and H. Y. S. Tse in the resistivity measurements; the technical staff of the Keck Laboratory especially J. E. Brown and J. A. Wysocki in preparing the alloys; Mrs. Betty Wolar in typing the thesis drafts and Mrs. Marilyn Hawn in typing the thesis. The author is also grateful for being able to work in the amiable research environment of the Keck Engineering Laboratory.

Financial aid was gratefully received from the Atomic Energy Commission, the Francis J. Cole Trust and the California Institute of Technology.

ABSTRACT

Amorphous alloys $Pd_{41}Ni_{41}B_{18}$ containing up to 4 at.% of Cr or Fe were obtained by rapid quenching from the liquid state. The electrical resistivity of these alloys was measured as a function of concentration and temperature in order to gain some understanding of the effect of spin correlation on electronic conduction in amorphous solids. The resistivity vs. temperature curve (ρ vs. T) for the amorphous alloys containing Cr exhibit all the characteristics of a Kondo system. An excellent agreement is found between the present resistivity data and Hamann's theoretical prediction. It is shown that the resistivity of all the Cr alloys studied can be adequately represented by a universal function of reduced temperature (T/T_K) which is defined as the ratio of temperature to Kondo temperature. The experimental results are used to make a comparison between the Kondo theory and the Hamann theory. The latter is found to be superior to the former. It is also found that when the interaction between magnetic spins is no longer negligible, the experimental results show two important deviations from those obtained in dilute magnetic systems: (1) the unitarity limit ρ_o does not scale with the concentration and (2) the Kondo temperature increases linearly with concentration. The electrical resistivity of the basic alloy containing up to 4 at.% of Fe was also measured. The temperature dependence of the ρ vs. T curves agrees very well with the theory of Turner and Long. It is also found that the alloys are ferro-

magnetic only above a certain critical Fe concentration. A simple physical model based on the interaction between the s electron polarization spheres about the magnetic spins is proposed. This model successfully explains the observed deviations in the Cr alloys mentioned above. It also accounts for the existence of a critical concentration for ferromagnetism in the Fe alloys. Estimated values of the radii of the polarization spheres around the Cr and the Fe spins in the amorphous alloys and the corresponding exchange integrals are given. Based on this information it is concluded that the direct coupling between d spins is weaker in an amorphous alloy than in a corresponding crystalline alloy. Hence, amorphous alloys are ideally suited for studying the effects of s electron correlations.

TABLE OF CONTENTS

PART	TITLE	PAGE
I.	INTRODUCTION	1
II.	EXPERIMENTAL PROCEDURES	3
	A. Alloys and Specimen Preparation	3
	B. Electrical Resistivity Measurements	4
	C. Magnetic Measurements	5
III.	BRIEF REVIEW OF RELEVANT THEORIES	8
	A. Formation of Localized Moments	8
	B. Theories related to the Cr[B] System	10
	1. Kondo's Theory	10
	2. Nagaoka's Approach	20
	3. Hamann's Formulation	22
	C. Theories related to the Fe[B] System	23
	1. Yosida's Treatment	23
	2. Turner and Long's Theory	25
	3. Mannari's Theory of $d\rho/dT$	28
	D. Theory of Magnetic Susceptibility	29
IV.	EXPERIMENTAL RESULTS	31
	A. The [B] Alloy	31
	B. The Cr[B] System	31
	1. Electrical Resistivity as a Function of Temperature	31
	2. Electrical Resistivity as a Function of $\mathrm{Log}_{10}T$	31

3. Magnetic Susceptibility vs. T for $Cr_{3.0}[B]_{97.0}$ 42

C. The Fe[B] System 42

1. Electrical Resistivity as a Function of Temperature 42

2. Magnetic Susceptibility and Magnetization vs. T for $Fe_{2.5}[B]_{97.5}$ 48

3. Inductance Bridge Results 48

V. DISCUSSION OF RESULTS 57

A. The Cr[B] System 57

1. General Discussion 57

2. Fitting the Experimental Data to Hamann's Expression 59

3. Average Background and Normalization Procedure 66

4. Concentration Dependence of the Unitarity Limit ρ_o 67

5. Concentration Dependence of the Kondo Temperature T_K 70

6. Determination of the Spin Value of Cr in [B] 72

7. Supporting Evidence from Magnetic Susceptibility 72

8. The Meaning of T_K 75

9. A Comparison Between the Theories of Kondo and Hamann. 76

(i) The Slope of Logarithmic Temperature Dependence 77

(ii) Universal Curve Based on Kondo's Theory 80

(iii) Universal Curve Based on Hamann's Theory 83

10. Estimation of the Fermi Energy E_F 85

11. Estimation of the s-d Exchange Integral J_{sd} 86

12. Simple Physical Model and the Estimation of the Polarization Cloud Radius ξ 87

B. The Fe[B] System 93

1. General Discussion 93

2. The $T^{3/2}$ Dependence of ρ, Background and Normalization Procedure 94

3. Linear T Dependence Below T_c 99

4. Linear T Dependence at High Temperature; Matthiessen's Rule 101

5. $\Delta\rho$ vs. T 101

6. Temperature Derivative of the Resistivity $d\rho/dT$ 104

7. Concentration Dependence of the $\ell n|T-T_c|$ Slope in $d\rho/dT$ 114

8. Inductance Bridge Measurements and the Concentration Dependence of T_c(I.B.) and T_c(R) 118

9. Magnetometer Measurement 122

10. $\Delta\rho_{max}[T_c]$ vs. Concentration 124

11. $\Delta\rho_{step}$ vs Concentration 128

12. An Attempt in Arriving at a Universal Curve for $\Delta\rho/\Delta\rho_{max}[T_c]$ vs. T/T_c 131

13. Estimation of J_{dd}, $J_{eff\ s-d}$ and Giant Moment 136

14. Simple Physical Model and ξ Estimation 138

VI. SUMMARY AND CONCLUSIONS 148

References 154

I. INTRODUCTION

Magnetism in metals has been a leading unsolved problem in solid state physics for many years. Considerable effort has been devoted to this problem. A microscopic theory of magnetism in metal, that is based on first principle, still does not exist. With the anticipation that the studies will constitute a sound first step towards the eventual understanding of bulk magnetism (for example in iron metal), experimental and theoretical investigators in this field in recent years have concentrated their effort on the equally fundamental, but perhaps simpler, problem of very dilute amounts of magnetic impurity atoms in a metallic host.

Dilute magnetic alloys can be classified by their low temperature resistivity into at least two classes. The first class, of which Mn Cu is typical, exhibits a resistivity minimum, with resistivity rising logarithmically with decreasing temperature, called the Kondo effect. The second class, of which Fe Pd is typical, has a kink near a critical temperature T_c in the resistivity vs. temperature curve. Below the temperature T_c the resistivity decreases rapidly with temperature. The underlying mechanism in both types of phenomenon is the scattering of s electrons from the localized d electrons, the so called s-d interaction.

Considerable understanding of the very dilute magnetic impurity problem has now been gained. Recently, there are several excellent review articles reviewing the progress in this field up to the present.[1][2][3] As a second step in the study of metallic magnetism, an attempt is made to correlate the experimental results for the non-

dilute concentration problem with the theories developed for the very dilute problem. It is intended to find out to which extent the theories are still directly applicable and where and what modifications are needed. It is hoped that some of the discrepancies between theory and experiment will emerge to provide a suggestion for further research, both experimental and theoretical.

The present study is an experimental investigation of the electrical resistivity resulting from adding up to 4 at. % of Cr and Fe to an amorphous metallic conductor. This amorphous alloy, $Pd_{41}Ni_{41}B_{18}$, henceforth denoted by [B], is obtained by rapid quenching from the liquid state via the Piston-Anvil method[4]. An amorphous host is chosen because it is intended to study the nature of the interactions associated with magnetic impurities in a metal with a minimum extraneous influence of crystal structure effects, crystal fields effects etc. Moreover, the amorphous state is of current interest[5], but it is still not well understood. It is hoped that the present study will give some insight on this problem as well.

II. EXPERIMENTAL PROCEDURES

A. Alloys and Specimen Preparation

The amorphous alloys prepared for this study have the general composition $M_c[B]_{100-c}$ where M stands for Cr or Fe and [B] stands for $Pd_{41}Ni_{41}B_{18}$ as has been defined in the introduction. The impurity concentration c varies from 0 to 4 in both cases. The alloys were prepared by induction melting of the appropriate quantities (total of about 2 g) of the constituents (99.99% purity for the palladium, 99.9% for the nickel, and 99.5% for the boron) in a quartz crucible under an argon atmosphere. In addition, a very high purity [B] alloy, symbolized by VHP[B], was prepared with 99.999% pure Pd, 99.999% pure Ni and 99.9999% pure boron. Since the weight loss after melting was less than 0.2%, it was assumed that the actual composition of the alloy was the nominal one.

The amorphous state of the alloys was obtained by quenching from the liquid state. The "piston and anvil" technique of rapid quenching[4] was used. In this technique, a small globule of liquid alloy is contained in a fused silica tube for about 30 seconds before quenching. This time is short enough to prevent reaction between the liquid alloys and the fused silica tube. However, some reaction was observed for the alloys containing Cr which may have some effect on the chemical composition of the quenched foils. Since the rapid quenching technique does not always yield reproducible results[6], every foil used in the present study was carefully checked by x-ray diffraction. A diffraction pattern was recorded with a Norelco diffractometer at 2θ angles between 34° and 50° and in angular steps of 0.05° (in 2θ), each step

corresponding to a total of 12,800 counts. Within this angular range, the diffraction pattern of the quenched foil exhibits a very broad maximum typical of a liquid structure. The presence of microcrystals (if any) in the foil can be detected by weak Bragg reflections superimposed on the broad maximum. The quenched foils which show any deviations from the liquid structure diffraction pattern were not used in the present study.

A typical amorphous foil quenched from the liquid state is about 2.5 cm in diameter and 40μ thick. From this foil, a rectangular specimen of about 20x3mm was cut for resistivity measurements. Current and potential leads, made of 0.005" Pt-10% Rh wires, were spot welded to the specimen. For the magnetic susceptibility measurements, one or two foils were cut into small pieces (1.5 x 2.0 mm) and the amount used varied from 30 mg. to 100 mg.

B. Electrical Resistivity Measurements

The resistivity of the amorphous alloys was measured by the standard four-point method as a function of temperature (4^{o} - 500^{o}K) and magnetic impurity concentrations. The temperature was measured with an accuracy of $\pm 0.2^{o}$K by a combination of copper-constantan thermocouple and a Germanium resistance thermometer. The main source of error arises from the uncertainty in the determination of the thickness. This gives rise to an uncertainty of ± 20%. The actual experimental points are partially shown in Fig. 4. as dots to indicate the scattering typical in the resistivity measurements other than that caused by uncertainties in the dimension measurements. In the magnetic impurity problem the usual analysis assumes that the Matthies-

sen's rule is applicable and involves subtracting the resistivity of the host alloy from the resistivity of the sample at corresponding temperatures. Even assuming that the Matthiessen's rule holds, in view of the deviations arising from the thickness measurements, this procedure cannot be followed unless a normalization procedure is first carried out. Further details will be given in Sections (V. A. 3.)† and (V. B. 2.).

C. Magnetic Measurements

Magnetic moments of the $Cr_{3.0}[B]_{97.0}$ and $Fe_{2.5}[B]_{97.5}$ alloys were measured between 4°K and 300°K and in magnetic fields up to 8.4 kilogauss. The measurements were made in the null-coil pendulum magnetometer whose design and performance are described in detail in Ref. 7. The magnetic susceptibility was obtained from the magnetic isothermals (magnetization vs. magnetic field at constant temperature). Strictly speaking, one should consider χ for the impurity only. The ordinary analysis involves subtracting χ_{host} from the $\chi_{host + impurity}$. In the present case, however, the subtraction between two susceptibility curves was a highly unreliable process due to experimental uncertainties, and it was not carried out. Instead, the inverse of the total susceptibility was plotted against temperature. This should show the correct qualitative trend, which constitutes the main interest in the magnetic susceptibility measurements in this investigation. For a ferromagnetic system, the Curie point was de-

†The notation Section (V. A. 3.) refers to section 3 of part A in Chapter V. (See the table of contents). A similar interpretation for this notation will be adopted throughout this thesis.

termined using an a-c inductance Wheatstone bridge. A schematic diagram of the bridge is shown in Fig. 1. One arm of the bridge is a coil wound around the sample called the sample coil. At 4.2°K, the bridge was balanced so that the voltage V_{AB} across the two points A and B was zero. When the sample changed its magnetic state as a result of the increase in temperature, V_{AB} deviated sharply from null due to an abrupt change in the inductance of the sample coil.

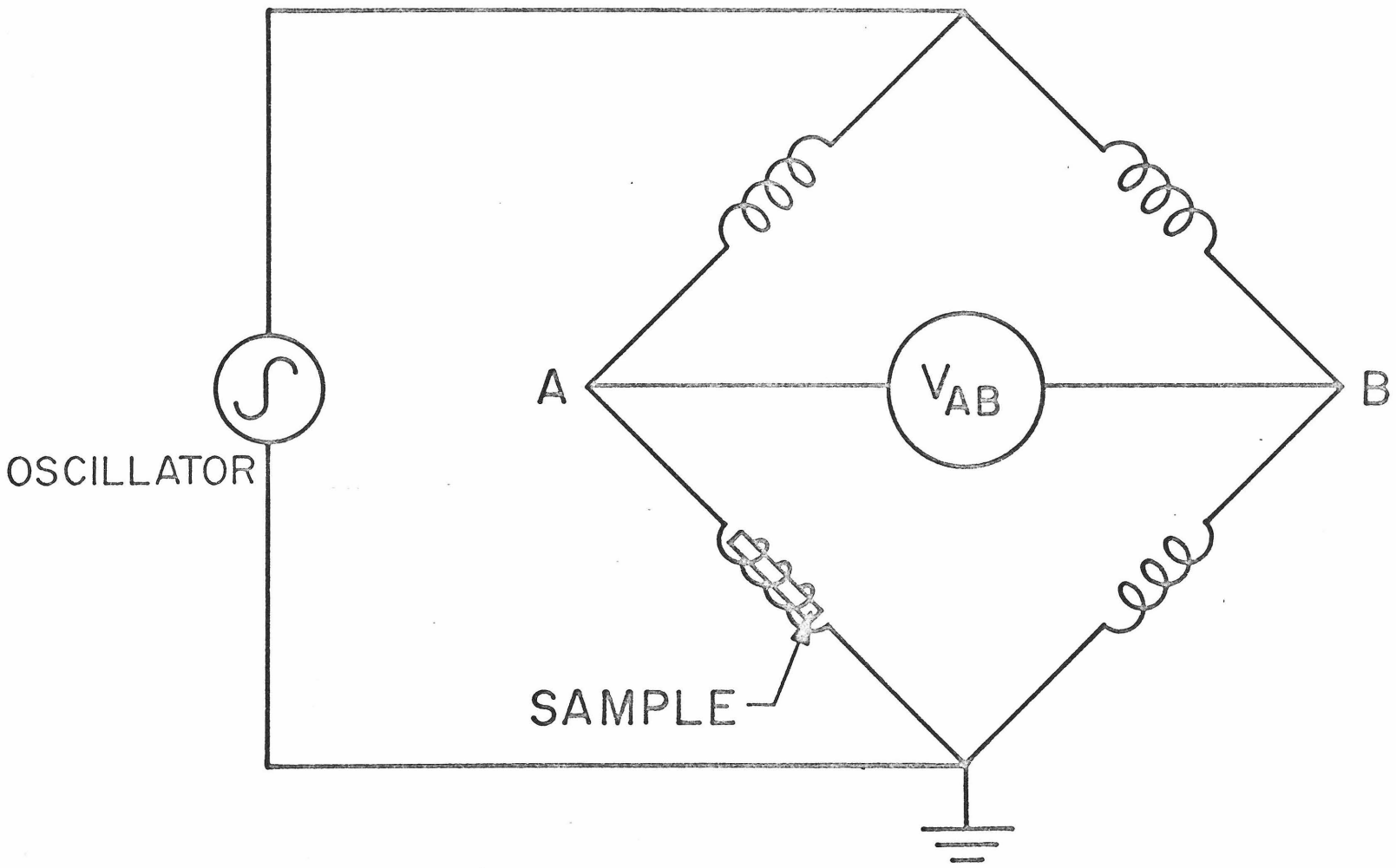

Fig. 1. Schematic diagram of an a-c Wheatstone bridge.

III. BRIEF REVIEW OF RELEVANT THEORIES

This chapter contains a brief interpretive review of some of the theoretical concepts relevant to this experimental investigation.

A. Formation of Localized Moments

When a magnetic impurity is introduced substitutionally into a metal, a magnetic moment may or may not exist. This is by itself a complicated problem. Friedel[8] pioneers in this field by introducing his virtual-bound-state concept. He notes that the metallic conduction band is so broad that the impurity energy levels would in general lie within it. There is strong intermixing between the impurity state and the continuum of conduction electron states with the result that the atomic d levels are broadened and shifted in energy from their unperturbed values. Such a state is not strictly localized because it has a finite energy width and hence would decay into the continuum. However, under appropriate conditions, one finds the screening charge is quite localized at the impurity site such that one can construct a localized charge density in the neighborhood of the impurity. Friedel points out that the mechanism responsible for Hund's rule would operate to separate the energy of the virtual bound states for spin-up electrons from that of the electrons of opposite spin. In this conceptual framework, a net moment exists if the number of virtual states lying below the Fermi level E_F for one spin exceeds that for the opposite spin.

Anderson[9] has expressed these ideas on a more quantitative basis using the Hartree-Fock approximation for a dilute magnetic system at $T = 0^{\circ}K$. He assumes that a localized moment exists, and

can be represented by a single d-orbital level with energy - E_d (energy is measured from the Fermi level E_F) so that it is occupied by an electron of say, spin-down. A spin-up electron trying to occupy the same level will see the full repulsive Coulomb interaction U between it and the d electron already on the impurity. This spin-up electron can only occupy a level of energy $-E_d + U$, which must be empty by the assumption that a moment exists, and hence must lie above the Fermi level. However, the conduction electrons, through the s-d mixing interaction, will again cause both levels to be broadened and shifted. The broadening of the spin-down level pushes the high energy tail of its energy distribution above the Fermi level so that it can become partially empty. For similar reasons, the spin-up level will become partially filled. This s-d mixing allows the spin-up and spin-down levels to be brought closer together in energy, and this effect is opposite to that of the Coulomb interaction U. Hence if the s-d interaction is too strong, the state collapses to two degenerate levels, and no moment exists. Later work actually suggests that for the present example a local moment can exist only in the case when the spin-down state is nearly always occupied, and the spin-up state nearly always empty[10].

One may also view the existence of moments from a dynamic point of view by considering the different characteristic times. The important question becomes whether the fluctuations in the spin density can be sufficiently slow so that, on the time scale of a given experimental probe, there appears to be a moment. Much work has been done recently along this line[11].

B. Theories Related to the Cr[B] System

1. Kondo's Theory

Kondo[12] has taken the first step towards a real understanding of the magnetic impurity problem. His main assumptions will first be reviewed briefly.

(1) Sarachik et al.[13] has recently shown a one to one correspondence between the appearance of a minimum in the resistivity vs. temperature curve and the existence of a magnetic moment (in the sense of the sample having strongly temperature dependent susceptibility). Kondo accepts this as being universally true and assumes the existence of a well defined localized moment $\vec{S}_n$. He by-passes the question of moment formation, and only treats those cases in which magnetic moments exist and are localized.

(2) Kondo assumes that the basic interaction is between the conduction s electrons and the localized magnetic moment $\vec{S}_n$ quite independent of other properties of the system like the crystalline structure.

(3) The strength of the interaction is characterized by the s-d exchange integral defined by:

$$J_{sd} = N \int d^3r\, d^3r'\, \bar{\Phi}^{*}_{d_n}(\vec{r})\, \bar{\Phi}_{\vec{k}'}(\vec{r}')\, \frac{e^2}{|\vec{r}-\vec{r}'|}\, \bar{\Phi}_{d_n}(\vec{r}')\, \bar{\Phi}_{\vec{k}}(\vec{r}) \qquad (1)$$

where Φ_{d_n} is the wave function of the localized impurity d electron,

$\phi_{\vec{K}}$, $\phi_{\vec{K}'}$, are the wave functions of the conduction s electron states. The quantity J_{sd} has its origin in the Coulomb interaction and the Pauli exclusion principle. In general, J_{sd} is a function of $\vec{K}$ and $\vec{K}'$. However, Kondo assumes that he can set J_{sd} to be a constant J independent of $\vec{K}$ and $\vec{K}'$. In this way, J may be considered as a phenomenological parameter whose value is to be determined from fitting experimental results.

(4) Kondo assumes that the amount of impurities under consideration is dilute in the sense of being non-interacting with each other. In that case, the scattering probability per unit time $W(\vec{K} \to \vec{K}')$ is additive and hence proportional to the concentration c.

(5) Kondo further assumes that the perturbation theory approach is applicable to the problem at hand. Mathematically, the perturbing Hamiltonian that Kondo considers is:

$$H'_{sd} = -2 \frac{J}{N} \sum_{n\alpha} \vec{s}_\alpha \cdot \vec{S}_n \tag{2}$$

where $\vec{s}_s$ = spin of the conduction electron, and $\vec{S}_n$ = spin of the localized impurity. In the language of second quantization, it is:

$$H'_{sd} = -\frac{J}{N} \sum_{n \vec{K} \vec{K}'} e^{i(\vec{K}'-\vec{K})\cdot\vec{R}_n} \left\{ (a^\dagger_{\vec{K}'+} a_{\vec{K}+} - a^\dagger_{\vec{K}'-} a_{\vec{K}-}) S_{nz} + a^\dagger_{\vec{K}+} a_{\vec{K}-} S_{n-} + a^\dagger_{\vec{K}'-} a_{\vec{K}+} S_{n+} \right\} \tag{3}$$

This describes the scattering of a conduction electron in the state $\vec{K}$ by a magnetic impurity $\vec{S}_n$ into the final state $\vec{K}'$.

Kondo applies the perturbation theory to this Hamiltonian to calculate the temperature dependence of resistivity. It is recalled that ρ = resistivity in Ohm-cm, and

$$\frac{1}{\rho} = -\left(\frac{e^2}{12\pi^3}\right)\int \tau_{\vec{K}} v_{\vec{K}}^2 \frac{\partial f^o}{\partial E_{\vec{K}}} d^3K \tag{4}$$

where,

$$\frac{1}{\tau_{\vec{K}}} = \sum_{\vec{K}'} \left\{ W(\vec{K}\pm \rightarrow \vec{K}'\pm) + W(\vec{K}\pm \rightarrow \vec{K}'\mp) \right\} \tag{5}$$

$W(\vec{K}+ \rightarrow \vec{K}'-)$ = the probability per unit time for a transition from the state $\vec{K}+$ to the state $\vec{K}'-$ etc.; $\tau_{\vec{K}}$ = the life time of the state $\vec{K}$ in sec.; $E_{\vec{K}}$ = the energy of a s electron in the state $\vec{K}$; $v_{\vec{K}}$ = the speed of a s electron in the state $\vec{K}$; f^o = the Fermi distribution function at equilibrium; and e = the electronic charge. Hence, the resistivity calculation essentially reduces to the problem of correctly evaluating the probability of transition per unit time, W. The quantity W holds the key to the solution.

Obviously one should consider starting with initial states consisting of the s electrons of spin-up as well as with those of spin-down. The final states should also include all possibilities containing both spin orientations. However, for the purpose of demonstration, only the special case $W(\vec{K}+ \rightarrow \vec{K}'+)$ will be considered. The extension to the remaining cases is straightforward.

The first order process is a direct scatteri ng of $\vec{K}+$ into $\vec{K}'+$ as indicated in Fig. 2a.

$$W(\vec{\kappa}+ \rightarrow \vec{\kappa}'+) = \frac{2\pi}{\hbar}\,\delta(E_{\vec{\kappa}+} - E_{\vec{\kappa}'+})\left\{H'_{\vec{\kappa}\vec{\kappa}'}\,H'_{\vec{\kappa}'\vec{\kappa}}\right\}$$
$$= \frac{2\pi}{\hbar}\left(\frac{J}{N}\right)^2 M_n^2\,\delta(E_{\vec{\kappa}+} - E_{\vec{\kappa}'+}) \qquad (6)$$

where $M_n = S_{nZ}$.

The value of W in first order is temperature independent.

The second order process allows much more possibilities, and they are described in Fig. 2b. The first column indicates the Feynman diagrams. The second column indicates the initial conditions. The initial state starts out with an electron in the state $\vec{K}+$ in the conduction band and the Z-component of the localized impurity M_n. Hence the Z-component of the total angular momentum of the system is $M_n + \frac{1}{2}$. This must stay constant throughout the process. The fourth column indicates the final state with a conduction electon in the state $\vec{K}'$ and a Z-component of the impurity spin M_n. It is crucial to consider the conduction electrons and the impurity spin as one system. The intermediate state $\vec{Q}$ contains four different possibilities, and according to quantum mechanics all four would occur with appropriate probabilities. (a) In the case of process (I), $\vec{K}+$ may be scattered into $\vec{Q}+$ with no change in the Z-component of the impurity spin. This process would occur only if the state $\vec{Q}+$ is originally empty. Hence, this process is weighed by the factor $(1-f^{o}_{\vec{Q}})$ where f^{o} = the Fermi function. (b) In the case of process (II), there is the different possibility of having a spin-up electron in the state $\vec{Q}+$ jump

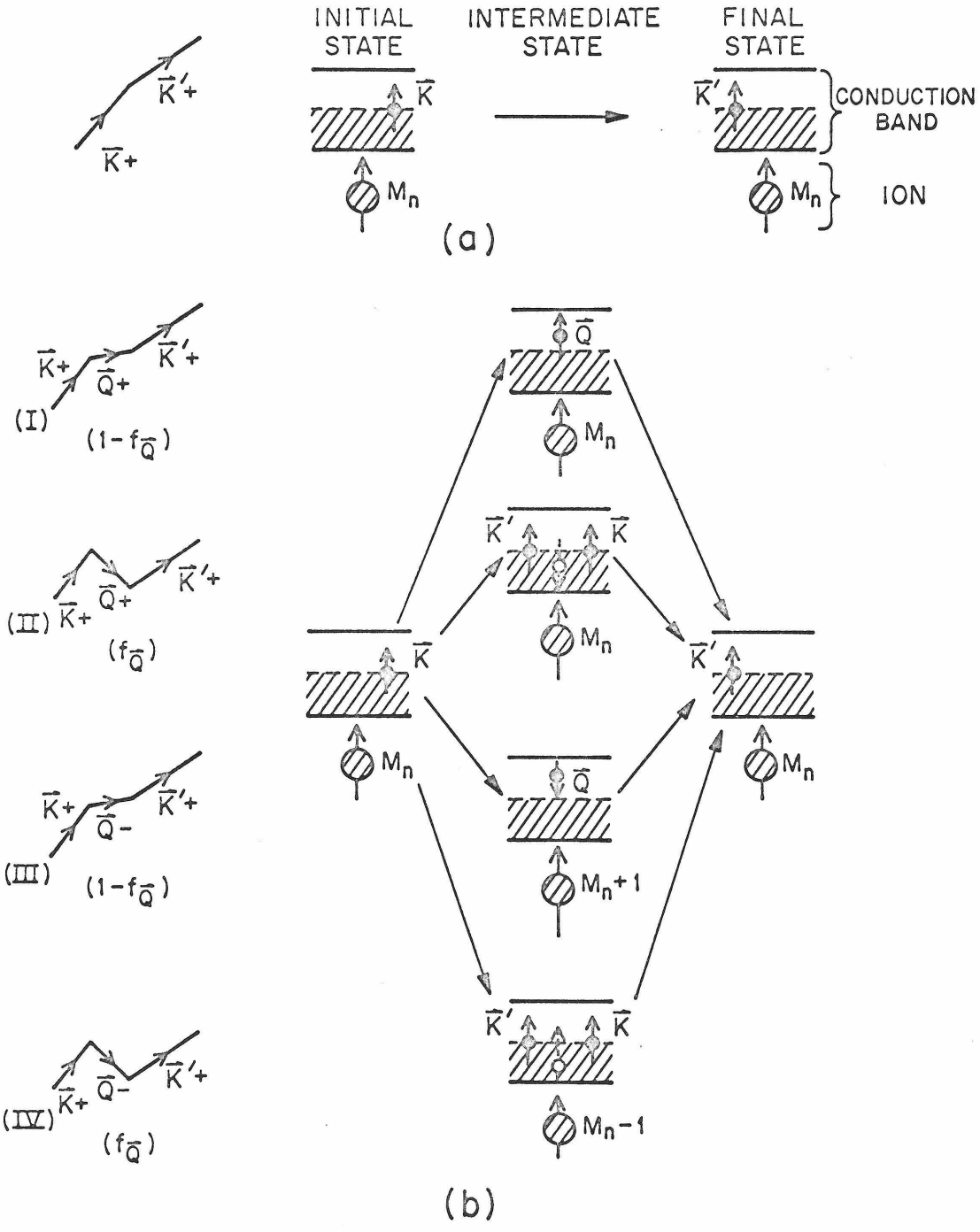

Fig. 2. Schematic diagrams showing the possible 1st. and 2nd. order processes in the s-d interaction.

out into the state $\vec{K}'+$ while the original electron $\vec{K}+$ still remains. A hole exists in the energy state $E_{\vec{Q}}$ with an equivalent spin down, and is indicated by the dashed line. Again the Z-component of the total spin of the conduction electron-impurity system remains the same if S_{nZ} is unchanged. The intermediate state in process (II) cannot occur unless $\vec{Q}+$ is an occupied state at the beginning. Hence, this process is weighed by the factor $f^{o}_{\vec{Q}}$. From process (I), one gets a contribution to $W(\vec{K}+\rightarrow\vec{K}'+)$ given by

$$2\left(-\frac{J}{N}\right)^{3}\sum_{n} M_{n}^{3}\sum_{\vec{Q}}\frac{1-f^{o}_{\vec{Q}}}{E_{\vec{K}}-E_{\vec{Q}}} \tag{7}$$

From process (II) one gets a contribution to $W(\vec{K}+\rightarrow\vec{K}'+)$ given by

$$2\left(-\frac{J}{N}\right)^{3}\sum_{n} M_{n}^{3}\sum_{\vec{Q}}\frac{+f^{o}_{\vec{Q}}}{E_{\vec{K}'}-E_{\vec{Q}}} \tag{8}$$

Conservation of energy requires $E_{\vec{K}} = E_{\vec{K}'}$. The sum of processes (I) and (II) contributes to W a term:

$$2\left(-\frac{J}{N}\right)^{3}\sum_{n} M_{n}^{3}\sum_{\vec{Q}}\frac{1}{E_{\vec{K}}-E_{\vec{Q}}} \tag{9}$$

This term vanishes if one assumes that $\sum_{n} M_{n}^{3} = 0$ in a paramagnetic system. (c) In the case of process (III) $\vec{K}+$ is scattered into $\vec{Q}-$. This is possible only if $\vec{Q}-$ is an originally empty state (hence a weight factor $(1-f^{o}_{\vec{Q}})$) and some other part of the system must increase the Z-component of its spin by one unit so as to conserve the Z-component of the total angular momentum. In this case, it is

achieved via the impurity Z-spin going from M_n to M_n+1. (d) In the case of process (IV), an electron in the state $\vec{Q}-$ jumps into the final state $\vec{K}'+$ while the initial electron remains in the state $\vec{K}+$. Again, one needs to have the state $\vec{Q}-$ originally occupied and hence a weight factor $f^{o}_{\vec{Q}}$. However, there is now the absence of a down-spin electron and that means a hole with an effective spin-up (s_Z of hole = +). Including $\vec{K}'+$, there is an excess of one unit in the Z-component of total s electron angular momentum in the intermediate state. In order to conserve the Z-component of angular momentum of the system, the impurity spin should decrease its Z-component from M_n to M_n-1. Process (III) contributes to $W(\vec{K}+\rightarrow\vec{K}'+)$ a term

$$2\left(-\frac{J}{N}\right)^3 \sum_n M_n(S-M_n)(S+M_n+1) \sum_{\vec{Q}} \frac{1-f^{o}_{\vec{Q}}}{E_{\vec{K}}-E_{\vec{Q}}} \tag{10}$$

Process (IV) gives a term

$$2\left(-\frac{J}{N}\right)^3 \sum_n M_n(S+M_n)(S-M_n+1) \sum_{\vec{Q}} \frac{-f^{o}_{\vec{Q}}}{E_{\vec{Q}}-E_{\vec{K}'}} \tag{11}$$

After using the conservation of energy ($E_{\vec{K}} = E_{\vec{K}'}$) and keeping only the term containing $f^{o}_{\vec{Q}}$, Kondo obtains the result:

$$W(\vec{K}+\rightarrow\vec{K}'+) \longrightarrow 4\left(\frac{J}{N}\right)^3 \sum_n M_n^2 \sum_{\vec{Q}} \frac{f^{o}_{\vec{Q}}}{E_{\vec{Q}}-E_{\vec{K}}} \tag{12}$$

For a paramagnetic system

$$\sum_n M_n^2 = \frac{C}{3} S(S+1)N \tag{13}$$

Kondo has indicated that combining the other possibilities of spin orientations in the initial and final states, one gets

$$W(\vec{K}\pm \rightarrow \vec{K}'\mp) = \frac{4\pi J^2 S(S+1)C}{3\hbar N}\left\{1 + \frac{4J}{N}\sum_{\vec{Q}} \frac{f^0_{\vec{Q}}}{E_{\vec{Q}} - E_{\vec{K}}}\right\}\delta(E_{\vec{K}} - E_{\vec{K}'}) \propto \frac{1}{\tau_{\vec{K}}} \tag{14}$$

Kondo has shown that at low temperatures

$$\sum_{\vec{Q}} \frac{f^0_{\vec{Q}}}{E_{\vec{Q}} - E_{\vec{K}}} = \frac{3ZN}{2E_F}\left\{1 + \frac{K}{2K_F} \ln \frac{K - K_F}{K + K_F}\right\} \tag{15}$$

and $\quad (K - K_F) \propto T$

and ends up with an expression for the resistivity due to s-d interaction:

$$\rho_{sd} = c\rho_M\left(1 + \frac{3ZJ}{E_F} \ln T\right) \tag{16}$$

where,

$$\rho_M = \frac{3\pi m J^2 S(S+1)}{2e^2\hbar E_F}\left(\frac{V}{N}\right) \tag{17}$$

Z = the number of conduction electrons per atom; N = the total number of atoms and V = the volume of the sample. It should be pointed out that a ℓn T term results only if the intermediate state can flip a spin (i.e. $\vec{Q}$ has the opposite spin orientation to that of the initial state). This, in turn, is only allowed if the impurity atom can change the Z-component of its spin in a compensating way so as to conserve the total angular momentum. If, for some reason, this moment is turned off on the impurity ion (i.e., $\vec{S}_n = 0 \Rightarrow S_{nZ} = 0$) the spin-flip processes are no longer allowed. Then the ℓn T term ceases to exist. Even if $\vec{S}$ should exist, but if S_Z cannot change easily, one likewise does not expect a ℓn T dependence in ρ. The resistivity of the sample may be written as

$$\rho = \rho_r + c\rho_A + c\rho_M(1 + 3ZJ\ell nT/E_F) + \rho_{electron\text{-}phonon} \tag{18}$$

where ρ_r = the residual resistivity of the host; $c\rho_A$ = the resistivity due to the impurity potential and is temperature independent; c = the concentration; $\rho_{electron\text{-}phonon} = A(c)\,T^n$; n = an integer and A = the coefficient of temperature dependence and may, in general, be concentration dependent.

As long as J is negative, when $T \to 0$, ρ_{sd} goes up (towards ∞) while $\rho_{\text{electron-phonon}}$ drops in magnitude. On approaching high temperatures, $\rho_{\text{electron-phonon}}$ goes up while ρ_{sd} drops in magnitude. Hence a minimum occurs in the resistivity vs. temperature curve. If one sets $\rho_r' = \rho_r + c\rho_A + c\rho_M$, still a temperature independent quantity, one may write

$$\rho = \rho_r' - D(c) \ln T + A(c) T^n \tag{19}$$

$$\text{where} \quad D(c) = \frac{c 9\pi m |J|^3 z \left(\frac{V}{N}\right) S(S+1)}{2 e^2 \hbar E_F^2} \tag{20}$$

The temperature T_m at which ρ is minimum is given by $T_m = [D(c)/nA(c)]^{\frac{1}{n}}$. Alternately one may write

$$A(c) = \frac{D(c)}{n T_m^n} \tag{21}$$

Usually A(c) is assumed to be independent of c. (Matthiessen's rule holds). If this is truly the case

$$T_m \propto [D(c)]^{1/n} \tag{22}$$

2. Nagaoka's Approach

As $T \to 0$, Kondo's expression for the resistivity $\rho_{sd} \to \infty$ for $J_{sd} < 0$. The quantity $1/\tau_K^{\rightarrow}$ diverges and a situation of instability would seem to exist. This is obviously unphysical. Nagaoka[14] has pioneered in solving this problem. He adopts Kondo's assumptions with the exception of the one on perturbation theory. He further assumes that $S_n = \frac{1}{2}$. He believes that the divergence indicates the inadequacy of the perturbational treatment. He appreciates the physical similarity of the present situation to the superconductivity problem. By analogy with the Cooper pair concept[15], he expects the correlation between the conduction electrons and the localized spin to be an important quantity. Using Kondo's Hamiltonian, he treats the magnetic impurity problem by the method of retarded double time Green's function which has earlier been applied by Zubarev[16] to the problem of superconductivity producing the BCS results[17]. Nagaoka shows that the conduction electron states, and hence the perturbational treatment, will break down below a critical temperature T_K defined by

$$1 = \frac{|J|\rho}{N} \int_0^L \frac{1}{\eta} \tanh \frac{\eta}{2kT_K} \, d\eta \qquad (23)$$

where, $\eta = E - E_F$ i.e., the energy measured from the Fermi level; and L = the width of the conduction band. This defines the Kondo tem-

perature.

At $T > T_k$ Nagaoka also obtains a $\ell n\ T$ dependence for ρ_{sd}; at $T \ll T_K$, he shows that $\rho_{sd} \sim \rho_o [\ 1-(T/T_R)^2]$ where $T_R \sim T_K$. Below the Kondo temperature T_K (similar to the superconductivity case) Nagaoka claims that there is a cloud of spin polarization forming around the impurity spin. This polarization has a dependence on distance: $p(r) \sim -(\sin k_F r/k_F r)^2$ $r \ll 10^{-4}$cm. It should be noted that it is of much longer range than the usual Ruderman-Kittel-Kasuya-Yosida type polarization[18]. Another interesting feature is that it is always negative or antiparallel to the localized spin. The magnitude does vary in space but the sign remains unchanged. On this basis, Nagaoka postulates the existence of the quasi-bound state. The quasi-bound state energy is of the order of $\sim kT_K$. It is not a true bound state in the sense that a sharp transition occurs at T_K. Rather, the transition is gradual and the spin compensating cloud surrounding the impurity spin is the collective result of a large number of conduction s electrons, each contributing a little bit. With this view point, one can see why ρ_{sd} should level off at $T \ll T_K$. As the conduction electrons complete their collective compensation of the impurity spin, the latter is essentially turned off ($S \to 0$). Hence, the two processes (III) and (IV) in Fig. 2b. no longer exist, and Kondo's $\ell n\ T$ mechanism is, as a consequence, absent. The weakness in the Nagaoka treatment is that it gives us no information on how the resistivity should behave around and at the critical temperature T_K, and how the Kondo $\ell n\ T$ region connects to the spin-compensate-state region at $T \ll T_K$.

3. Hamann's Formulation

Hamann [19] starts to treat the magnetic impurity problem using Nagaoka's method of decoupled equation of motion for double time Green's functions. The approximation used is lowest order non-trivial decoupling, and this correctly treats the logarithmic divergences[20], which are the salient features of the Kondo problem. The beauty of Hamann's solution is that he obtains an expression for ρ_{sd} valid for all temperatures T. He shows that

$$\rho_{sd} = \frac{2\pi c}{ne^2 k_F}\left\{1 - \frac{\ln(T/T_K)}{\left[\ln^2(T/T_K) + S(S+1)\pi^2\right]^{1/2}}\right\} \tag{24}$$

where T_K = the Kondo temperature; S = the spin value; c = the impurity concentration; n = the electron density and k_F = the Fermi wave vector. This result is qualitatively the same as the work of Suhl and Wong [21]. No instability occurs at $T = T_K$, and as the temperature changes from above T_K towards $T < T_K$ the resistivity changes in a smooth manner. This region around T_K has been neglected by most theories. Equation (24) is a most valuable expression for an experimentalist, since it correlates the data continuously through the physically interesting transition region between the Kondo $\ln T$ regime and the quasi-bound state regime. At $T << T_K$ one gets essentially $\rho_{sd} = 4\pi c/ne^2 k_F$ which is consistent with a spin-compen-

sate-state idea. (This is also required by the need to approach the unitarity limit)[1]. At $T >> T_K$, ρ_{sd} essentially $\rightarrow 0$.

C. Theories Related to the Fe [B] System

1. Yosida's Treatment

Yosida[22] has investigated the resistivity of magnetically ordered alloys, assuming the molecular field theory approach is valid. He concentrates only on the anomalous part of the resistivity neglecting the electron-phonon contribution. His treatment follows the line of Kasuya[23] who has calculated the anomalous resistivity arising from the s-d exchange interaction in the ferromagnetic iron group. Yosida assumes that the spin dependent part of the perturbing Hamiltonian arises from the exchange interaction between conduction s electrons and localized d electrons. Following Slater [24], Yosida treats this exchange interaction as an effective potential having opposite signs for electrons of opposite spin orientations. Hence up- and down-spin electrons would see different effective potentials. The spin independent part of the perturbing Hamiltonian arises mainly from the ordinary screened Coulomb potential around the impurity ion. The difference in potential corresponding to different spin orientations results in a difference in scattering probabilities through the cross term of the spin dependent interaction and the spin independent interaction. This cross term is proportional to the total magnetization M of the impurity.

With this Yosida arrives at an expression for the resistivity which can be written as:

$$R = \frac{3\pi m \Omega}{4 e^2 \hbar E_F N} c \left[2V^2 + \alpha(J_{exch}) - \beta(J_{exch}, V) \right] \qquad (25)$$

where $\alpha(J_{exch})$ is given by:

$$J_{exch}^2 \left\{ \langle S_z^2 \rangle^+ + \left[S(S+1) - \langle S_z^2 \rangle^+ - \langle S_z \rangle^+ \right] \left(1 + \tanh \frac{g\mu H}{kT}^+\right) + \langle S_z^2 \rangle^- + \left[S(S+1) - \langle S_z^2 \rangle^- - \langle S_z \rangle^- \right] \left(1 + \tanh \frac{g\mu H}{kT}^-\right) \right\}$$

$\beta(J_{exch}, V)$ is given by:

$$\frac{4 J_{exch}^2 V^2 \left(\langle S_z \rangle^+ + \langle S_z \rangle^- \right)^2}{2V^2 + J_{exch}^2 \left\{ \langle S_z^2 \rangle^+ + \langle S_z^2 \rangle^- + \left[S^2 + S - \langle S_z^2 \rangle^+ - \langle S_z \rangle^+ \right] \left(1 + \tanh \frac{g\mu H}{kT}^+\right) + \left(S^2 + S - \langle S_z^2 \rangle^- - \langle S_z \rangle^- \right) \left(1 + \tanh \frac{g\mu H}{kT}^-\right) \right]}$$

J_{exch} = the spin dependent interaction strength;

V = the spin independent interaction strength;

and c = the concentration of magnetic ions.

The symbols ± refer to + or - groups of ions. In general one may divide the ions into two groups. The ions of one group are subjected to the field H^+, and those belonging to the other group are subjected to the field H^-. The quantities H^+ and H^- are the sums of the molecular fields and the external field.

2. Turner and Long's Theory

Following the line of attack of Doniach and Wohlfarth[25] and Cole and Turner[26], Turner and Long [27] have been the first to calculate the resistivity of ferromagnetic alloys resulting from the addition of magnetic impurities like Fe in polarizable hosts like Pd, the d band of which contains holes. Based on the work of Izuyama, Kim and Kubo [28] they assume that the repulsion between the d holes of opposite spin on the same site in these hosts gives rise to an enhanced Pauli susceptibility for the d band. Hence when a magnetic impurity is added to these hosts, a large polarization of the d holes takes place due to this enhanced Pauli susceptibility. This phenomenon has some significant effect on the conduction s electron-localized Fe impurity scattering process. As in all magnetic impurity problems, there is the direct scattering of a s electron from an Fe impurity characterized by $J_{s\text{-}Fe}$. In addition, the s electron may scatter from a d hole-particle pair (characterized by $J_{s\text{-hole}}$) which propagates on and then, after some time t would scatter from the Fe impurity (characterized by $J_{Fe\text{-hole}}$). Due to this indirect process there is now an effective exchange integral taking the place of the ordinary exchange integral J. Turner and Long show that the Fourier transform of J_{eff} is given by:

$$J_{eff}(q,\omega) = J_{s-Fe} + J_{s-hole}\bar{\chi}_{host}(o,o)J_{Fe-hole} \qquad (26)$$

where, $\bar{\chi}_{host}(o, o)$ = the Fourier transform of the host susceptibility

evaluated at q = o, ω = o; $J_{s\text{-}Fe}$ = the Fourier transform of the s electron-Fe impurity exchange integral; $J_{s\text{-}hole}$ = the Fourier transform of the s electron-hole exchange integral; and $J_{Fe\text{-}hole}$ = the Fourier transform of the Fe impurity-hole exchange integral. Turner and Long have calculated the susceptibility by the method of Green's function. They also assume that for $T \rightarrow 0$ the situation can be adequately described by the theory of non-interacting spin waves. For $T \rightarrow T_c$, they assume that the molecular field theory approach gives an adequate description of the physical conditions.

The total Hamiltonian that they consider consists of the following six terms.

Just as in non-polarizable systems, there are: (1) the kinetic energy of the conduction s electrons, (2) the scattering of the s electrons from the Hartree Fock potential arising from the introduction of the Fe impurities, and (3) the coupling of the s electrons to the Fe impurity spins. However, due to the presence of the d holes in the host metal, there are in addition: (4) the kinetic energy of the d holes including the short range repulsion between the holes of opposite sign on the same site, (5) the coupling of the Fe impurity spins to the d holes and (6) the coupling of the s electrons to the d holes.

Turner and Long concentrate on the resistivity in the ferromagnetic temperature range. For resistivity, one is mostly interested in the s electrons. They reason that the additional resistivity of the alloy due to the addition of Fe impurities arises (1) from the scatterings of the s electrons from the Hartree Fock potential due to the presence of the Fe impurities, and (2) from the scattering of the

s electrons from the localized Fe spins both directly and indirectly.

For $T \to 0$, considering the dominant contribution to ρ to be caused by spin waves, Turner and Long follow the approach of Yosida [22] and arrive at an expression for the resistivity.

$$\rho(T) = \rho_r + c\rho_A + D'_{Fe}\, c \left(\frac{T}{T_c}\right)^{3/2} \qquad (27)$$

where ρ_A and D'_{Fe} are independent of temperature T but dependent on J_{eff} and V, V being the Hartree Fock potential. The term ρ_r is the residual resistivity of the host.

The important thing to notice is the $T^{3/2}$ temperature dependence. There are 3 contributions to this term. The first arises from the conduction s electron spin-flip scattering from the coupled Fe impurity -d band system resulting in the creation of a spin deviation which propagates as a spin wave. Contrary to the situation in ferromagnets possessing periodicity in which case one gets a T^2 dependence, Turner and Long claim that for the electron-magnon scattering in a non-periodic system, one should obtain a $T^{3/2}$ dependence for the resistivity. This is so because momentum is no longer conserved and the scattering rate is proportional to the number of spin waves present which in turn is proportional to $T^{3/2}$. The second contribution comes from the non spin-flip part of the exchange scattering, and is proportional to $\langle M^2 \rangle$. For spin waves as $T \to 0$, $M^2(T)$ $= (M(o) - DT^{3/2})^2 \cong M^2(o) - 2DT^{3/2}M(o)$. The third contribution comes from the interference effect between the potential scattering

and the non spin-flip part of the exchange scattering. In the limit of strong potential scattering, one gets a term $\propto \langle M \rangle^2$. For a ferromagnetic system, this is again $\propto T^{3/2}$.

As $T \to T_c$, Turner and Long adopt the expression derived by Yosida [22] for magnetically ordered systems given in Section (III.C.1.). At T near T_c, one may set $\langle\ \rangle^+ = \langle\ \rangle^-$ and $H^+ = H^- = B$. Using Yosida's expression and expanding to the leading power in $(T-T_c)$, they obtain:

$$\int_{T \to T_c} \rho(T) = \frac{3\pi m^* c}{2e^2 \hbar E_F}\left(\frac{\Omega}{N}\right)\left\{V^2 + J_{eff}^2 S(S+1) - \frac{J_{eff}^2 S(S+1)}{2S^2+2S+1}\left[5 - \frac{40V^2 S(S+1)}{3(V^2+J_{eff}^2 S(S+1))}\right]\frac{T-T_c}{T_c}\right\} \quad (28)$$

Hence they predict a term linear in T for ρ just below the Curie temperature T_c.

3. Mannari's Theory of $d\rho/dT$.

Mannari[29] also assumes the s-d interaction model, and concentrates his analysis on the region near the Curie point T_c. He assumes that the singularity in the critical region arises from the spin-disorder scattering through the s-d interaction. He treats this problem in terms of pair correlation functions. Mannari argues that the main contribution to ρ(which is weighed by a factor $(1 - \cos\theta)$) comes from the short range part of the spin correlation function, and no singularity arises. In $d\rho/dT$, however, the long range part of the spin correlation function also contributes giving rise to a singularity. In an amorphous system, where long range correlation is

less prominant, one expects the singularity in $d\rho/dT$ to be partially smeared out. Using the s-d interaction model, Mannari obtains an expression for $d\rho/dT \propto \ell n \mid T-T_c \mid$.

D. Theory of Magnetic Susceptibility

Magnetic moment measurements can provide some supporting information which is helpful in understanding the resistivity of the alloys containing the transition elements Cr and Fe. The temperature dependence of the inverse magnetic susceptibility ($1/\chi$) obtained from the observed magnetic isothermals gives a direct indication on whether or not an alloy possesses localized moments. The following operational definition[1] will be adopted: a localized moment exists if the alloy has a temperature dependent $1/\chi$ vs. T curve in the form of a Curie law or a Curie-Weiss law. This constitutes the main interest in the magnetic measurements in this investigation. Just as Kondo[12] and others have assumed the existence of localized moments without worrying about moment formation, this investigation will likewise concentrate on those cases where magnetic moments exist.

In the paramagnetic temperature range one may write [30]

$$\chi = \frac{N \mu_{eff}^2}{3k(T-\theta_p)} \qquad (29)$$

where N is the number of transition metal atoms and μ_{eff} is the effective moment. From the slope of the $1/\chi$ vs. T curve, one may get an estimate of μ_{eff}. Assuming that the orbital motion is quenched and that only the electron spin contributes to the magnetic

moment, one may write $\mu_{eff} = g\mu_B \sqrt{S(S+1)}$ with g = 2.0. The sign of θ_p depends on whether the long range interaction between the transition metal atoms is ferromagnetic or antiferromagnetic. Blandin and Friedel[31] have considered the d-d spin interaction of the form $H' = \sum_{i,j} (J_{dd})_{ij} \vec{S}_i \cdot \vec{S}_j$ and obtained the susceptibility correct to the order of J_{dd}^2. They find that $\theta_p = 2S(S+1)\, c\, J_{dd}/3k$ where c is the concentration, $\vec{S}$ is the spin of the transition metal atom, and $J_{dd} = \sum_j (J_{dd})_{ij}$ is the d-d spin interaction exchange integral. When the system becomes ferromagnetic, the magnetization σ increases by a factor of a hundred or more. On the other hand, for Kondo systems, existing theories[14], [19], [32] predict that as the temperature goes below $T = T_K$ the magnetic moment should decrease due to the formation of the quasi-bound state. As a result, there is an increase in the slope of the $1/\chi$ vs. T curve below $T = T_K$.

IV. EXPERIMENTAL RESULTS

A. The [B] Alloy

The resistivity ρ for pure [B] is plotted as a function of temperature from $4^{\circ}K$ to $500^{\circ}K$ in Fig. 3. At high temperatures (above $60^{\circ}K$), $\rho_{[B]}$ varies linearly with temperature. The coefficient of T is approximately 1.58×10^{-2} $\mu\Omega$-cm/$^{\circ}K$. Between $20^{\circ}K$ and $60^{\circ}K$, $\rho_{[B]}$ depends quadratically on T. At $12^{\circ}K$, a slight resistivity minimum is observed. This is seen more clearly in Fig. 4 where $\rho_{[B]}$ is plotted against temperature between $0^{\circ}K$ and $60^{\circ}K$. For comparison's purpose, the resistivity ρ for VHP [B] is also plotted as a function of temperature T between $0^{\circ}K$ and $60^{\circ}K$ in Fig. 4. It should be noted that the resistivity minimum is substantially reduced.

B. The Cr[B] System

1. Electrical resistivity as a Function of Temperature

The resistivities of $Cr_{0.5}[B]_{99.5}$, $Cr_{1.0}[B]_{99.0}$, $Cr_{1.5}[B]_{98.5}$, $Cr_{2.0}[B]_{98.0}$, $Cr_{2.5}[B]_{97.5}$, $Cr_{3.0}[B]_{97.0}$, and $Cr_{4.0}[B]_{96.}$ are plotted as a function of temperature between $4^{\circ}K$ and $300^{\circ}K$ in Figs. 5 to 8. Well defined resistivity minima are observed in all cases. For $Cr_{0.5}[B]_{99.5}$ and $Cr_{1.0}[B]_{99.0}$, a linear in T region exists at the high temperature end. As the concentration c increases from 1.5 at.% to 4.0 at.% the minimum region gets progressively broader.

2. Electrical Resistivity as a Function of $Log_{10}T$

The data in Figs. 5 to 8 are plotted against $\log_{10}T$ in Figs. 9 to 12. A linear region is observed for each of the concentrations studied. For each concentration, it is noticed that ρ deviates from the

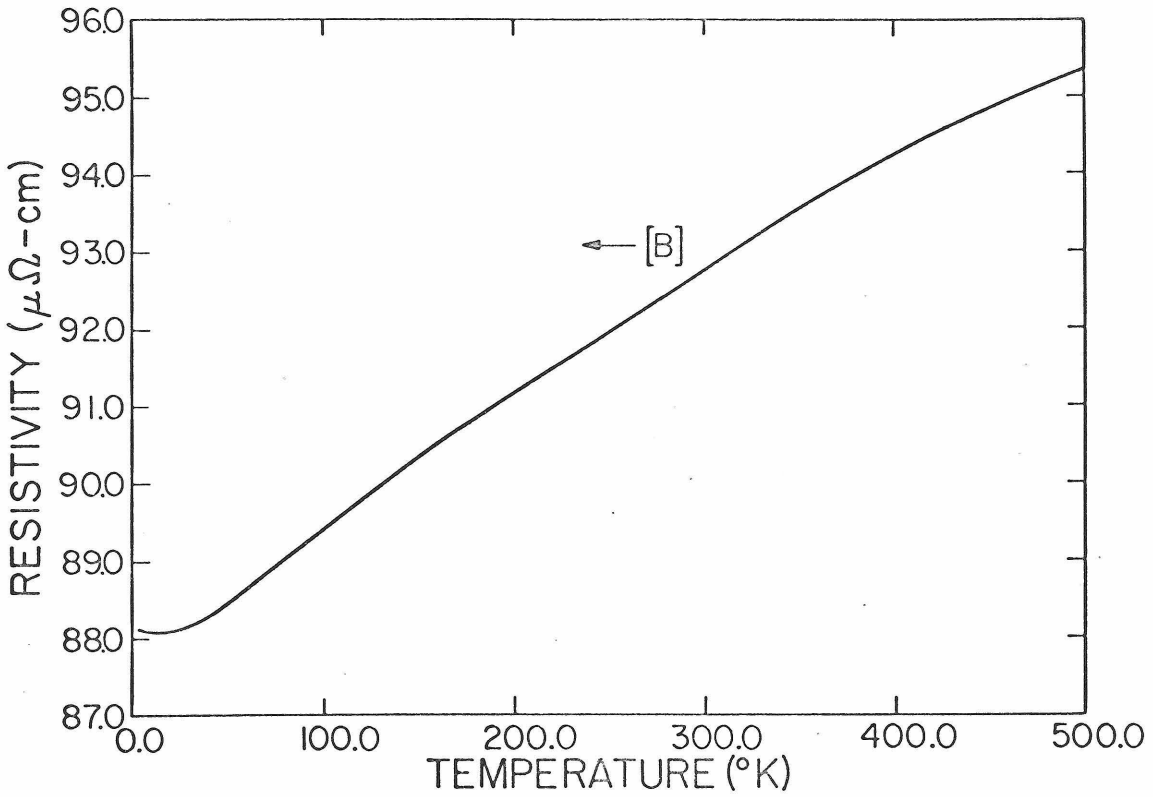

Fig. 3. Resistivity vs temperature curve for the [B] alloy.

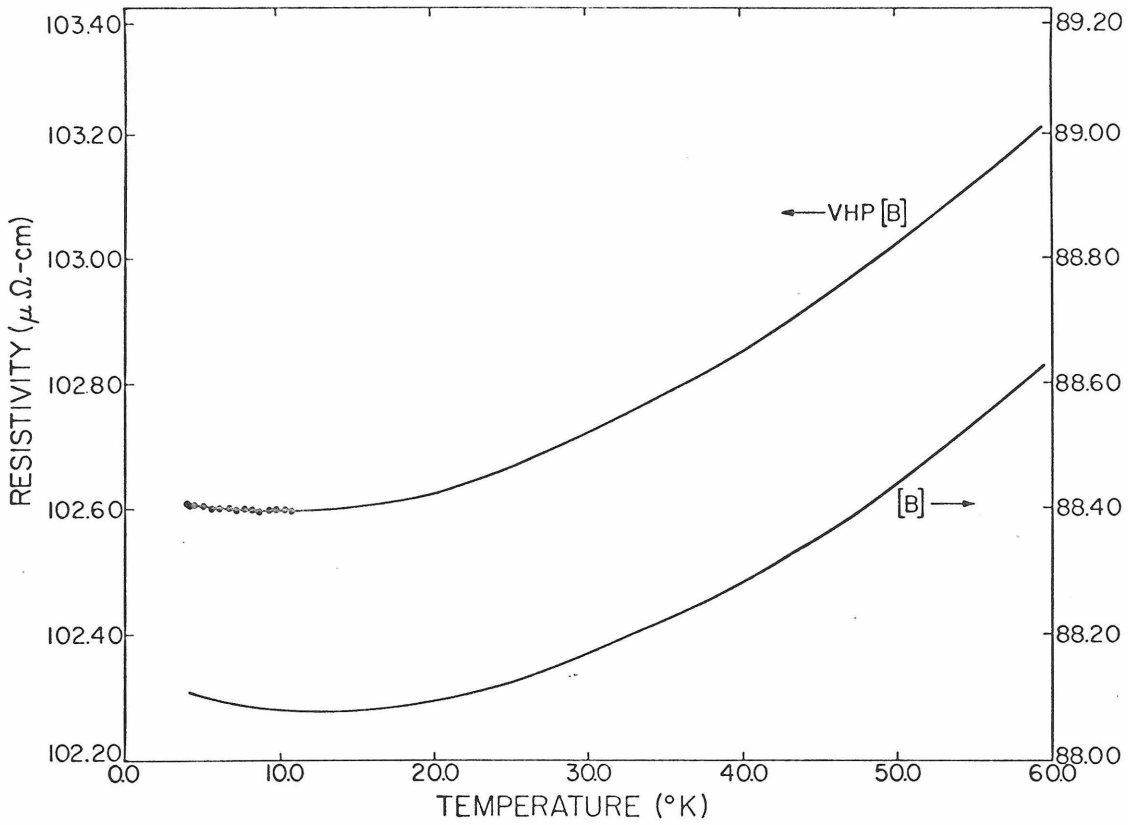

Fig. 4. Comparison of the resistivity vs temperature curves for the VHP[B] (Fe concentration less than 0.0013 at.%) and the [B] alloys. The actual experimental points are partially shown in this figure (dots) to indicate the scattering typical in the resistivity measurements.

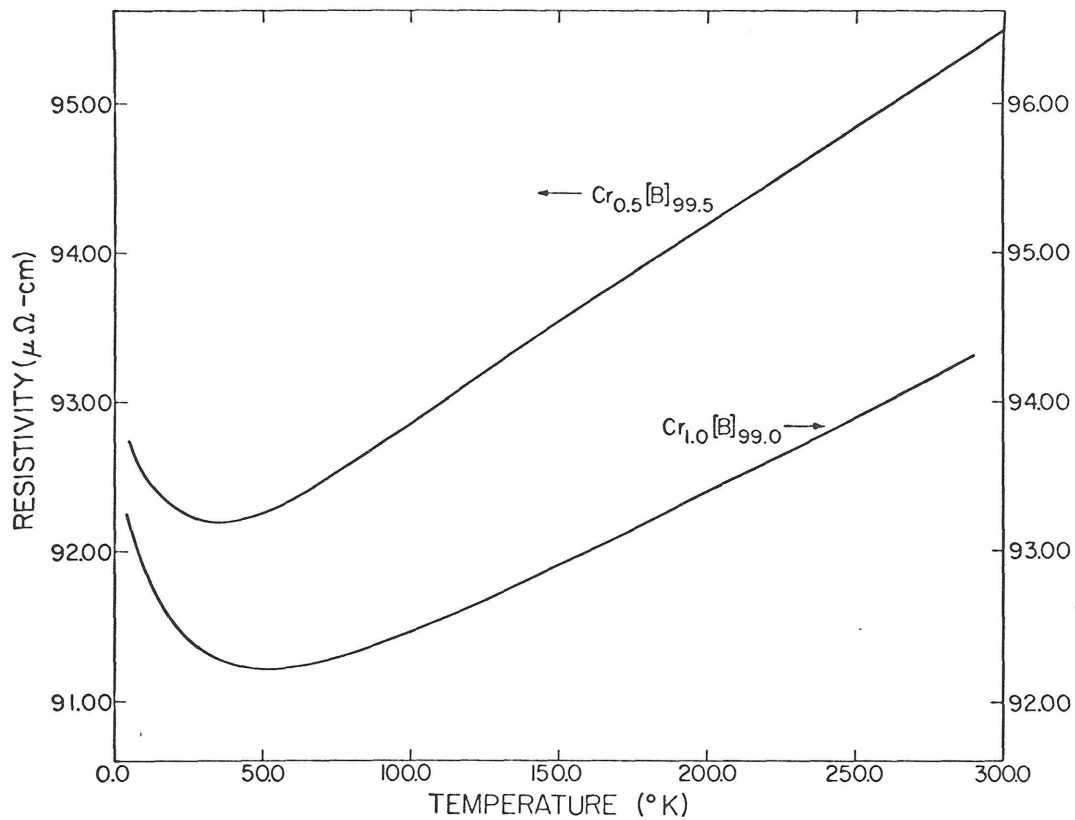

Fig. 5. Resistivity vs temperature curves for the $Cr_{0.5}[B]_{99.5}$ and $Cr_{1.0}[B]_{99.0}$ alloys.

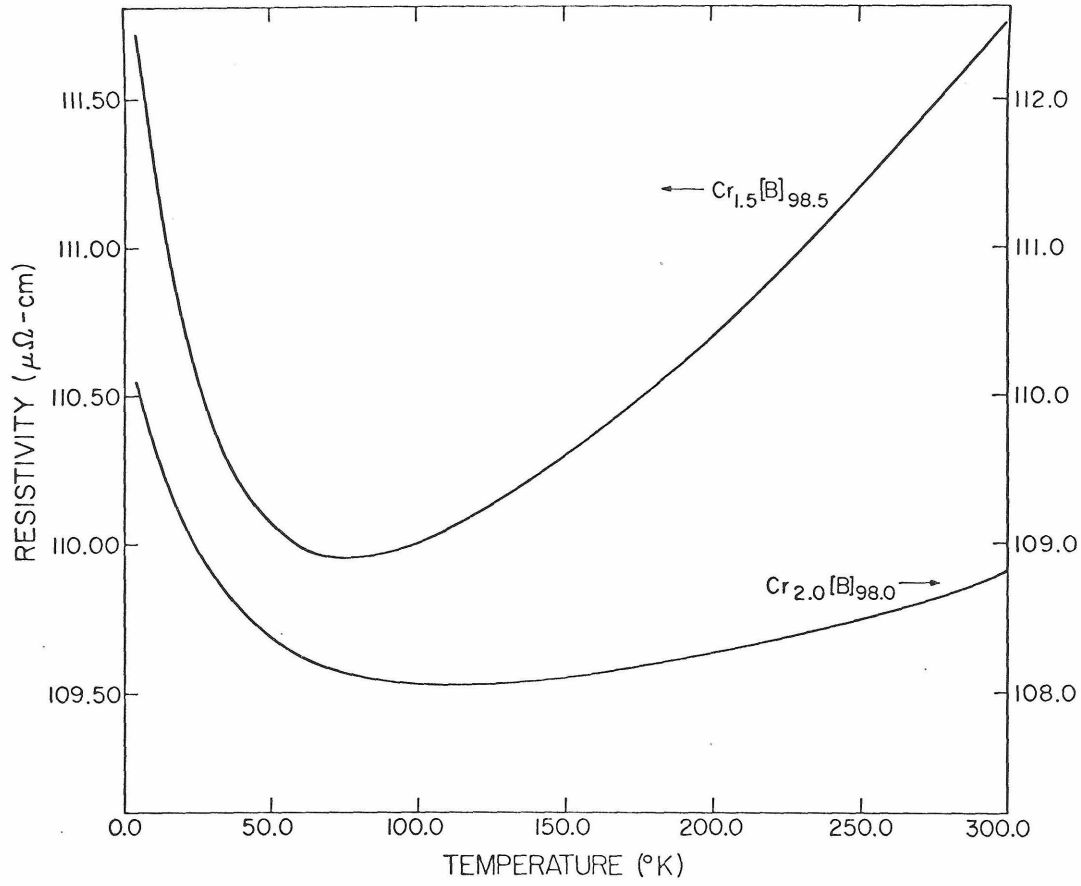

Fig. 6. Resistivity vs temperature curves for the $Cr_{1.5}[B]_{98.5}$ and $Cr_{2.0}[B]_{98.0}$ alloys.

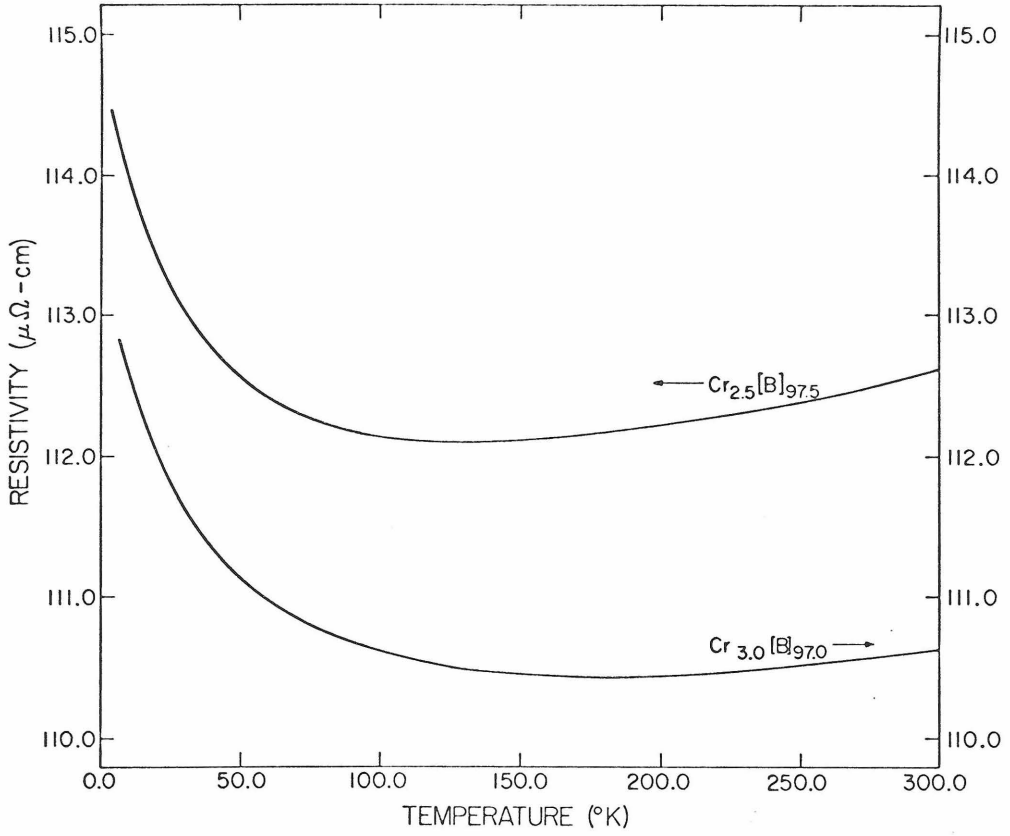

Fig. 7. Resistivity vs temperature curves for the $Cr_{2.5}[B]_{97.5}$ and $Cr_{3.0}[B]_{97.0}$ alloys.

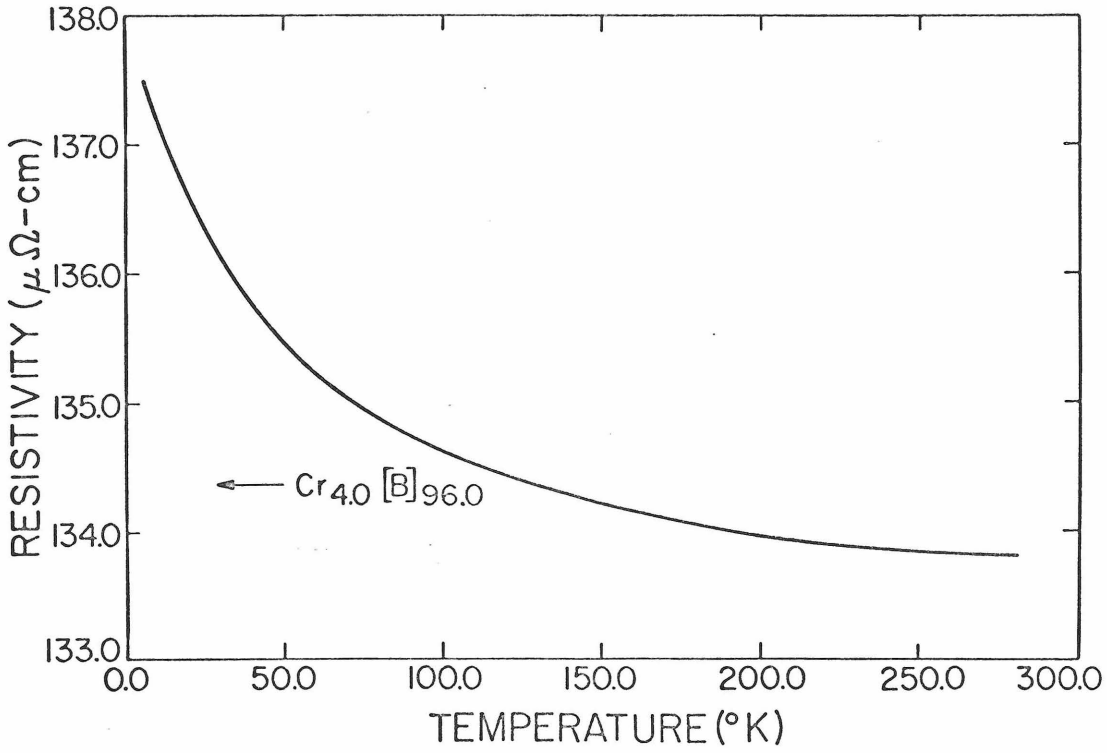

Fig. 8. Resistivity vs temperature curve for the $Cr_{4.0}[B]_{96.0}$ alloy.

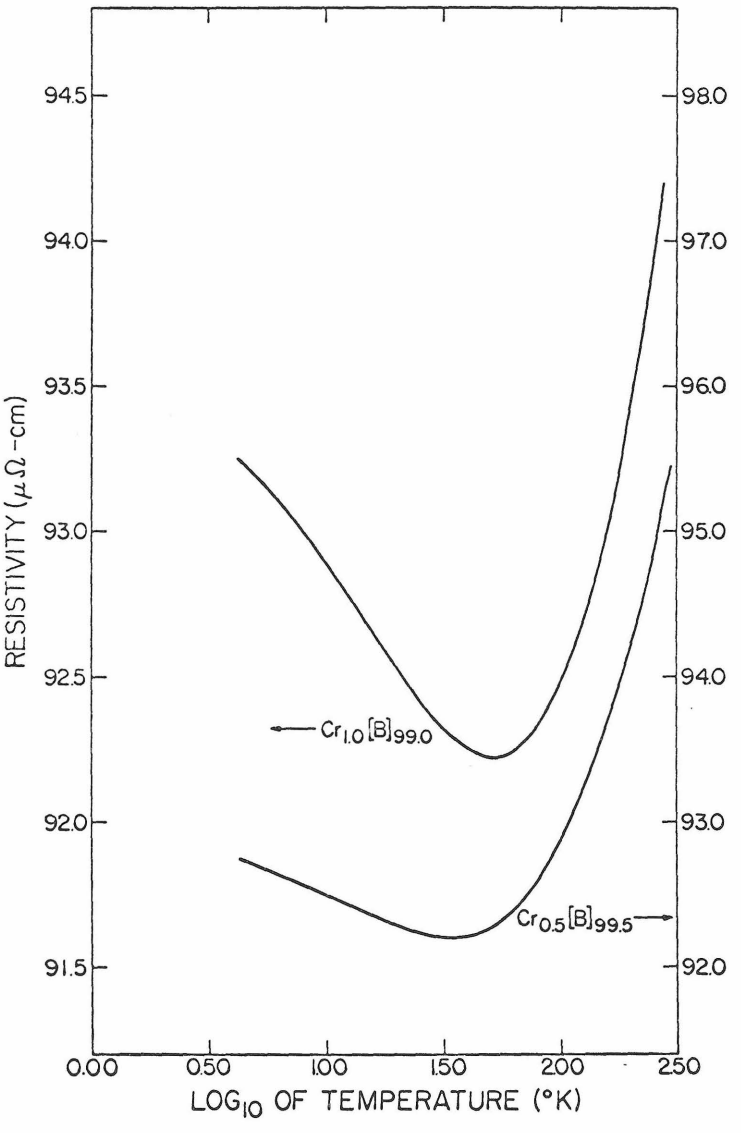

Fig. 9. Resistivity vs $\log_{10}$ of temperature curves for the $Cr_{1.0}[B]_{99.0}$ and $Cr_{0.5}[B]_{99.5}$ alloys.

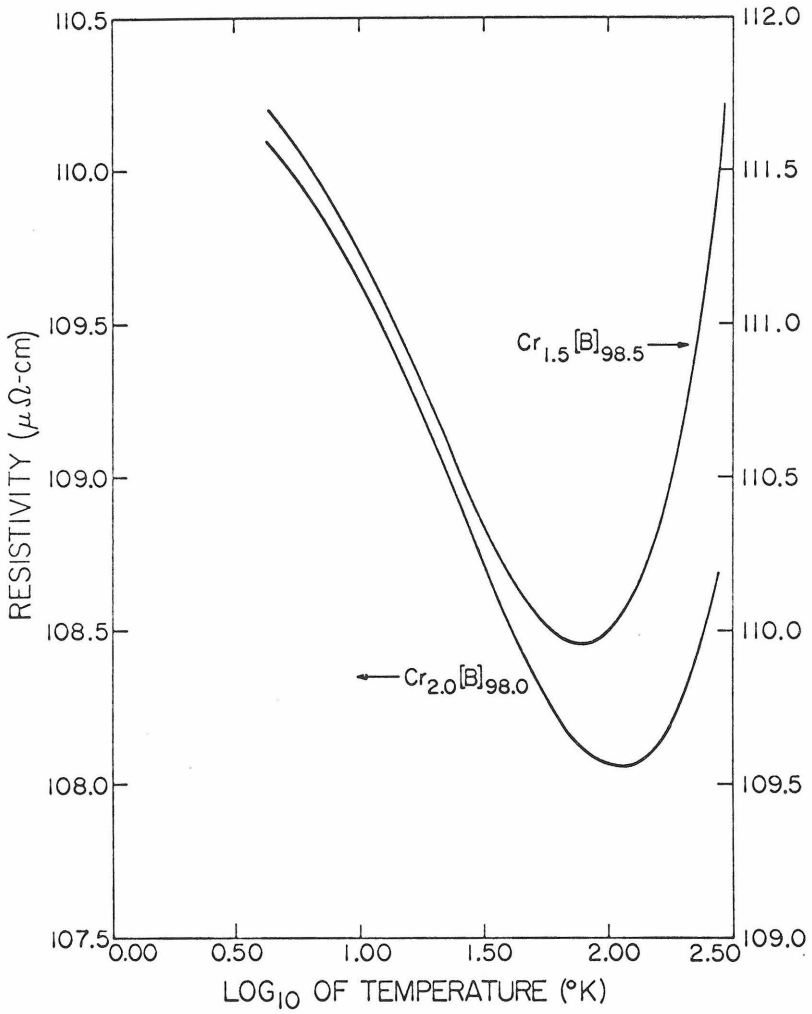

Fig. 10. Resistivity vs $\log_{10}$ of temperature curves for the $Cr_{1.5}[B]_{98.5}$ and $Cr_{2.0}[B]_{98.0}$ alloys.

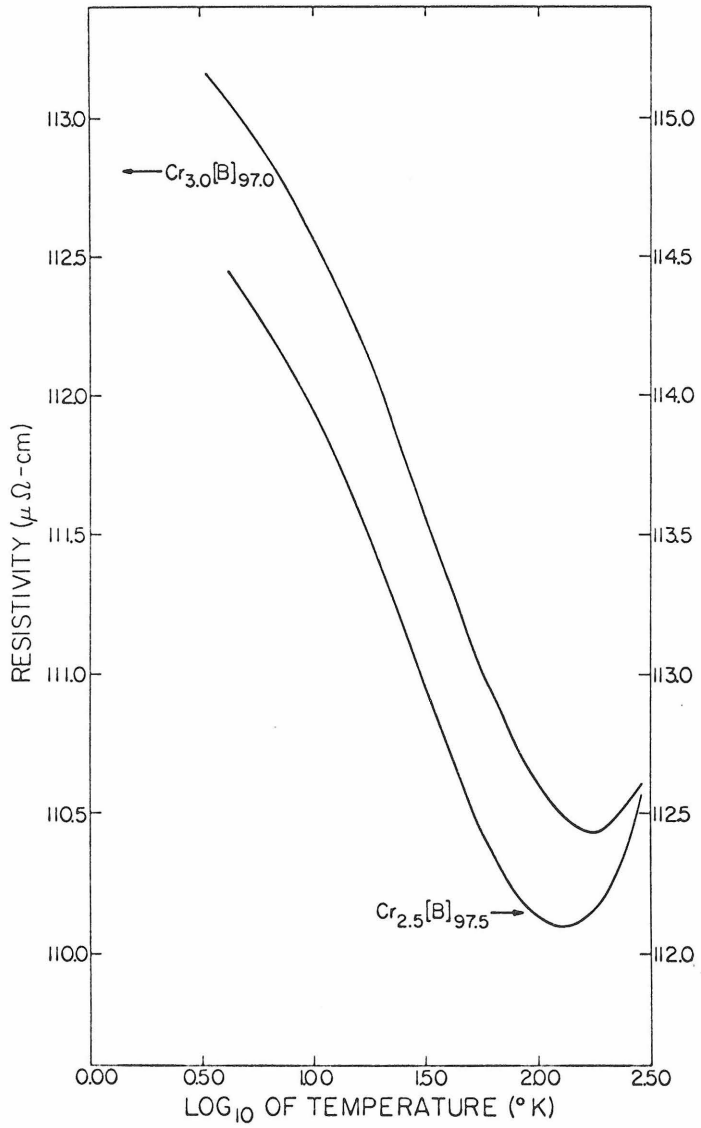

Fig. 11. Resistivity vs $\log_{10}$ of temperature curves for the $Cr_{3.0}[B]_{97.0}$ and $Cr_{2.5}[B]_{97.5}$ alloys.

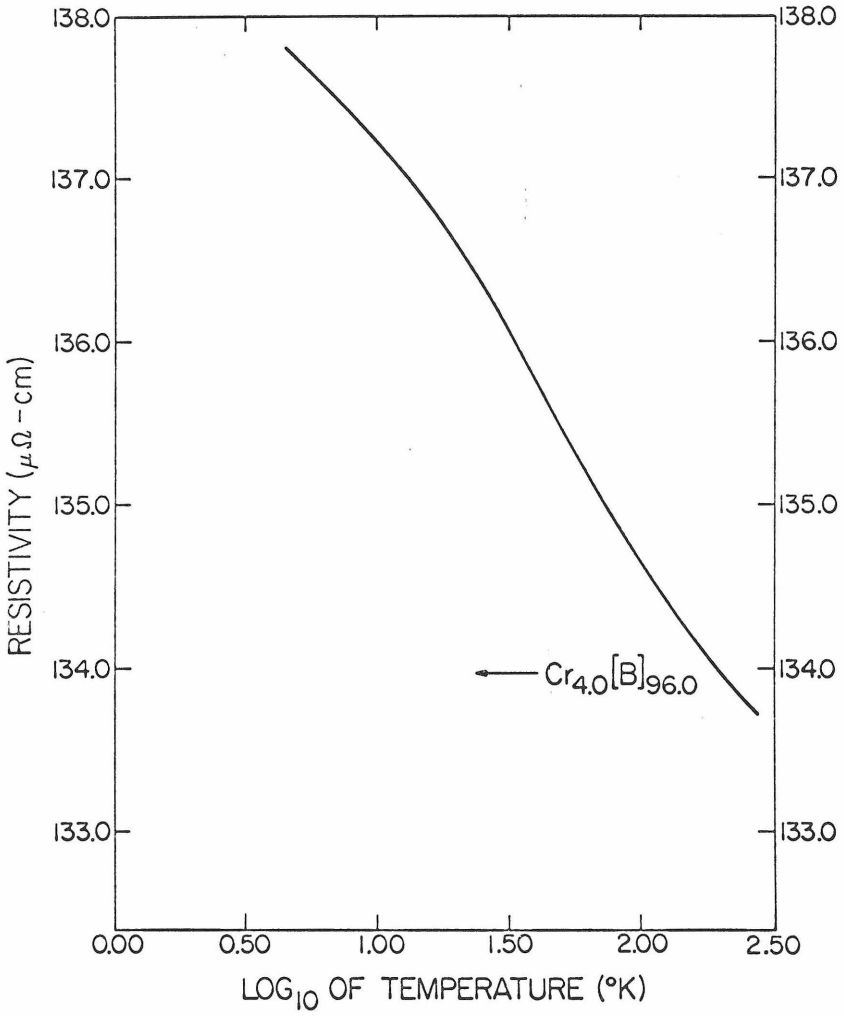

Fig. 12. Resistivity vs $\log_{10}$ of temperature curve for the $Cr_{4.0}[B]_{96.0}$ alloy.

$\log_{10}T$ dependence when $T = T_{d\ lower}$ (at the low temperature end) and when $T = T_{d\ upper}$ (near the minimum). The quantities $T_{d\ upper}$, $T_{d\ lower}$ and ΔT ($T_{d\ upper} - T_{d\ lower}$, the approximate range in T over which a linear $\log_{10}T$ dependence is observed) are listed in Table 1. The quantity ΔT is plotted as a function of Cr concentration in Fig. 13. The temperature at which the resistivity is minimum, T_m can readily be determined. The values of T_m are listed as a function of c in Table 2.

3. Magnetic Susceptibility vs. T for $Cr_{3.0}[B]_{97.0}$

As supporting evidence, the reciprocal susceptibility for $Cr_{3.0}[B]_{97.0}$ is plotted as a function of temperature in Fig. 14. At high temperature $1/\chi$ varies linearly with temperature, obeying a Curie-Weiss temperature dependence with $\theta_p = -145^{\circ}K$. At low temperature (below $20^{\circ}K$), $1/\chi$ again varies linearly with temperature, although with a sharper slope. The transition between these two regions is very gradual. Extrapolating the two linear regions gives an intercept at $T = 31^{\circ}K$.

C. The Fe[B] System

1. Electrical Resistivity as a Function of Temperature

The resistivity vs. temperature curves for [B] containing low concentrations of Fe impurities (i.e., less than 0.45 at.%) are similar to the ρ vs. T curve for $Fe_{0.45}[B]_{99.55}$ shown in Fig. 15. It exhibits a slight minimum at $T \sim 15^{\circ}K$. At high temperatures, ρ is a linear function of temperature. The resistivity vs. temperature curves for [B] containing 0.6 to 1.0 at.% Fe show no minimum. The resistivity increases monotonically with temperature with no charac-

TABLE 1

Values of the characteristic temperatures and related functions for the $Cr_c[B]_{100-c}$ alloys.

Concentration (at.%)	T_K (^oK)	$T_{d\ upper}$ (^oK)	$T_{d\ lower}$ (^oK)	ΔT (^oK)	$\log_{10} T_K$	$\frac{1}{2}(\log_{10} T_{d\ upper} + \log_{10} T_{d\ lower})$
$Cr_{0.5}[B]_{99.5}$	12.7	22.1	6.3	15.8	1.1038	1.0719
$Cr_{1.0}[B]_{99.0}$	14.1	26.6	7.9	18.7	1.1492	1.1625
$Cr_{1.5}[B]_{98.5}$	17.0	31.6	10.3	21.3	1.2306	1.2563
$Cr_{2.0}[B]_{98.0}$	20.6	41.0	15.4	25.6	1.3139	1.4000
$Cr_{2.5}[B]_{97.5}$	25.2	55.4	16.3	39.1	1.4009	1.4781
$Cr_{3.0}[B]_{97.0}$	30.0	56.2	16.8	39.4	1.4770	1.4875
$Cr_{4.0}[B]_{96.0}$	38.2	86.6	21.8	64.9	1.5826	1.6345

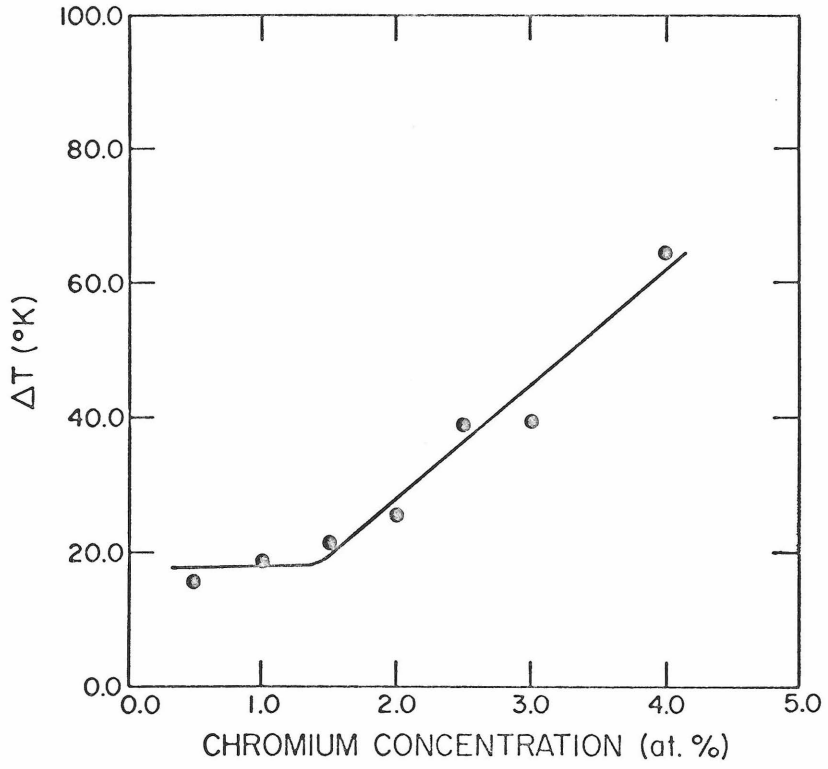

Fig. 13. $\Delta T = (T_{d\ upper} - T_{d\ lower})$ vs chromium concentration for the $Cr_c[B]_{100-c}$ alloys.

TABLE 2

Values of the parameters used in arriving at the universal curves of resistivity according to the Hamann theory and the Kondo theory for the $Cr_c[B]_{100-c}$ alloys.

Concentration (at.%)	T_K (^oK)	ρ_o ($\mu\Omega$ - cm)	$\langle B \rangle$ ($\mu\Omega$ - cm)	T_{min} (^oK)	ρ_{min} ($\mu\Omega$ - cm)	D (also denoted by SL) ($\mu\Omega$ - cm)
$Cr_{0.5}[B]_{99.5}$	12.7	1.71	91.56	34.5	92.19	0.292
$Cr_{1.0}[B]_{99.0}$	14.1	2.70	91.37	53.1	92.22	0.510
$Cr_{1.5}[B]_{98.5}$	17.0	4.11	108.75	75.0	109.95	0.754
$Cr_{2.0}[B]_{98.0}$	20.6	4.60	106.77	109.0	108.05	0.850
$Cr_{2.5}[B]_{97.5}$	25.2	4.88	110.73	129.6	112.09	0.933
$Cr_{3.0}[B]_{97.0}$	30.0	5.06	109.08	171.0	110.43	0.977
$Cr_{4.0}[B]_{96.0}$	38.2	6.53	132.54			1.245

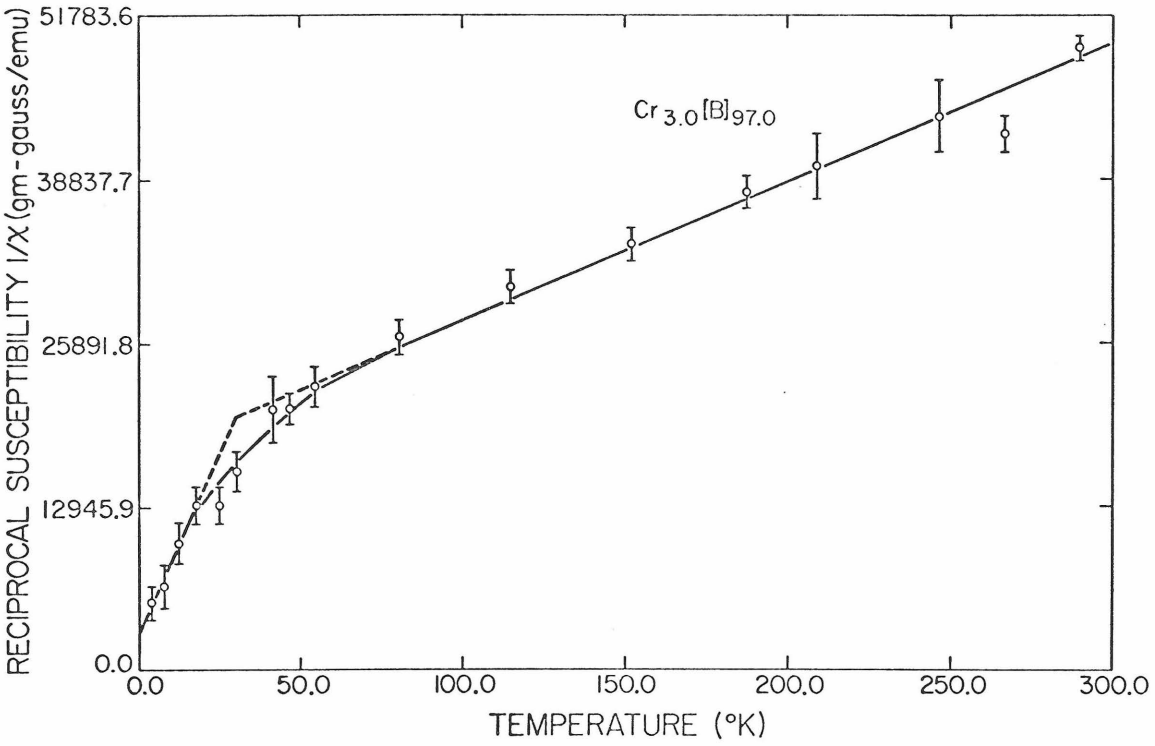

Fig. 14. Reciprocal susceptibility vs temperature curve for the $Cr_{3.0}[B]_{97.0}$ alloy.

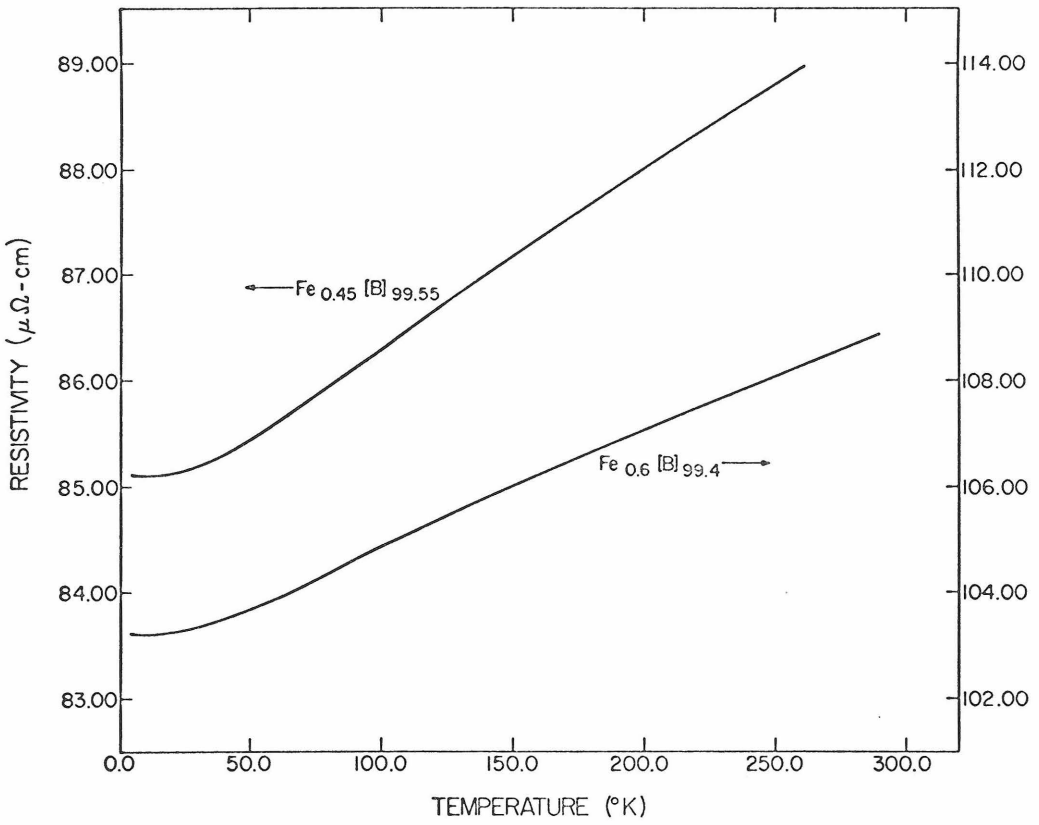

Fig. 15. Resistivity vs temperature curves for the $Fe_{0.45}[B]_{99.55}$ and $Fe_{0.6}[B]_{99.4}$ alloys.

teristic anomaly. As examples, the resistivity curves for $Fe_{0.6}[B]_{99.4}$, $Fe_{0.7}[B]_{99.3}$ and $Fe_{0.8}[B]_{99.2}$ are shown in Figs. 15 and 16. The resistivity vs. temperature curves for [B] containing 1.50 to 4.0 at.% Fe are shown in Figs. 17 to 19. A very striking kink occurs in each of the resistivity vs. temperature curves. The transition T_c, around which the kink occurs, increases with concentration. At high temperatures, ρ possesses a linear dependence on temperature. Below the characteristic temperature T_c there is a region where ρ decreases linearly with T. At temperatures well below T_c, ρ has a $T^{3/2}$ dependence.

2. Magnetic Susceptibility and Magnetization vs. T for $Fe_{2.5}[B]_{97.5}$

The reciprocal susceptibility of the alloy $Fe_{2.5}[B]_{97.5}$ is plotted vs. T in the paramagnetic temperature range in Fig. 20. At the high temperature region, it is noticed that $1/\chi$ varies linearly with T. Extrapolating the straight line yields an intercept at 100°K. Fig. 21 shows the temperature dependence of magnetization for the same alloy for T below 70°K in the three lowest available applied magnetic fields - 390 Gauss, 810 Gauss and 1400 Gauss. For T below ~20°K, the magnetizations show signs of saturation with σ_{sat}~7 emu/gm. The temperature at the midpoint of the "fall-off" part of the σ vs. T curve decreases as the external applied field is decreased. This temperature varies from 27°K at H_{app} = 1400 Gauss to 24°K at H_{app} = 390 Gauss.

3. Inductance Bridge Results

An example of the results obtained from the a-c inductance

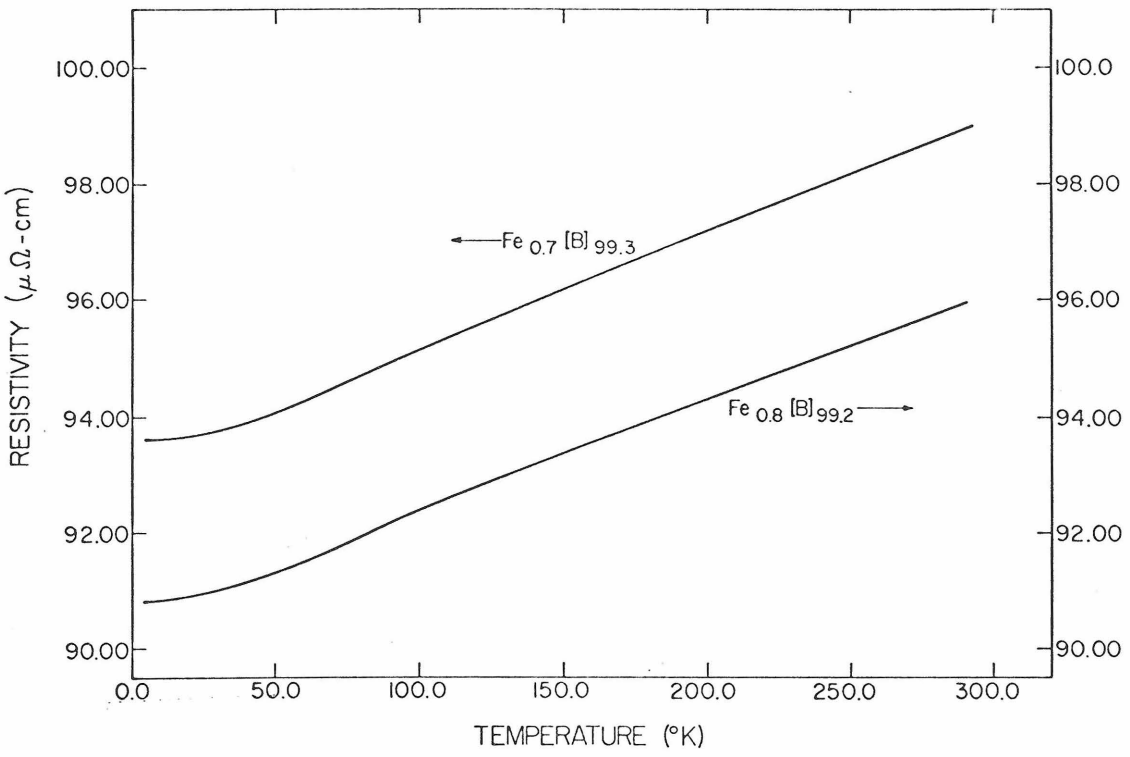

Fig. 16. Resistivity vs temperature curves for the $Fe_{0.7}[B]_{99.3}$ and $Fe_{0.8}[B]_{99.2}$ alloys.

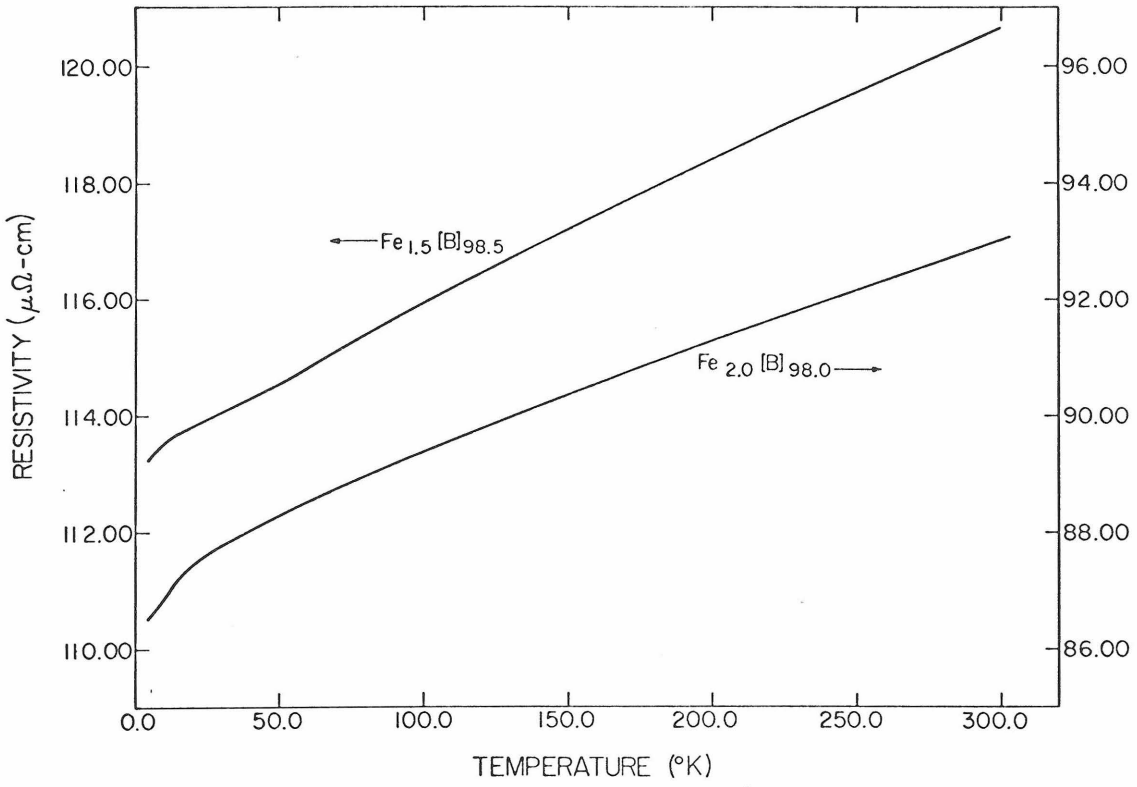

Fig. 17. Resistivity vs temperature curves for the $Fe_{1.5}[B]_{98.5}$ and $Fe_{2.0}[B]_{98.0}$ alloys.

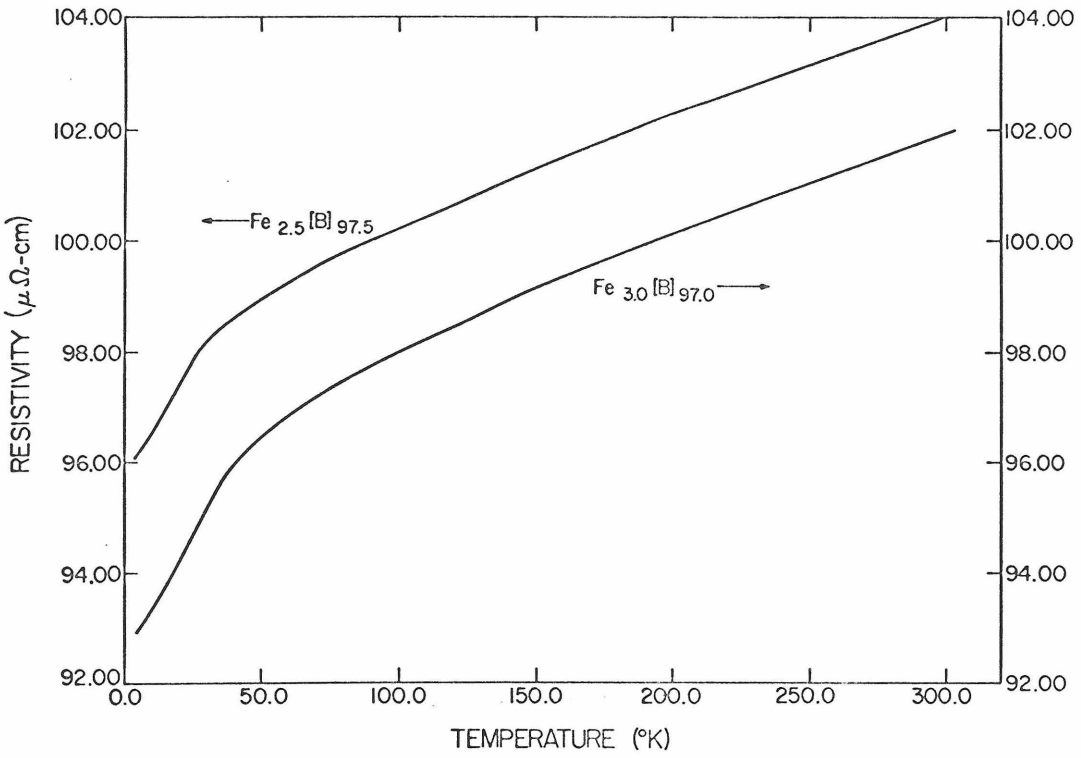

Fig. 18. Resistivity vs temperature curves for the $Fe_{2.5}[B]_{97.5}$ and $Fe_{3.0}[B]_{97.0}$ alloys.

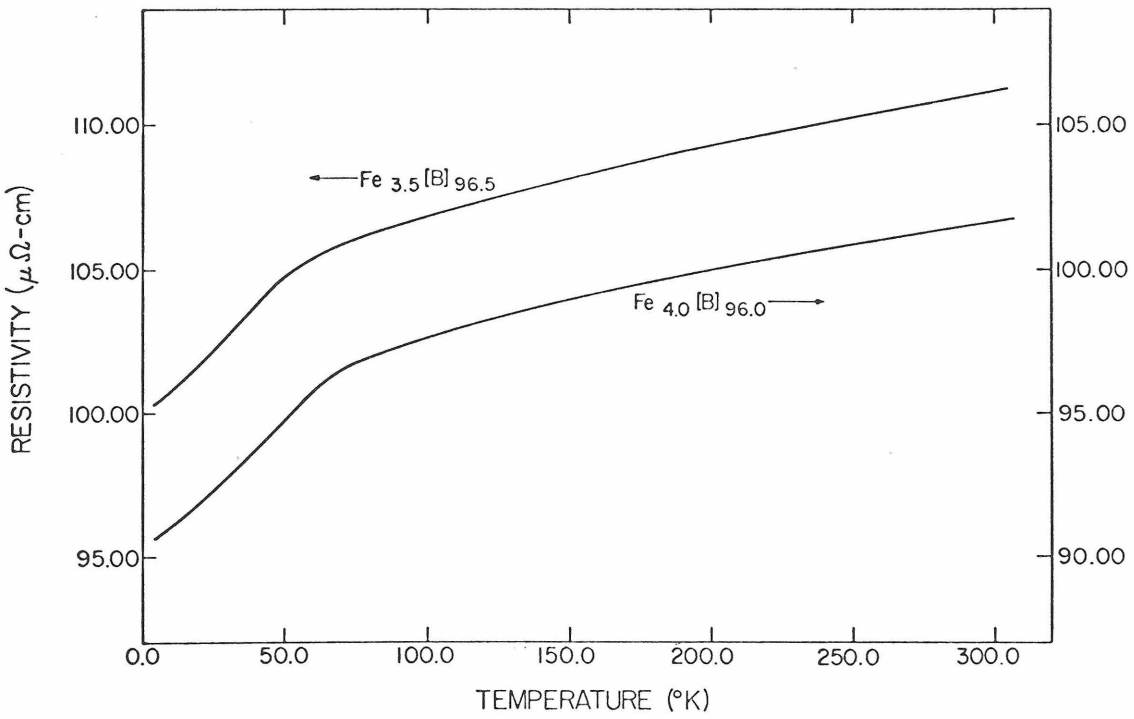

Fig. 19. Resistivity vs temperature curves for the $Fe_{3.5}[B]_{96.5}$ and $Fe_{4.0}[B]_{96.0}$ alloys.

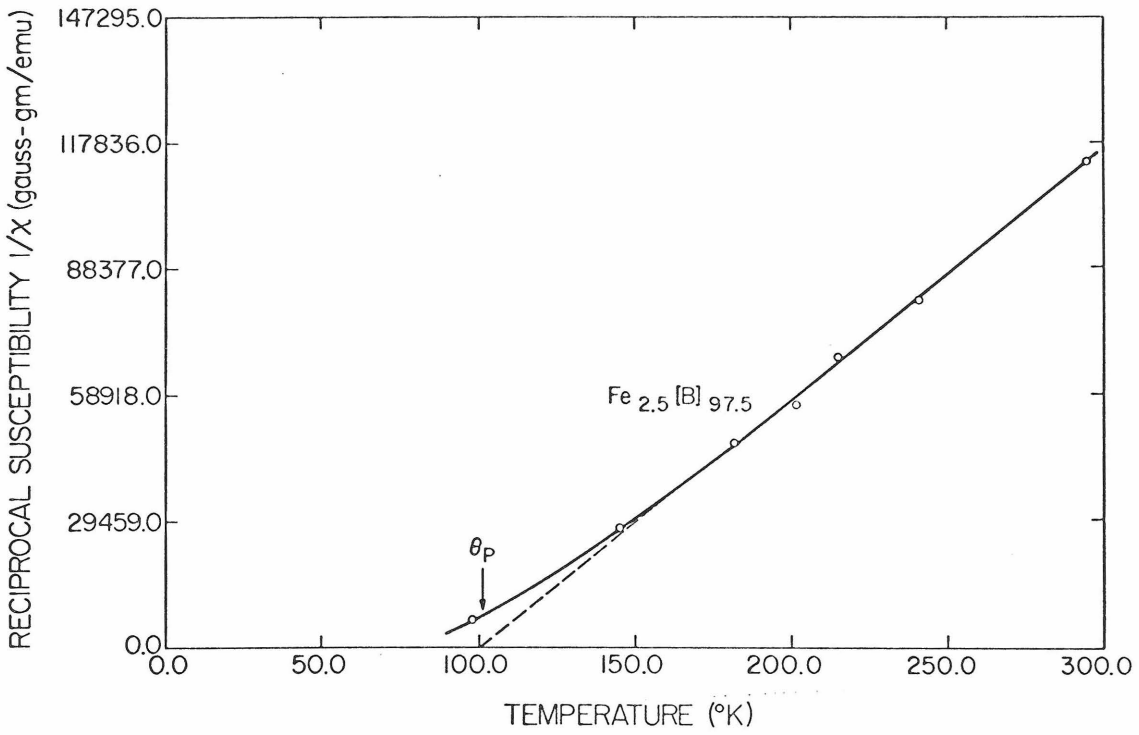

Fig. 20. Reciprocal susceptibility vs temperature curve for the $Fe_{2.5}[B]_{97.5}$ alloy.

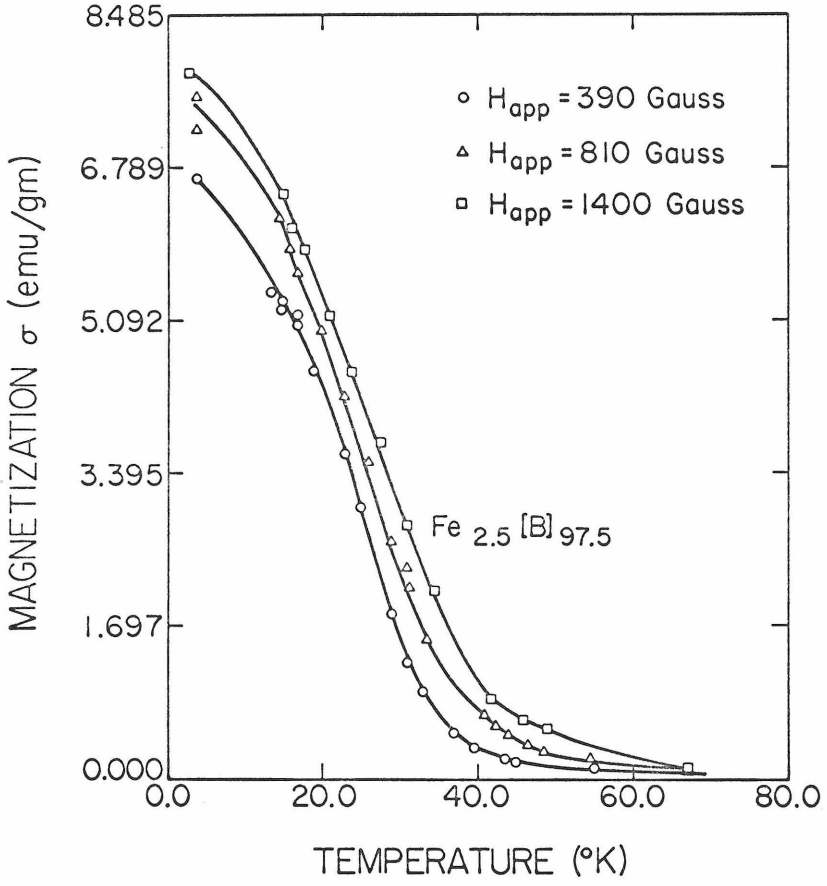

Fig. 21. Magnetization vs temperature curves for the $Fe_{2.5}[B]_{97.5}$ alloy.

Wheatstone bridge is presented in Fig. 22. The voltage inbalance V_{AB} in arbitrary units is plotted against the temperature for the alloy $Fe_{2.5}[B]_{97.5}$. It should be noticed that the changes in the voltage V_{AB} are quite pronounced around 24.8°K.

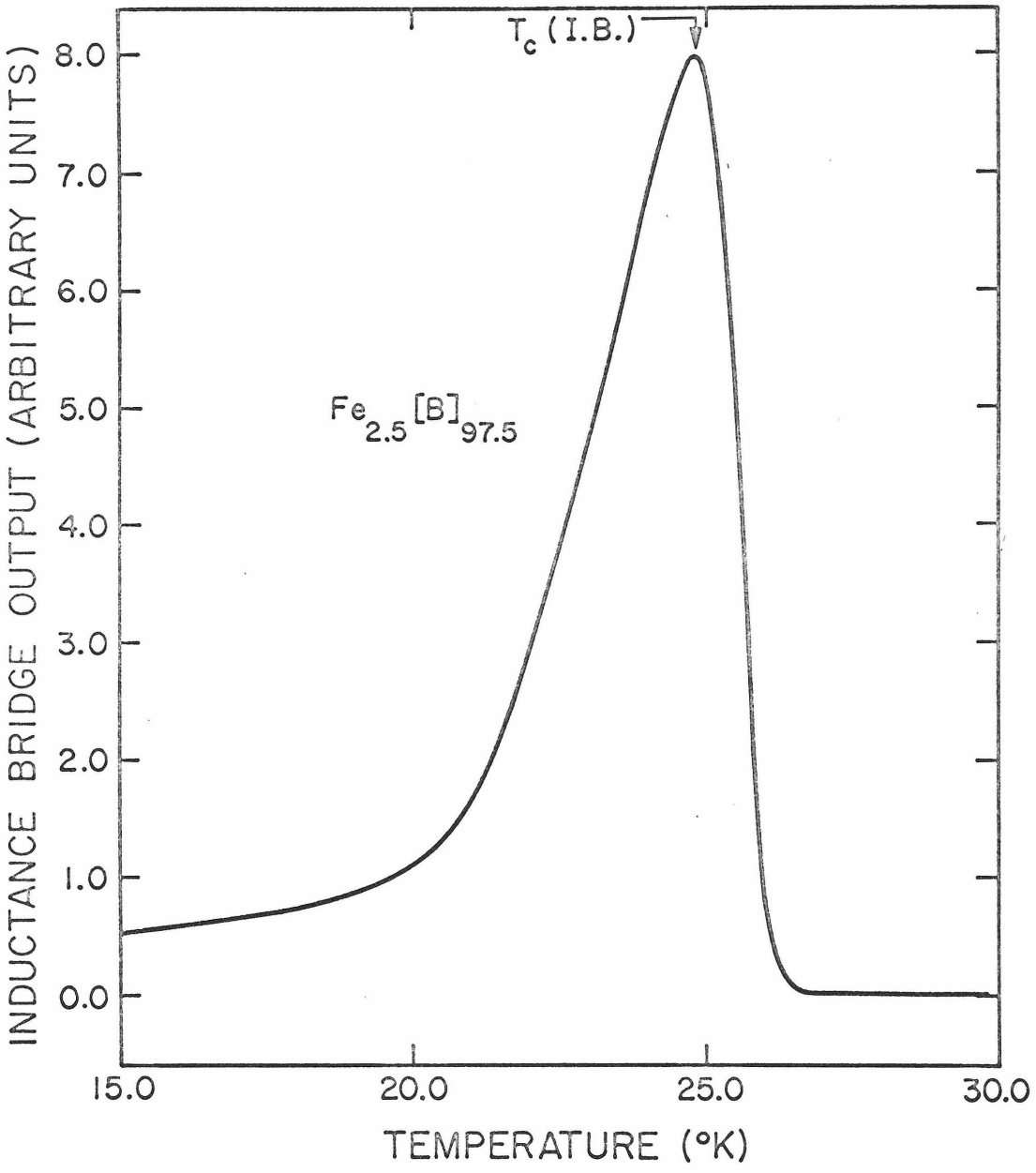

Fig. 22. Output of inductance bridge vs temperature curve for the $Fe_{2.5}[B]_{97.5}$ alloy.

V. DISCUSSION OF RESULTS

A. The Cr[B] System

1. General Discussion

The above brief review of Kondo's and Nagaoka's formulations of the Kondo effect has described several salient features in the resistivity vs. temperature curves for a Kondo system and these will be compared with the experimental results obtained in this investigation.

(1) Kondo predicts that ρ_{sd} should vary as $\ell n\ T$ at low temperature. The usual analysis involves subtracting the host resistivity from the resistivity for samples containing magnetic impurities at corresponding temperatures so as to focus the attention on ρ_{sd}. In Figs. 9 to 12, the raw data ρ are plotted as a function of $\log_{10} T$. It is noticed that the total ρ already exhibit a remarkable $\ell n\ T$ dependence. This suggests that $\rho_{sd} >> \rho_{\text{electron-phonon}}$ over that region where ρ depends linearly on $\ell n\ T$.

(2) As the conduction electrons start to compensate the impurity Cr spin, the Kondo mechanism is expected to begin to be less important. Consequently, the resistivity is expected to be insensitive to temperature. Below $T_{d\ \text{lower}}$, it is noticed that ρ indeed deviates from a $\ell n\ T$ behavior and starts to level off. This behavior is consistent with Nagaoka's spin-compensate-state idea.

(3) Kondo shows that ρ_{sd} and $\rho_{\text{electron-phonon}}$ together give a resistivity minimum. Expecting this phenomenon to occur at low temperature, he assumes that $\rho_{\text{electron-phonon}}$ is proportional to T^5,

which is correct for a crystalline system, like Cu, at low temperature. On this basis, Kondo predicts that T_m is proportional to $c^{1/5}$. Subsequently, several high T_m systems (AuV, $Pd_{80-c}Si_{20}Cr_c$ etc.) [33][34] have been found and the minimum temperatures do not vary according to $c^{1/5}$.

In the present system, the values of T_m for Cr concentrations above 1 at.% lie in the temperature range (above 60°K) where the resistivity of the host alloy, $\rho_{[B]}$, varies linearly with temperature. It should be recalled that $\rho_{[B]}$ arises almost entirely from the electron-phonon interaction. Assuming that the electron-phonon contribution to ρ in the alloy $Cr_c[B]_{100-c}$ (for $4.0 > c > 1.0$) also possesses a linear temperature dependence in this temperature range, and basing on $T_m = (D/nA)^{1/n}$ with $n = 1$, one expects T_m to vary with c in the same way as D does if A is independent of c. A comparison between T_m vs. c and D vs. c (both in Table 2) indicates that they have quite different concentration dependences. This means A, the temperature coefficient of resistivity due to the electron-phonon interaction, has a concentration dependence of its own.

(4) From Fig. 5, it is noticed that one can find a region at high temperature, where ρ is a linear function of T, for $Cr_{0.5}[B]_{99.5}$ and $Cr_{1.0}[B]_{99.0}$. Their slopes can be measured directly. For each of the concentrations shown in Figs. 6 to 8, the minimum region is so broad that no linear in T region is manifest. The coefficient A can be estimated as follows:

$$A = D/T_m \quad (c > 1.0 \text{ at. } \%) \tag{21}$$

The values of D and T_m (for c from 1.5 at.% to 4.0 at. %) in Table 2 have been used to estimate the corresponding values of A, which are listed in Table 3. The measured slopes for $Cr_{0.5}[B]_{99.5}$ and $Cr_{1.0}[B]_{99.0}$ are also included in Table 3 for completeness. The values of A are normalized by the procedure outlined in Section (V.A.3.) and are also listed in Table 3. Fig. 23 shows a plot of normalized A vs. concentration c, and a complicated concentration dependence is seen. This suggests that the addition of Cr impurities to [B] has a significant effect on the electron-phonon scattering process. Since the values of A are lower than that observed in pure [B], the electron-phonon scattering process is probably weaker in Cr[B]. ($\rho_{\text{electron-phonon Cr[B]}} < \rho_{[B]}$). Matthiessen's rule does not hold. Hence, the usual approach of obtaining ρ_{sd} by simple subtraction ($\rho - \rho_{[B]}$) cannot be justified in this system.

2. Fitting the Experimental Data to Hamann's Expression

The emphasis in the resistivity study of a Kondo system should be on ρ_{sd}, the resistivity arising from s-d interaction. To further analyze ρ_{sd}, an attempt was made to fit the experimental data in Figs. 5 to 8 to Hamann's expression for ρ_{sd} given in the brief review of relevant theories in the above. For convenience Equation (24) is repeated here

$$\rho_{sd} = \frac{\rho_0}{2}\left\{1 - \frac{\ln(T/T_K)}{[\ln^2(T/T_K) + S(S+1)\pi^2]^{1/2}}\right\} \qquad (24')$$

TABLE 3

Coefficients of logarithmic temperature dependence and linear temperature dependence for the $Cr_c[B]_{100-c}$ alloys.

Concentration (at.%)	$\Delta\rho/\log_{10}T$ ($\mu\Omega$ - cm)	$\Delta\rho/\ln T$ ($\mu\Omega$ - cm)	$\rho_o/(4S(S+1)\pi^2)^{1/2}$ ($\mu\Omega$ - cm)	Slope A ($\mu\Omega$-cm/^oK)	Normalized Slope A ($\mu\Omega$ - cm/^oK)
$Cr_{0.5}[B]_{99.5}$	0.674	0.293	0.313	0.0130	0.0130
$Cr_{1.0}[B]_{99.0}$	1.174	0.510	0.495	0.0097	0.0097
$Cr_{1.5}[B]_{98.5}$	1.735	0.754	0.756	0.0101	0.0084
$Cr_{2.0}[B]_{98.0}$	1.958	0.850	0.852	0.0078	0.0067
$Cr_{2.5}[B]_{97.5}$	2.148	0.933	0.896	0.0071	0.0059
$Cr_{3.0}[B]_{97.0}$	2.250	0.977	0.931	0.0057	0.0048
$Cr_{4.0}[B]_{96.0}$	2.866	1.245	1.200	0.0046	0.0032

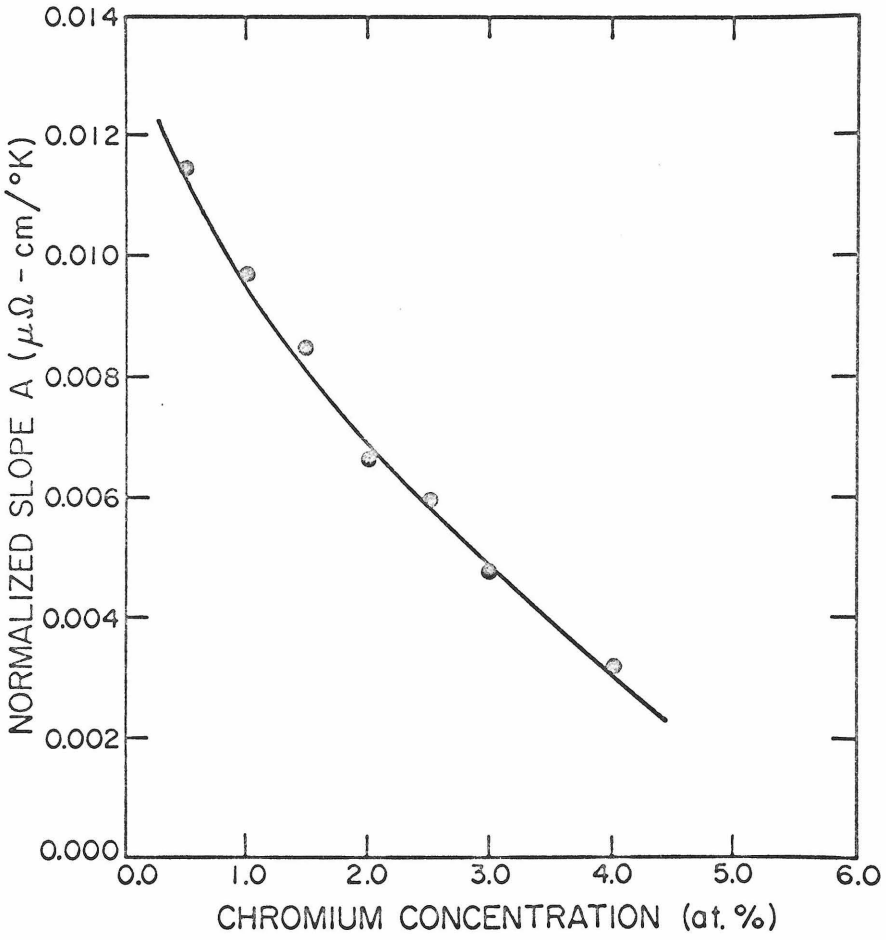

Fig. 23. Normalized linear slope A vs chromium concentration curve for the $Cr_c[B]_{100-c}$ alloys.

There are three parameters ρ_o (the unitarity limit), the Kondo temperature T_K, and the impurity spin value S. The potential scattering background is taken into account by including a temperature independent quantity <B>. In other words it is assumed that $\rho \cong \rho_{sd} + <B>$. By comparison with Equation (18), this essentially means setting $<B> = \rho_r + c\,\rho_A + \langle \rho_{\text{electron-phonon}} \rangle$ = a temperature independent quantity. Strictly speaking, this is correct only for $T < 15^o$ when the temperature dependent electron-phonon interaction is virtually non-existent. However, if the data to be fitted are restricted to the range of $T << T_{min}$ so that $\rho_{sd} >> \rho_{\text{electron-phonon}}$, the assumption is deemed reasonable. This viewpoint is consistent with the observation that the plots of ρ vs. $\log_{10} T$ exhibit well defined linear regions without going through any subtraction procedure as noted in Section (V.A.1.).

The parameters ρ_o, T_K and <B> are varied in order to fit the experimental data for ρ to the Equation (24') using a non-linear least square fit program on the computer. The value of S is also varied. The best fits are achieved with $S = \frac{1}{2}$. The results of fitting are shown in Figs. 24 to 26 for $T < 60^oK$. The circles indicate the experimental curve. The solid lines are the predicted curves based on Equation (24') using the fitted parameters. The agreement seems to be satisfactory. There is a discrepancy at the low temperature end. This is understandable because the Nagaoka approach, on which Hamann bases his calculation, does not treat the ground state correctly.[1] The predicted curves for $Cr_{0.5}[B]_{99.5}$ and $Cr_{1.0}[B]_{99.0}$ fall below the experimental curves as T moves towards the respective minimum tem-

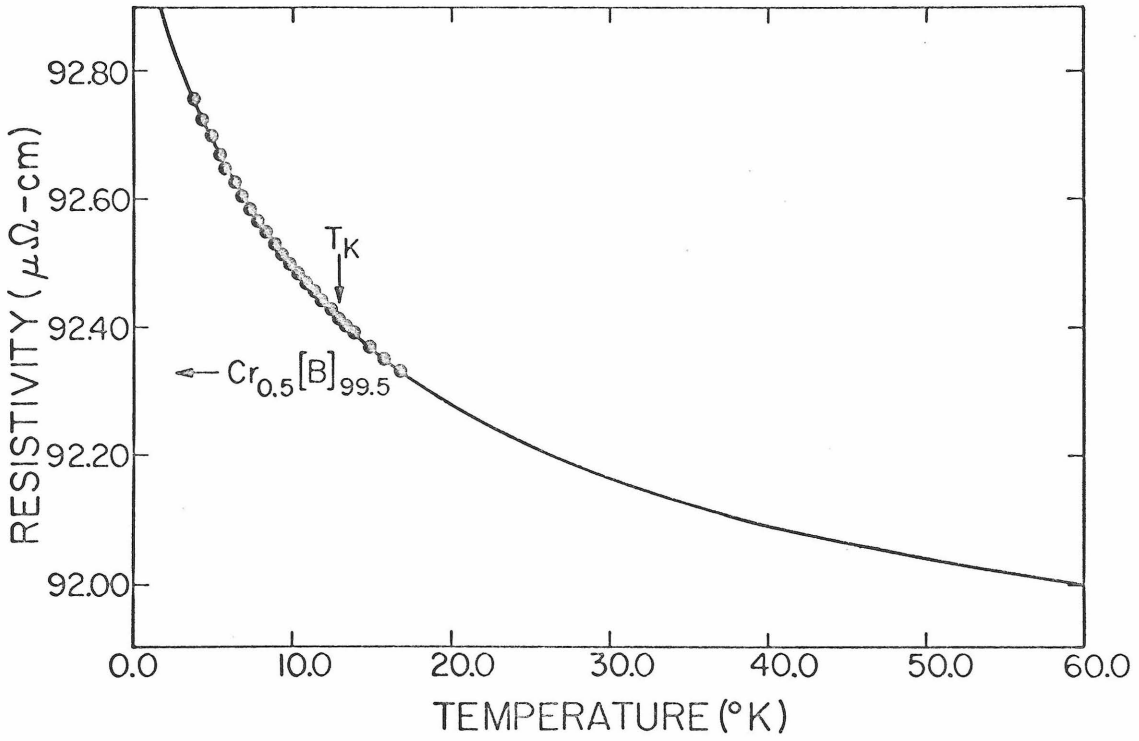

Fig. 24. Comparison of Hamann's theory (curve) with the resistivity data (dots) for the $Cr_{0.5}[B]_{99.5}$ alloy. The arrow indicates the Kondo temperature.

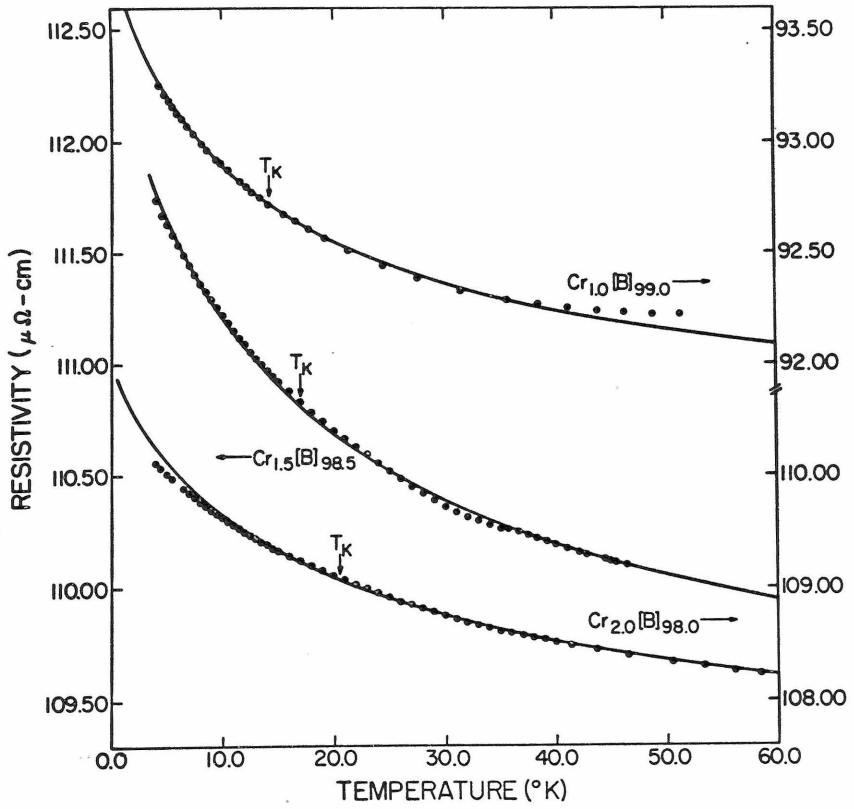

Fig. 25. Comparison of Hamann's theory (curve) with the resistivity data (dots) for the $Cr_{1.0}[B]_{99.0}$, $Cr_{1.5}[B]_{98.5}$ and $Cr_{2.0}[B]_{98.0}$ alloys. The arrows indicate the Kondo temperatures.

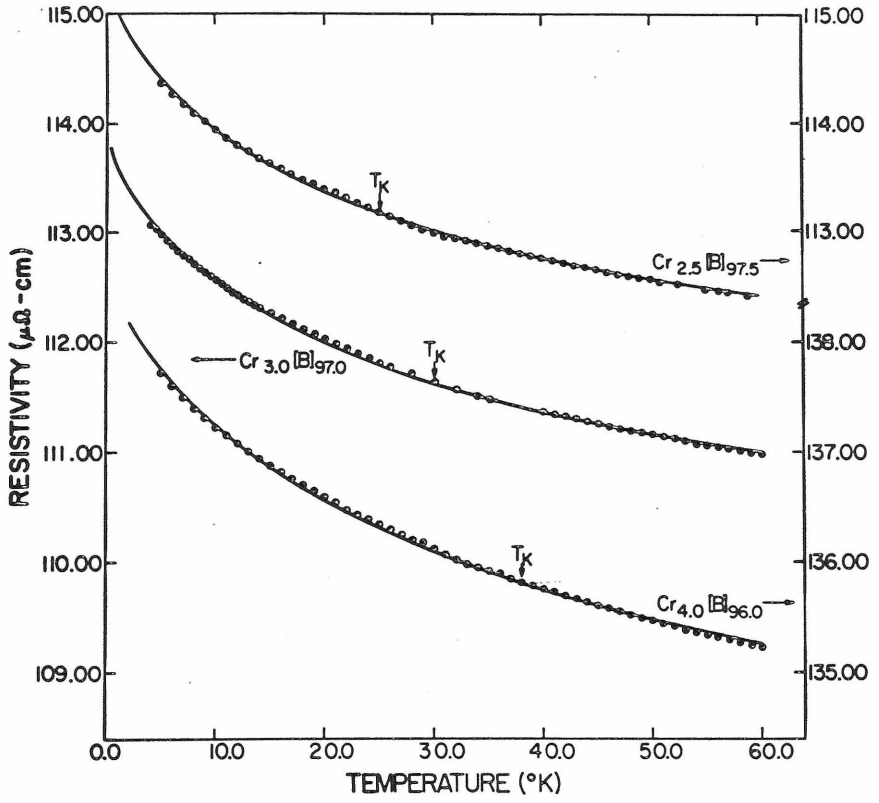

Fig. 26. Comparison of Hamann's theory (curve) with the resistivity data (dots) for the $Cr_{2.5}[B]_{97.5}$, $Cr_{3.0}[B]_{97.0}$, and $Cr_{4.0}[B]_{96.0}$ alloys. The arrows indicate the respective Kondo temperatures.

peratures. This is to be expected because the predicted curve contains only ρ_{sd}. At temperatures which are comparable to the corresponding values of T_m one should add the now important $\rho_{\text{electron-phonon}}$ to the predicted curves in order to obtain the experimental curves.

3. Average Background and Normalization Procedure

The values of $\langle B \rangle$ obtained from the above fitting procedure are listed against their corresponding concentrations c in Table 2. There is a large scatter in the values of $\langle B \rangle$ for the various concentrations. This reflects the uncertainty in the measurement of the thickness for quenched foils. The estimated variation is ± 20% as mentioned earlier in the section on experimental procedure. A closer examination of $\langle B \rangle$ indicates that it may be used as a criterion in normalizing the data for different concentrations. $\langle B \rangle = \rho_r + c\,\rho_A + \langle \rho_{\text{electron-phonon}} \rangle$ where $\langle \rho_{\text{electron-phonon}} \rangle$ = the average electron-phonon contribution to ρ. For the present amorphous alloy, [B], $\rho_r \cong 90\,\mu\,\Omega$ - cm. Between 4°K and 60°K, $\rho_{[B]}$ changes by $\sim 0.5\,\mu\,\Omega$ - cm as can be seen from Fig. 4. It has been noted that this variation is mainly due to the electron-phonon scattering process. In the alloys containing Cr, $\langle \rho_{\text{electron-phonon}} \rangle$ is expected to be $\leq 0.25\,\mu\,\Omega$ - cm since the electron-phonon scattering in Cr[B] is probably weaker than that in pure [B]. The term $\langle \rho_{\text{electron-phonon}} \rangle$ is hence negligible compared to ρ_r. The term $c\,\rho_A$ is the residual resistivity due to the presence of Cr impurities. In crystalline systems, ρ_A the residual resistivity due to per atomic % of impurity $\sim 2\mu\,\Omega$ - cm/at.%[35]. It is expected to be even smaller in amorphous systems. In any case, even in the case of 4 at.% of Cr, $c\,\rho_A$ amounts to $\leq 8\,\mu\Omega$-cm. This is about 9% of ρ_r. To

within 9%, $\langle B \rangle \cong \rho_r$ and one would expect all the $\langle B \rangle$'s to be the same. In order to consider the resistivities for different concentrations on a more comparable basis, the $\langle B \rangle$ of $Cr_{1.0}[B]_{99.0}$ has been chosen arbitrarily to be the standard, and all the other values of $\langle B \rangle$ are normalized to this standard value with proportionate adjustments in their resistivities. Although this criterion still leaves the absolute value of the resistivities uncertain by ± 20%, the relative error from concentration to concentration becomes less than 9%. This will at least ensure that the analysis will yield the correct qualitative dependence on concentration.

4. Concentration Dependence of the Unitarity Limit ρ_o

According to Hamann's expression, ρ_o is the value taken on by ρ_{sd} at T = 0. Hence ρ_o is the unitarity limit. The values of ρ_o for the various concentrations are listed in Table 2. Fig. 27 is a plot of ρ_o vs. concentration. The normalization procedure outlined in section (V.A.3.) has been applied to the values of ρ_o and these corrected values of ρ_o called ρ_o' are plotted in Fig. 28. It should be noted that the qualitative concentration dependence is unchanged while the scatter among the points is reduced. For the lower impurity concentrations, i.e., $Cr_{0.5}[B]_{99.5}$ and $Cr_{1.0}[B]_{99.0}$, the values of ρ_o fall on a straight line passing through the origin. As the concentration increases beyond 1 at.% ρ_o still increases but at a slower rate. From then on ρ_o is no longer proportional to c. From Fig. 28, it is found that $\rho_o = (3.5 + 0.4c)\ \mu\Omega$ - cm, for c > 1 at.%. Beyond 1 at.%, each additional amount of impurity only contributes 40% of its strength to participate in the s-d interaction.

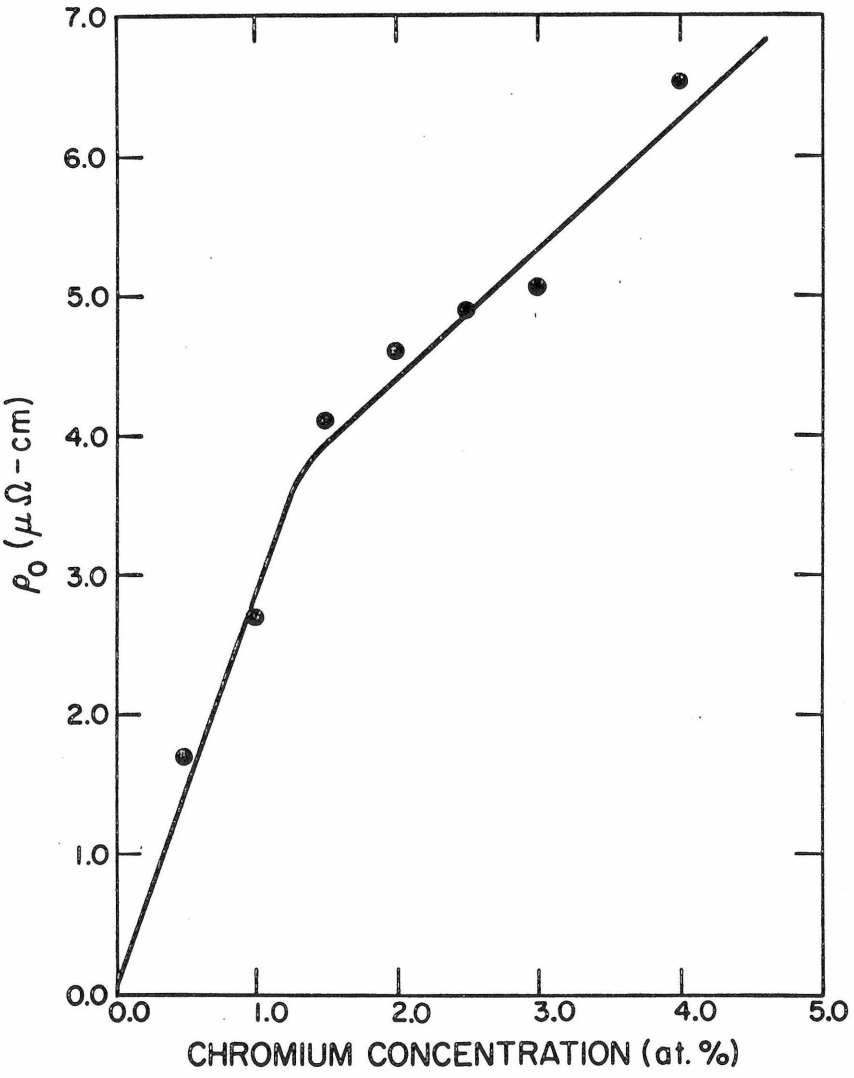

Fig. 27. Unitarity limit ρ_o vs chromium concentration curve for the $Cr_c[B]_{100-c}$ alloys.

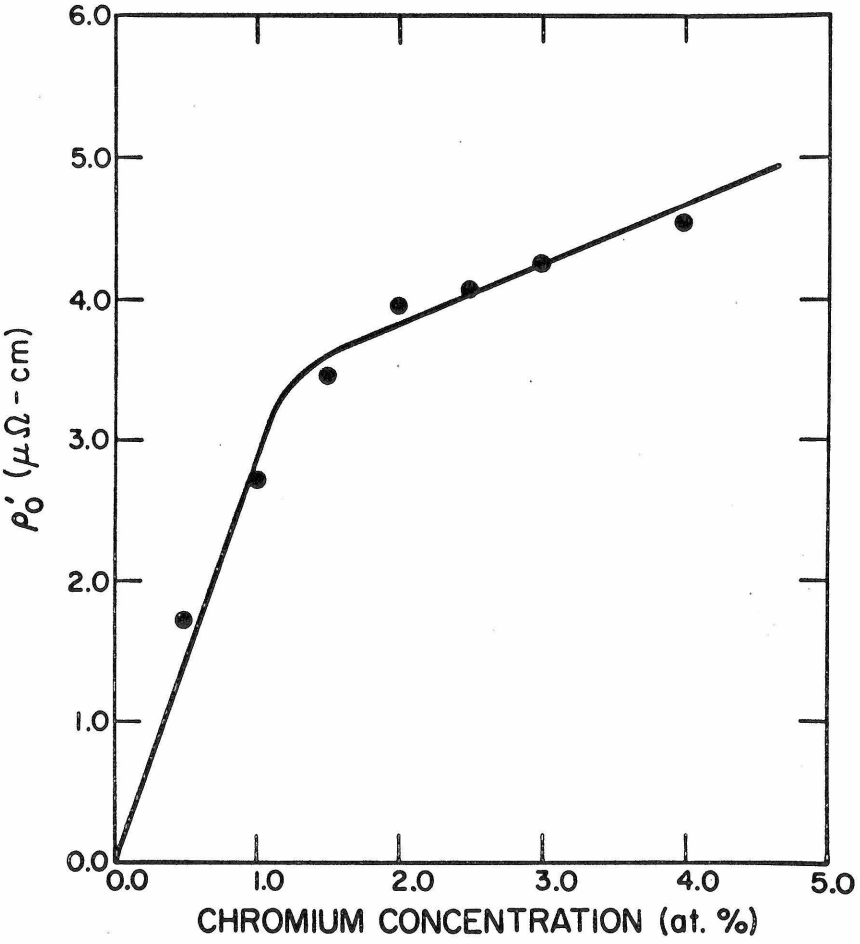

Fig. 28. Unitarity limit (ρ_o') normalized to $Cr_{1.0}[B]_{99.0}$ vs chromium concentration curve for the $Cr_c[B]_{100-c}$ alloys.

Most of the theoretical treatments of the magnetic impurity problem have concentrated on the very dilute case, (in the sense of having no significant correlation effects among the impurity spins), with the result that ρ_{sd} is proportional to c. In particular Hamann predicts that $\rho_o \propto 2\pi c/Ne^2\hbar k_F$ and hence a plot of ρ_o vs. c should go through the origin for dilute systems. From Fig. 28, it is seen that $Cr_{0.5}[B]_{99.5}$ and $Cr_{1.0}[B]_{99.0}$ seem to qualify as dilute systems. This view is supported by the value for ρ_o/at.% based on the most dilute case of $Cr_{0.5}[B]$. The result is ρ_o/at.% = 3.5 $\mu\Omega$-cm/at.%, and compares favorably with the value obtained for a free electron system[36][1].

$$\rho_{o\,free}/at.\% = 3.8(25)\,\mu\Omega\text{-}cm/at.\% \qquad (30)$$

In the present case S = $\frac{1}{2}$ (from best fit) and $\rho_{o\,free}$/ at.% = 3.8 $\mu\Omega$ -cm/at.%. Up to 1 at.%, the impurity spins are relatively independent, although it should be noted that at 1 at.% ρ_o already lies slightly below the line in Fig. 28, suggesting that some minor correlation effects has started. This is the first discrepancy between the theory for dilute alloys and the experimental results for moderate concentrations of impurities.

5. Concentration Dependence of the Kondo Temperature T_K

The values of the Kondo temperature, T_K, obtained from fitting the curves are listed in Table 2 and plotted in Fig. 29 as a function of concentration c. According to all existing theories[14][19][21],

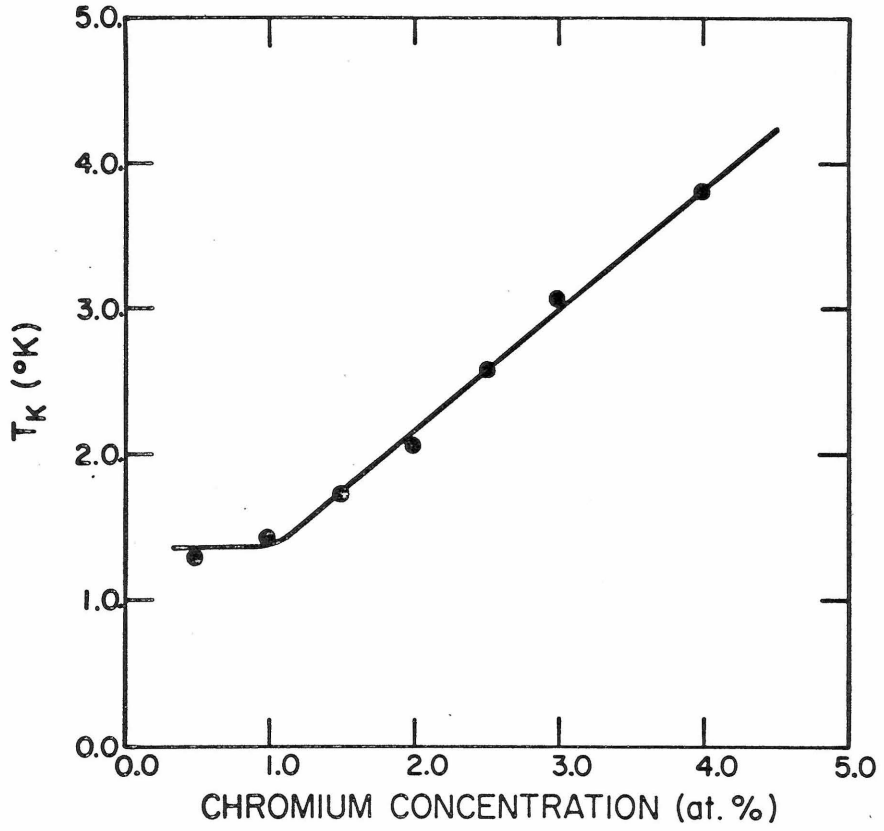

Fig. 29. The Kondo temperature T_K vs chromium concentration for the $Cr_c[B]_{100-c}$ alloys.

T_K is a concentration independent quantity. From Fig. 29, this prediction is consistant with the $Cr_{0.5}[B]_{99.5}$ and $Cr_{1.0}[B]_{99.0}$ results. However, above 1 at. % of Cr, T_K starts rising linearly with concentration. This is another disagreement between the theory developed for the dilute alloys and the experimental findings from the alloys containing moderate amounts of impurities. The values for T_K are not subject to the normalization process.

6. Determination of the Spin Value of Cr in [B]

It has been mentioned that the best fit of the experimental curves to Hamann's expression is achieved with $S = \frac{1}{2}$. For comparison, the data for $Cr_{3.0}[B]_{97.0}$ have been used to fit Hamann's expression again with S = 3/2 and S = 5/2. The results of these fits are shown in Fig. 30. The fit with $S = \frac{1}{2}$ is included again for the sake of comparison. The choice of $S = \frac{1}{2}$ should be self-evident. The experimental value of ρ_o/at.% = 3.5 $\mu\Omega$- cm/at.% is also consistent with $S = \frac{1}{2}$ assuming the free electron system expression of ρ_o/at.% = 3.8(2S) $\mu\Omega$ -cm/at.%.

7. Supporting Evidence from Magnetic Susceptibility

In the interest of gaining some supporting evidence, the magnetization of the alloy $Cr_{3.0}[B]_{97.0}$ has been measured on the magnetometer. It would be interesting to find out if there is any change in the magnetic properties as the temperature goes from above the Kondo temperature T_K to below T_K. This particular alloy has been chosen because it has a relatively high T_K so as to ensure a sufficient number of data points below T_K to define the low temperature part of the $1/\chi$ vs. T curve. From the plot of $1/\chi$ vs. T for $Cr_{3.0}[B]_{97.0}$ in Fig. 14,

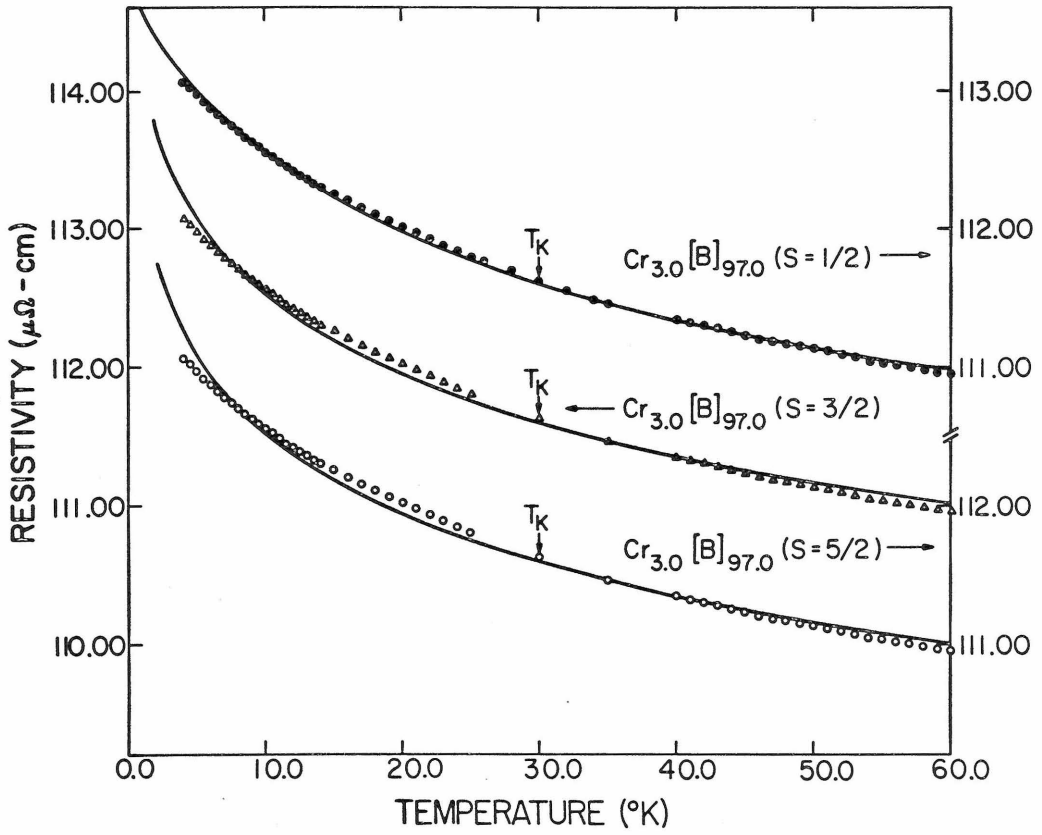

Fig. 30. Resistivity (points) as a function of temperature for $Cr_{3.0}[B]_{97.0}$ compared with Hamann's theorectical expression for S=1/2 , S=3/2 and S=5/2. The arrows indicate the Kondo temperature.

it is clear that $1/\chi$ obeys a Curie-Weiss law at the high temperature end. By the operational definition given in section (III. D.), the presence of localized moment, which has been suggested by the data's good fit to the Kondo-Nagaoka-Hamann theories, is confirmed. Linearly extrapolating the high temperature part of the $1/\chi$ curve to zero gives an intercept at $\theta = -140^{\circ}K$. Employing the empirical rule $\theta = -4.5T_K$ [1], one obtains $T_K = 31.1^{\circ}K$. This is close to the value for $T_K = 30^{\circ}K$ obtained from the resistivity measurement. It has also been noted in Section (IV. B. 3.) that the intercept resulting from the straight line extrapolations of the high and low temperature ends of the $1/\chi$ vs. T curve occurs at $T = 31^{\circ}K$. This temperature is again close to the determined Kondo temperature for $Cr_{3.0}[B]_{97.0}$. It should be emphasized that $1/\chi$ changes smoothly from the low temperature end to the high temperature end in a temperature interval around T_K. This is consistent with the notion of a gradual formation of the spin-compensate-state.

Bearing in mind the difficulty involved in obtaining quantitative data from the present magnetometer, an attempt has been made nevertheless to determine μ_{eff} from the slope of the $1/\chi$ vs. T curve. From Section (III. D.) it is recalled that the slope of the $1/\chi$ vs. T curve is given by $3k/N\mu_{eff}^2 = (2.15 \times 1.292 \times 10^5) / (50.0 \times 4.99)$ gm-Gauss/emu - $^{\circ}K$. This gives μ_{eff}^2 at high temperature $= 16.5\mu_B^2$ which is consistent with $S = 3/2$. Usually this is interpreted as the bare spin value and is in disagreement with the previously determined value of $S = \frac{1}{2}$. However, it may be more tolerable in comparison with the situation in Cr Cu, the most well known Kondo system in-

volving Cr. In that case, from a fit of the low temperature resistivity data to Hamann's expression yields $S = \frac{1}{2}$[1]; from the $1/\chi$ slope, one gets $S = 3/2$[37]; and from the value of ρ_o/at.%, one gets $S = 5/2$[38]. Moreover in the present case the $1/\chi$ vs. T slope at low temperature gives $\mu^2_{\text{eff at low temperature}} = 3.2\ \mu_B^2$. This is consistent with $S = \frac{1}{2}$. It should also be recalled that the data used in fitting Hamann's resistivity expression (from which one gets $S = \frac{1}{2}$) have all been low temperature data. On the other hand, the use of $S = 3/2$ would give ρ_o/at.% = 11.4 $\mu\ \Omega$- cm/at.% (assuming Equation (30)) and is very different from the experimental result of 3.5 $\mu\ \Omega$- cm/at.%. It should be mentioned that the uncertainty in the magnetic susceptibility measurement does not give sufficient confidence in the quantitative results and further similar experiments do not seem advisable at this time.

8. The Meaning of T_K

In the Nagaoka-Kondo formulation, T_K is the temperature below which the perturbational treatment breaks down. It is only above T_K that there is a ℓn T dependence in the resistivity. The energy kT_K is of the order of the quasi-bound state binding energy. Based on Hamann's theory, one finds that T_K is also the parameter which controls the range in temperature over which ρ_{sd} is important. When $\ell n\ (T/T_K) >> \sqrt{S(S+1)}\,\pi$, $\rho_{sd} \to 0$. From the resistivity and magnetic susceptibility results (Figs.24 to 26 and Fig. 14) it is learned that a transition does occur centering at T_K, but the transition is by no means a sharp one like, for example, in type I superconductors. One may say that T_K is the temperature at the centre of a gradual transi-

tion or a quasi-transition. From the good fit that the Hamann resistivity expression gives to the experimental data, one sees that T_K also governs the detailed manner in which ρ goes from the essentially Kondo $\ell n\, T$ regime to the unitarity limit regime. Combining this observation with Nagaoka's conceptual framework one may interpret T_K as the parameter governing the progress of the onset of the spin-compensate-state.

In the case of very dilute magnetic alloys, T_K is constant with respect to concentration. It has long been believed to be characteristic of the host and of the type of magnetic impurity (irrespective of concentration). In view of the present result, a more fundamental interpretation of T_K may be that it measures the s electron compensation of the localized spin which is a basic aspect of the problem. In line with Nagaoka's interpretation, it is a measure of how tightly bound is the resultant quasi-bound state. In this view, T_K characterizes the host and the type of magnetic impurity only in the sense that the s-d interaction is dependent on the host and the type of impurity involved. It may be more appropriate to say that it gives a faithful description of the s-d compensation property of the particular system (concentration dependent) under study. Hence, it is not too surprising that T_K also governs the degree of compensation accomplished at each temperature which in turn is reflected in changes in the electrical resistivity.

9. A Comparison Between the Theories of Kondo and Hamann

In the following, a brief comparison will be made between the Kondo theory and the Hamann theory, both of which give predictions

about the resistivity. On the basis of the experimental data, an attempt will be made to find out which theory is more applicable to describe the experimental results.

(i) The Slope of Logarithmic Temperature Dependence

The ℓn T dependence of the resistivity is the central feature in Kondo's theory. The coefficient of $\log_{10}T$ is a directly measurable quantity from the plots of ρ vs. $\log_{10}T$ in Figs. 9 to 12. Direct measurements yield the slopes $\Delta\rho/\log_{10}T$ in the linear in $\log_{10}T$ region. These slopes can be converted into $\Delta\rho/\ell n$ T by dividing $\Delta\rho/\log_{10}T$ by 2.3 and the results are plotted as a function of c in Fig. 31 (open circles).

Based on Hamann's expression for the resistivity, Equation (24), one can also obtain a logarithmic dependence on T at least at T near T_K. For T near T_K, $\ell n\,(T/T_K)\sim 0$ and the denominator in the second term is dominated by $S(S+1)\pi^2$. In this temperature range, one may write:

$$\rho \cong \rho_0/2\left[1 - \ell n\,(T/T_K)/\sqrt{S(S+1)\pi^2}\right] \qquad (31)$$

Examining the values of T_K determined (Table 1) and comparing the values of $T_{d\ upper}$ and $T_{d\ lower}$ (Table 1) where the resistivity is seen to deviate from a ℓn T dependence, one finds that $\ell n\ T_K$ does fall between $\ell n\ T_{d\ upper}$ and $\ell n\ T_{d\ lower}$. This indicates that the interpretation of Kondo's expression in terms of Hamann's expression

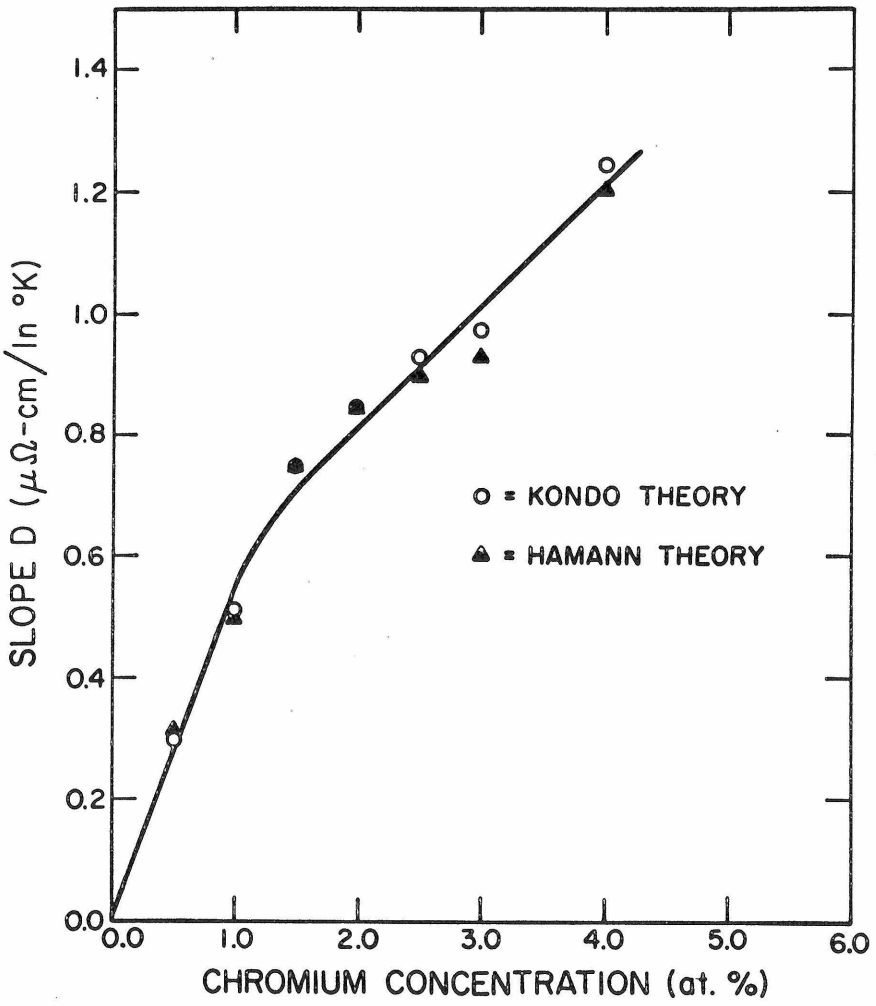

Fig. 31. Slope D vs chromium concentration for the $Cr_c[B]_{100-c}$ alloys.
(o) Kondo theory Slope D = $\Delta\rho/\ln T$
(▲) Hamann theroy Slope D = $\rho_o/(4S(S+1)\pi^2)^{1/2}$

given above is correct. In fact, in this light, the determination of $T_{d\ upper}$ and $T_{d\ lower}$ are, to a certain extent arbitrary. Based on Hamann's expression, as T moves away from T_K, there is a temperature where $\ell n^2(T/T_K)$ is equal to a significant fraction of $S(S+1)\pi^2$, which for $S = \frac{1}{2}$ is ~ 7.4. When this occurs one would observe ρ_{sd} deviating from a linear ℓn T dependence. The arbitrariness involved in determining the values of T_d reflects the arbitrariness in saying when $\ell n^2 T/T_k$ is a significant fraction of $S(S+1)\pi^2$ for the different concentrations by looking at the semi-log plots of ρ vs. T. Of course, if one were perfectly consistent in saying when ρ vs. ℓn T deviates from linearity at the upper and lower temperature ends, $\ell n\ T_K$ should be equal to $\frac{1}{2}(\ell n\ T_{d\ upper} + \ell n\ T_{d\ lower})$. Based on this interpretation of Hamann's expression, one can further say that the slope of the linear portion in a plot of ρ vs. ℓn T should be $\rho_o/(2\sqrt{S(S+1)\pi^2})$. Using the values of ρ_o in Table 2, one can compute the corresponding slope of ℓn T for each concentration c studied. The values of the slopes computed on this basis are listed in Table 3. and plotted in Fig. 31. There is good agreement between the measured slopes and those computed using Hamann's theory. In particular, the change in slope in the plot of slope vs. concentration can be understood. It just reflects the dependence of ρ_o on c. The agreement between the measured slope and the computed slope for each concentration is independent of the normalization process. From this consideration of slopes, one sees that the Kondo theory and the Hamann theory are equally correct.

(ii) Universal Curve Based on Kondo's Theory

For each composition, the minimum resistivity is subtracted from the resistivity at each point and the resulting difference is divided by the slope D of the $\ell n\ T$ term. This quotient is plotted against the corresponding temperature divided by the minimum temperature T_m. The values of T_m, ρ_m and D are listed as a function of c in Table 3. In this plot, the slope D is symbolized by SL. That is: one plots $(\rho-\rho_m)/SL$ vs. T/T_m for each composition. The results are shown in Fig. 32 and Fig. 33. One notices that the graphs do fall on sets of common curves over a certain T/T_m range. One may understand the rationale behind this plot by the following:

$$\text{At } T > 50_oK\text{: } \rho_{\text{electron-phonon}} \sim A\,T$$

Hence from Eq. (19): $\rho = A\,T - D\,\ell n\,T + \rho_r'$ and $T_m = D/A$

In terms of T_m, $\rho = D[\,(T/T_m) - \ell n(T/T_m)] + (\rho_r' - D\,\ell n\,T_m)$

$$\rho_m = D + (\rho_r' - D\,\ell n\,T_m)$$

It is recalled that $D = SL$

Hence $$(\rho-\rho_m)/SL = [\,(T/T_m) - \ell n\,(T/T_m)] - 1 \qquad (32)$$

should be a universal function of T/T_m and independent of c.

The plots in Figs. 32 and 33 deviate substantially from concentration to concentration at the low temperature end. This discrepancy is expected due to the fact that at low temperature, the spin-

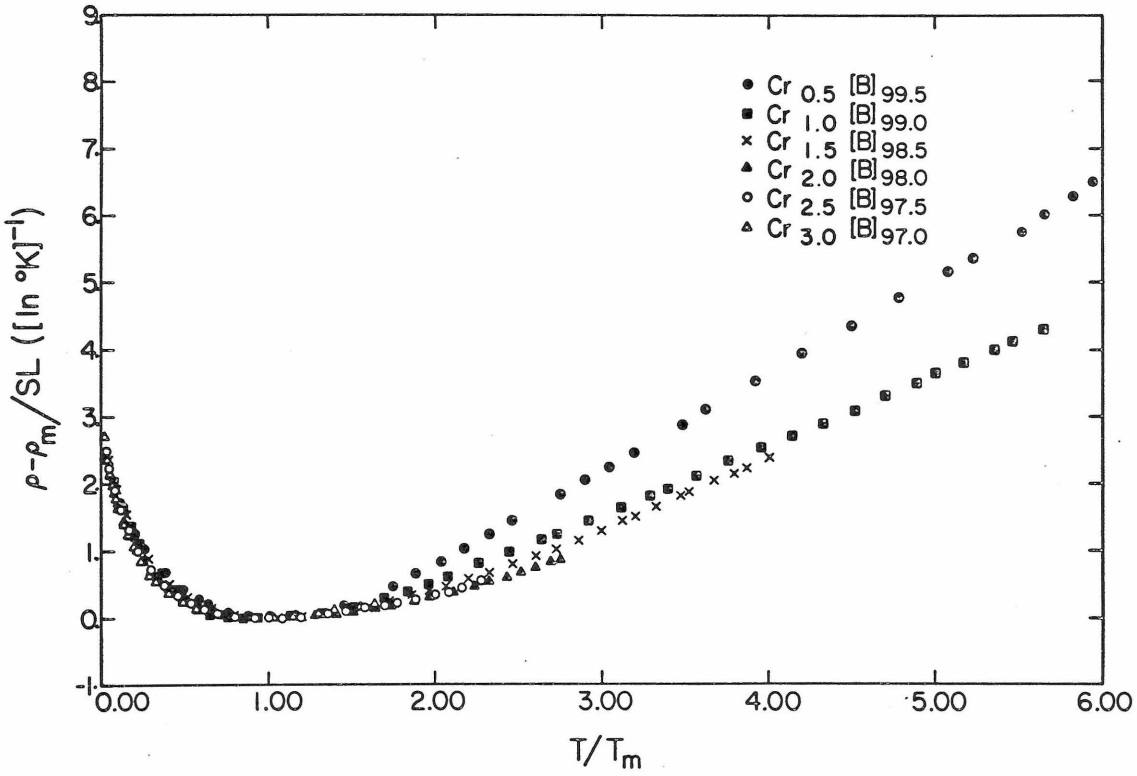

Fig. 32. $(\rho - \rho_m)/SL$ vs T/T_m curves for the $Cr_c[B]_{100-c}$ alloys.

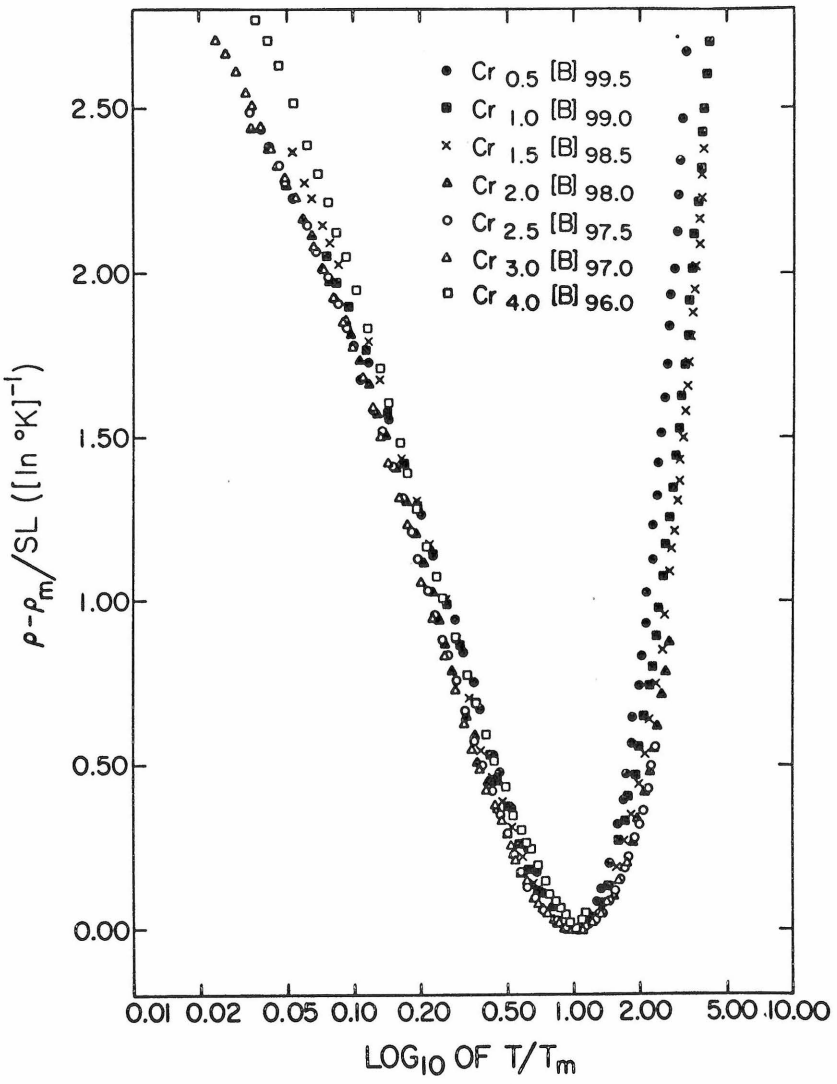

Fig. 33. $(\rho - \rho_m)/SL$ vs $\log_{10}$ of T/T_m curves for the $Cr_c[B]_{100-c}$ alloys.

compensate-state will set in and hence the Kondo ℓn T term is not expected to hold. Moreover, the $\rho_{\text{electron-phonon}}$ term cannot be represented by A T^n with n = 1 anymore. At the high temperature end, the curves do not match up either. The term $\rho_{\text{electron-phonon}}$ is believed to be correctly represented by AT. Hence the observed deviation among the curves in this high temperature range indicates that ρ_{sd} cannot be represented by a ℓn T term. Although the discrepancies are not too pronounced, it should be pointed out that they are not due to any error arising from the uncertainty in the dimension measurements and/or quenching rates. Any such deviations would have dropped out when the quantities $\rho - \rho_m$ are divided by the corresponding slopes. In the region surrounding T_m i.e., $T/T_m \cong 1$, the curves do match up reasonably well, although minor deviations can still be observed. This indicates that the Kondo ℓn T term gives a reasonably good description of the s-d interaction in the temperature range around T_m, even though some minor corrections are still required.

(iii) Universal Curve Based on Hamann's Theory

In Fig. 34, $(\rho - <\beta>)/\rho_o$ is plotted against $\ell n\,(T/T_K)$ for each concentration examined. The values of ρ_o, $< B >$ and T_K are obtained from the nonlinear least square fitting process and are listed in Table 2. The reasoning underlying this plot may be seen from the following: Using Hamann's theory, and assuming the sum of $\rho_{\text{electron-phonon}}$ and the temperature independent part of the resistivity can approximately be represented by a constant $< B >$, as mentioned in Section (V. A. 3.), one may write for

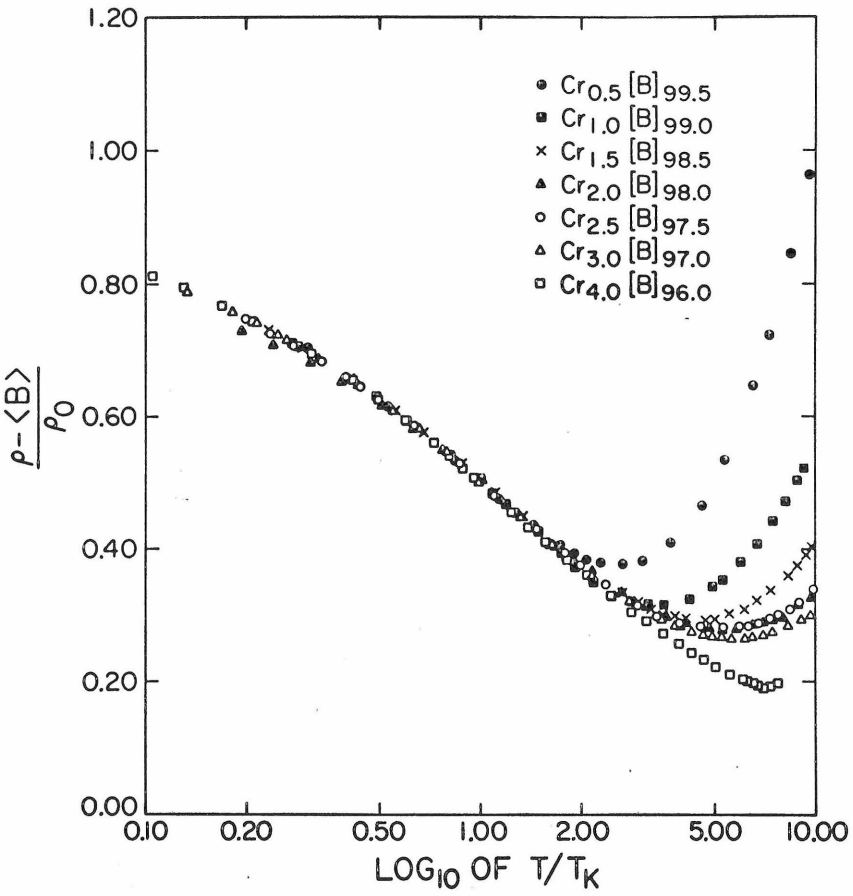

Fig. 34. $\frac{\rho-\langle B\rangle}{\rho_o}$ vs $\log_{10}$ of T/T_K curves for the $Cr_c[B]_{100-c}$ alloys.

$$T \ll T_m \quad \rho = \rho_o/2\left\{1 - \ell n(T/T_K)/\left[\ell n^2(T/T_K) + S(S+1)\pi^2\right]^{\frac{1}{2}}\right\} + <B>$$

Hence

$$(\rho - <B>)/\rho_o = 1/2\left\{1 - \ell n(T/T_K)/\left[\ell n^2(T/T_K) + S(S+1)\pi^2\right]^{\frac{1}{2}}\right\} \qquad (33)$$

It is manifestedly a function of $\ell n\,(T/T_K)$ only. At least based on Hamann's model, one can understand why one may expect a universal curve for $(\rho - <B>)/\rho_o$ vs. $\ell n\,(T/T_K)$. Of course, the plot is actually more general than the Hamann expression, Eq. (24'). From Fig. 34, one does see a universal resistivity curve, which shows that there is at least consistency in the fitting process from concentration to concentration. It gives even more credibility to the quantities ρ_o, T_K and $<B>$ obtained, and strongly suggests that they are actually correct and that the underlying assumptions are reasonable. Furthermore, it should be mentioned that Hamann's expression gives an excellent description of the resistivity even beyond the temperature where a fit has been attempted. The fact that a universal curve for the resistivity is obtained, indicates a significant step forward in the understanding of the magnetic impurity problem. It shows that the Hamann theory has at least the correct parameterization, and very probably even the correct result. It is definitely one step forward from the Kondo expression. On this basis, Hamann's expression is considered to be superior to Kondo's expression.

10. Estimation of the Fermi Energy E_F

From the preliminary measurements on Cr[B], Fe[B], Mn[B], Co[B], V[B], minima are found at least at low concentra-

tions of magnatic impurities. However, it is only in Cr [B] that well pronounced minima are observed. This suggests that well defined moments exist only for Cr in [B], while the other transition element impurities only possess marginal moments in [B]. Based on Friedel's model [8], the Fermi level in [B] has virtually covered both of the split d levels in each of the Fe, Mn, Co, and V cases. This implies that the E_F of [B] is relatively high. It is recalled that Cr, Fe, Mn etc., all show well pronounced minima in Cu. This means that the E_F of Cu (~ 7 ev) still leaves one of the split d levels in Cr, Mn and Fe unfilled. One may suggest that E_F of [B] > E_F of Cu. On the other hand, none of the transition elements retain a moment in Al. The E_F of Al (~ 11 ev) is too high. This suggests that E_F of Al > E_F of [B]. Hence 11 ev > E_F of [B] > 7 ev. As an educated guess, one may set E_F of [B] ~ 8.5 ev.

11. Estimation of the s-d Exchange Integral J_{sd}

According to Kondo's theory, the slope (per atomic %) of the ℓn T dependence in the resistivity is given by

$$\text{Slope/at.\%} = \frac{9\pi m Z S(S+1)}{2e^2\hbar E_F^2}\left(\frac{V}{N}\right)|J_{sd}|^3 \qquad (20)$$

where m = mass of electron;

Z = the number of conduction electrons per atom;

N = the total number of atoms in the sample;

V = the total volume of the sample;

E_F = the Fermi energy;

and J_{sd} = the s-d exchange integral.

According to Fig. 31, this slope is 5.5×10^{-7} Ω - cm/at.%. With $E_F \sim 8.5$ ev, $m = 5.1 \times 10^5 \frac{ev}{C^2}$, $S = \frac{1}{2}$, $Z = 1.33$ and $\frac{N}{V} = 8.4 \times 10^{22}$/c.c., one obtains J_{sd} for Cr in [B] = -0.36 ev.

12. Simple Physical Model and the Estimation of the Polarization Cloud Radius ξ

From the experimental result of the unitarity limit as a function of c, it is learned that between 1 at.% to 1.5 at.% of Cr impurity, the curve changes slope (see Fig. 28). This signals the onset of interaction between the impurities. Some insight concerning this may be gained from the following simple model. Following the suggestion of Kohn et. al.[39], the situation is depicted schematically in Fig. 35a. Each big arrow indicates the Cr impurity. The surrounding cloud of s electrons have spins pointing in the opposite direction as a result of the resistivity minimum phenomenon requires as a prerequisite J_{sd} negative. This is consistent with Nagaoka's quasi-bound state picture with the conduction electron spins cooperatively compensating the impurity Cr spin. For c < 1 at.% each Cr impurity spin is surrounded by its full demand of space filled with s electrons pointing in the opposite direction. As the impurity concentration increases, eventually it will get into the situation depicted in Fig. 35b. The electron spheres begin to touch. The impurity Cr spins are depicted as pointing in opposite directions. This reflects the tendency of Cr atoms to couple antiferromagnetically. It is suggested that the electrons in the double-shaded regions would not know which direction they should align with. The Cr atom I wants them to point up; the Cr

s electron polarization cloud
about a "Cr-impurity"

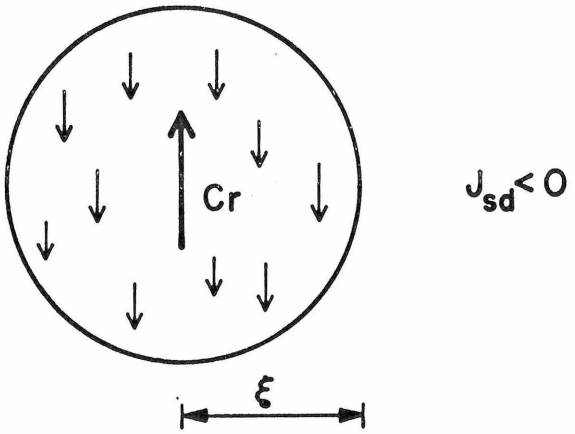

(a)

Cancellation of s electron polarization
in the overlap region (double-shaded)

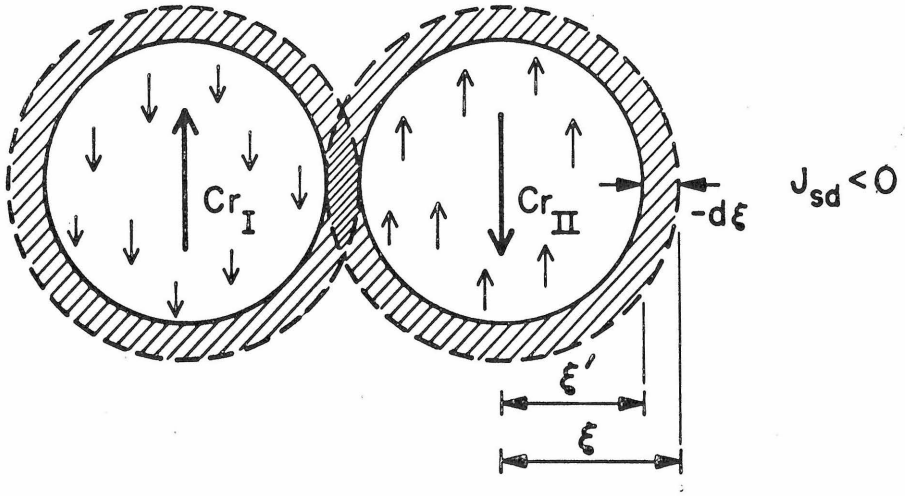

(b)

Fig. 35. The proposed model applied to the $Cr_c[B]_{100-c}$ alloys.

atom II wants them to point down. As a result, the electrons in the double-shaded region would align with neither. Hence the effective s electron cloud around the impurity spin is essentially confined to a sphere of radius $\xi' < \xi$.

Following Heeger [1] and Nagaoka [14], one may make an order of magnitude estimate in the following way. The electrons are confined to a region of space 2ξ. Based on the uncertainty principle, in order to build up a wave packet of spacial dimension 2ξ, there must at least be a momentum spread $\Delta p = \hbar\, \Delta k \geq \hbar/2\xi \Rightarrow \Delta k \gtrsim 1/2\xi$. When the quasi-bound state is formed, with energy of the order of kT_K, the available spread in momentum is usually estimated as $\Delta k \cong (kT_K/E_F)k_F$. As ξ is decreased, it will need a correspondingly larger spread in momentum in order to confine the electrons to the smaller space parameterized by ξ'. If it is assumed that k_F and E_F remain substantially constant as the concentration c is changed it would imply that T_K must increase after the effective spheres start touching. From the results that both ρ_o' and T_K vs. c change slope at $c \sim 1.2$ at.% one may conclude that the critical 2ξ is equal to ~ 13.5 Å. This is much smaller than the theoretical estimate of 1000 Å based on $2\xi \sim [(kT_K/E_F)k_F]^{-1}$. However, it is in order of magnitude agreement with the estimate of the extent of the quasi-spin density in Fe Cu based on NMR work.[40] Golibersuch and Heeger have estimated that the quasi-spin density, which contributes to the susceptibility, resides in a region of space less than 9 Å from the impurity.[40] Since the estimate of ξ given in the above is off numerically, a better estimate is called for.

It is suggested that the discrepancy arises from an incorrect estimate of Δk. The quantity Δk should reflect the basic scattering process in the following sense. If an electron starts out initially on the Fermi surface with energy E_F and momentum $\hbar k_F$, after one scattering, its change in momentum should be of the order of $\Delta k \sim$ Interaction Energy $\times (k_F/E_F)$. In the present case of the magnetic impurity problem, $\Delta k \sim (|J_{sd}|/E_F)k_F$. This may be seen as follows: Initially, one may write $(\hbar k_F)^2/2m = E_F$. After one scattering process, one has

$$[\hbar(k_F + \Delta k)]^2/2m = E_F \pm |J_{sd}|$$

$$(\hbar^2/2m)(k_F^2 + 2k_F \Delta k + \Delta k^2) = E_F \pm |J_{sd}|$$

Neglecting $(\Delta k)^2$,

$$k_F \Delta k/m \cong \pm |J_{sd}|/\hbar^2$$

$$\left.\begin{aligned} \Delta k_+ &= (m|J_{sd}|)/(\hbar^2 k_F) \\ \Delta k_- &= -(m|J_{sd}|)/(\hbar^2 k_F) \end{aligned}\right\} \Rightarrow \Delta k = (|J_{sd}| k_F)/E_F \qquad (34)$$

Hence $$2\xi \gtrsim 1/\Delta k \sim E_F/(k_F|J_{sd}|) \qquad (35)$$

With $E_F = 8.5$ eV, $|J_{sd}| = 0.36$ eV, one ends up with $2\xi \gtrsim 11$ Å. This estimate agrees very well with the experimentally determined value of 13.5 Å.

An alternate simple physical picture which explains T_K's dependence on concentration may be obtained from the following. Suppose one starts out with spheres of extent ξ as shown in Fig. 35a. Based on Nagaoka's theory that the bound state energy is of the order of kT_K, one may say that the energy arising from the quasi-bound state per impurity-s electron cloud is $U = -A\,kT_K$. The coefficient A is a positive constant. The simplifying assumption that the quasi-bound state energy U is distributed uniformly over the sphere ξ will be made. Hence, energy/unit volume $= U/(4/3)\pi\xi^3 = -AkT_K/(4/3)\pi\xi^3$. When the spheres touch, the electrons in the double-shaded region will not align along either Cr impurity. In fact they become unbound. The amount of work required to free the previously bound electrons in the region $(-d\xi)$ about ξ will be:

$$\Delta W = 4\pi\xi^2(-d\xi)\times(\text{energy/unit volume})$$
$$= 3\,Ak\,T_K\,d\xi/\xi$$

This is the amount of energy expended in order to make the electrons in $d\xi$ free from the quasi-bound state. At low temperature, assuming that the band structure and the Fermi level remain constant when the concentration is varied, it is believed that the only source of energy is the quasi-bound state itself. Based on energy balance, one may write

$$U(\xi-d\xi) = U(\xi) - 3\,AkT_K\,d\xi/\xi$$
$$U(\xi) - d\xi(dU/d\xi) = U(\xi) - 3\,AkT_K d\xi/\xi$$
$$-[d(-AkT_K)/d\xi]d\xi = -3\,AkT_K d\xi/\xi$$
$$d\,T_K/d\xi = -3\,T_K/\xi$$

$$d\,T_K/T_K = -\,3d\xi/\xi$$

After the spheres touch $T_K \propto T_{Ko}/\xi^3$ where T_{Ko} = the Kondo temperature before the spheres touch, and one expects $\xi^3 = V/c$ where V is the volume of the sample. Hence the end result becomes

$$T_K \propto T_{Ko}c \text{ for } c \geq 1.2 \text{ at.}\% \tag{36}$$

This linear dependence on concentration agrees very well with the experimental results (see Fig. 29).

It should be emphasized that no assumption is made to the effect that all the quasi-bound state energy resides in the conduction electrons. Since [B] is a polarizable host, (see the discussion on Fe[B] in Section (V.B.13.)), the Cr impurity may very well polarize a considerable number of surrounding host atoms having d holes. Conduction electrons are still expected to compensate around this impurity-host holes composite. The simple contention that electrons in the double-shaded region will not know which way to align and hence become free, applies equally well to the s and the d electrons. Moreover, the actual polarization p(r) does not have a sharp cut-off at ξ. Rather, the polarization p(r) is expected to vary as $\sim(\sin k_F r/k_F r)^2$ [14]. Hence ξ in our simple model would correspond to the distance from the origin to the first minimum or the second mimimum in the polarization cloud.

B. The Fe[B] System

1. General Discussion

The slight minima observed for low Fe concentrations are suspected to be a manifestation of the Kondo effect arising from the Fe impurities in the host [B]. It should be recalled that $\rho_{[B]}$ also exhibits a minimum. The contention that these minima are indeed due to Fe impurities is consistent with the observation that the depth of the minimum in $\rho_{VHP[B]}$ (99.9987 % Fe free) is greatly reduced (see Fig. 4). A systematic analysis of this Kondo effect along the line of analysis for Cr[B]is impossible. The available data barely show the regions around the minima. Any determination of ρ_o and T_K will be quite inaccurate. However, T_K is presumably $<<4^oK$. A systematic change of T_m with Fe concentration is not seen nor expected because at this temperature range (below 15^oK), ρ_{sd} is the only temperature dependent contribution to the resistivity. The present minimum just indicates the onset of the electron-phonon contribution to the resistivity. The absence of the minimum in the ρ vs. T curves for 0.6 at.% $\leq c \leq$ 1.0 at.% of Fe indicates that the ρ minimum effect has been cut off when $c \geq 0.6$ at.%. The behavior of the ρ vs. T curves in the concentration range 1.5 at. % $\leq c \leq$ 4.0 at.% is very similar to that for systems undergoing Curie transitions. They will be analyzed in greater details. In subsequent discussions, the transition temperature will be determined from the temperature derivative of resistivity, in which case it is specified as $T_c(R)$. It is also determined from the inductance bridge measurements in which case it is symbolized by $T_c(I.B)$. The symbol T_c will be used to denote the

transition temperature in general. If a distinction is required for exactness, T_c will be specified as either $T_c(R)$ or $T_c(I.B.)$.

2. The $T^{3/2}$ Dependence of ρ, Background and Normalization Procedure

Well below T_c, the temperature dependence of ρ obeys the $T^{3/2}$ law. In order to make this point manifest, ρ has been plotted against $T^{3/2}$ for a few representative concentrations in Figs.36 to 38. At the lower temperature end, the points do fall on a straight line. This is in complete accord with the predictions of Turner and Long. According to their theoretical approach, at $T << T_c$,

$$\rho \cong \rho_r + c\rho_A + D'_{Fe}\, T^{3/2}/\sqrt{c} \qquad (27)$$

where ρ_A and D'_{Fe} are constants independent of temperature and c is the concentration. The quantity ρ_r is the residual resistivity of the host. As mentioned in the review of relevant theories, Turner and Long have shown that there are three contributions to the $T^{3/2}$ term. In particular, due to the lack of periodicity in the impurity-d hole system resulting in the non-conservation of momentum, the s electron spin-flip scattering from the coupled impurity-d band system gives rise to a $T^{3/2}$ contribution. This is expected to be even more applicable in the present system where the host [B] is an amorphous alloy.

The coefficients of the $T^{3/2}$ term D_{Fe} (let $D_{Fe} = D'_{Fe}/\sqrt{c}$) are listed as a function of concentration in Table 4. Extrapolating the ρ vs. $T^{3/2}$ plots to $T^{3/2} = 0$ yields the value of $\rho_r + c\rho_A = R$. As in the Cr[B] system, due to the inaccuracy in the thickness determination, the ab-

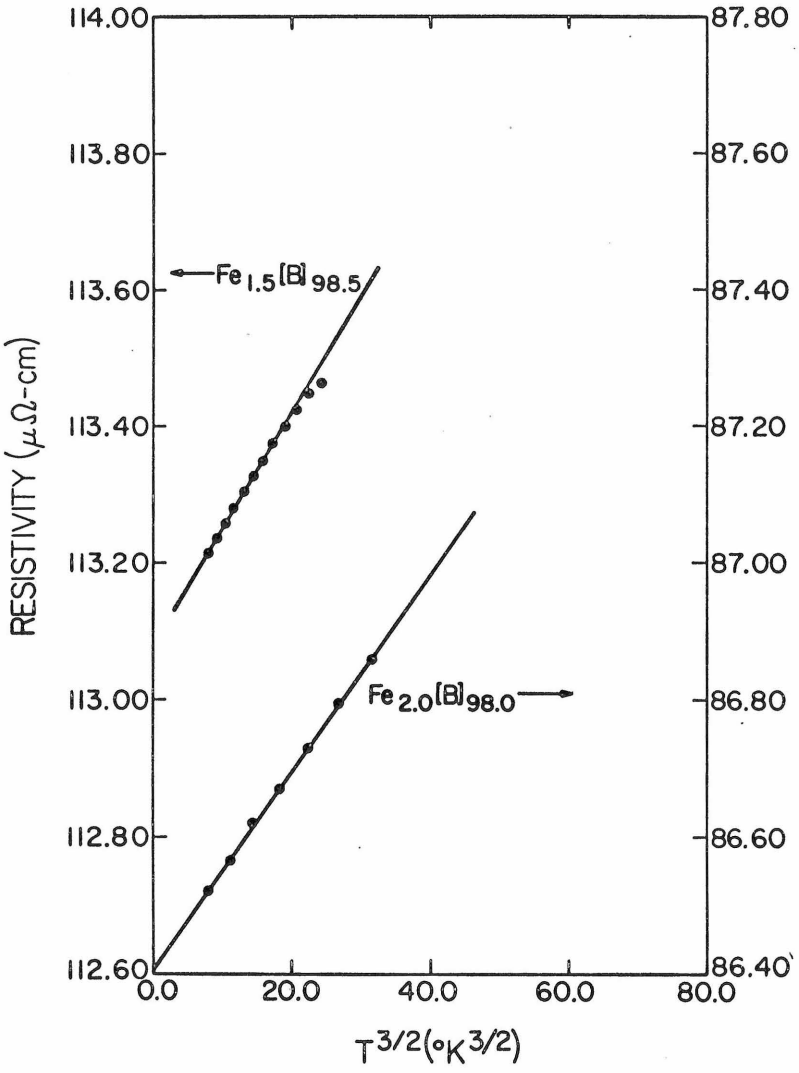

Fig. 36. Resistivity vs $T^{3/2}$ curves for the $Fe_{1.5}[B]_{98.5}$ and $Fe_{2.0}[B]_{98.0}$ alloys.

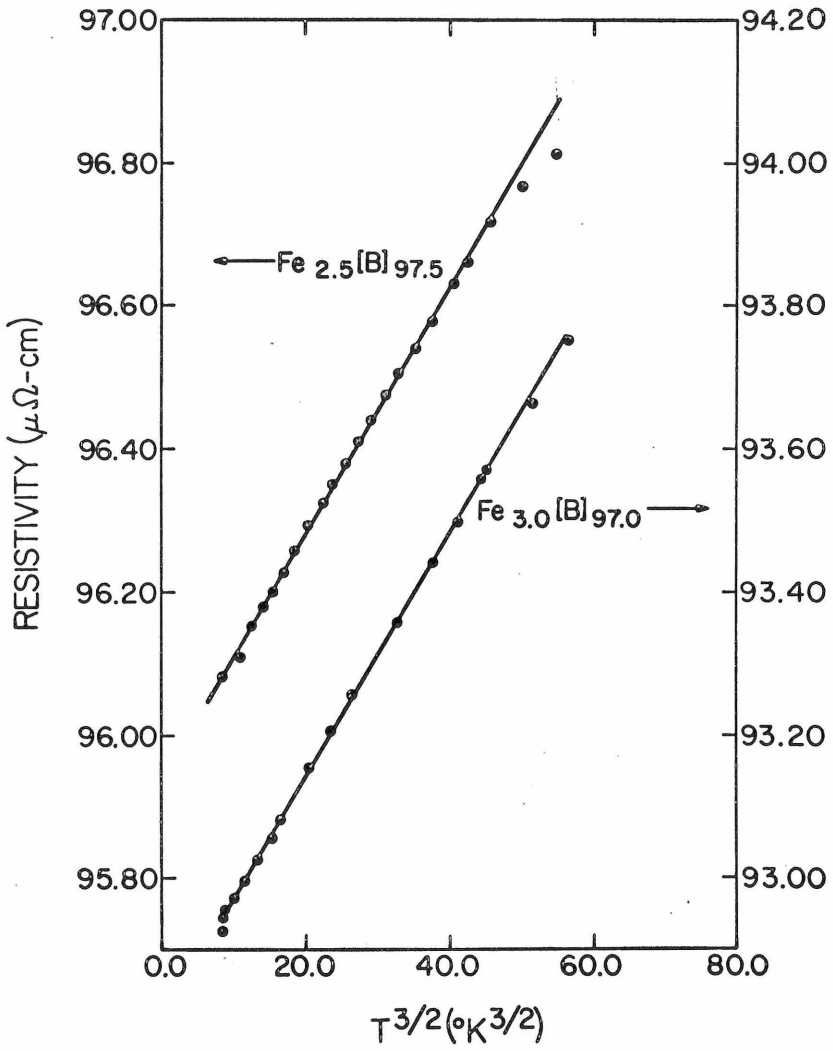

Fig. 37. Resistivity vs $T^{3/2}$ curves for the $Fe_{2.5}[B]_{97.5}$ and $Fe_{3.0}[B]_{97.0}$ alloys.

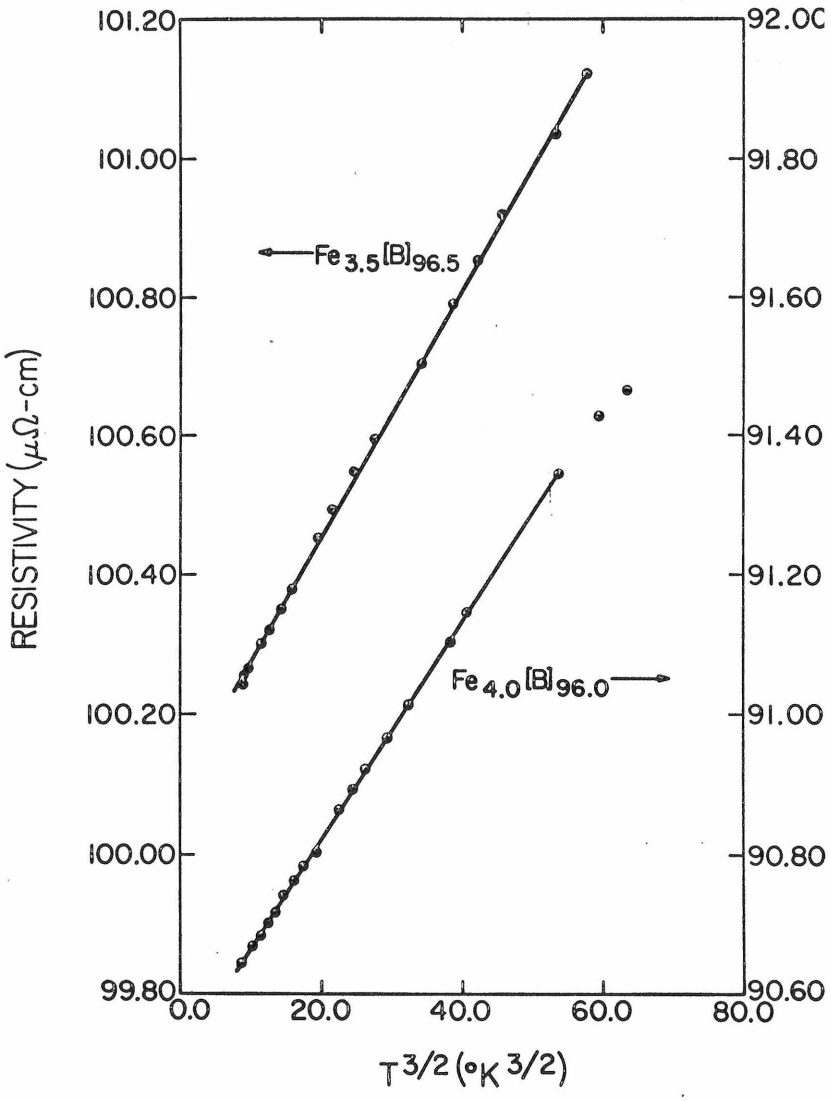

Fig. 38. Resistivity vs $T^{3/2}$ curves for the $Fe_{3.5}[B]_{96.5}$ and $Fe_{4.0}[B]_{96.0}$ alloys.

TABLE 4

Results from the analysis of resistivity of the $Fe_c[B]_{100-c}$ alloys.

Concentration (at.%)	R ($\mu\Omega$ - cm)	Slope of $T^{3/2}$ ($\mu\Omega$ - cm/$^oK^{3/2}$)		Linear Slope Below T_c ($\mu\Omega$ - cm/^oK)	High Temperature Slope ($\mu\Omega$ - cm/^oK)
		Non-Normalized	Normalized	Normalized	Normalized
$Fe_{1.5}[B]_{98.5}$	113.08	0.0185	0.0142	0.0474	0.0163
$Fe_{2.0}[B]_{98.0}$	86.41	0.0143	0.0143	0.0719	0.0170
$Fe_{2.5}[B]_{97.5}$	95.59	0.0176	0.0159	0.0833	0.0155
$Fe_{3.0}[B]_{97.0}$	92.80	0.0172	0.0161	0.0896	0.0164
$Fe_{3.5}[B]_{96.5}$	100.10	0.0180	0.0155	0.0899	0.0166
$Fe_{4.0}[B]_{96.0}$	90.51	0.0157	0.0150	0.0926	0.0163

solute values of the resistivities are uncertain by $\pm$ 20%. However, ρ_r should be identical in the various samples, and hence it can be used as a basis for normalization. Assuming that the term $c\rho_A$ is small compared to ρ_r, one may set all the values of R equal and normalize the corresponding quantities in each concentration accordingly. The R for $Fe_{2.0}[B]_{98.0}$ has been chosen arbitrarily as the standard. This will provide us with a common basis for comparing the different interesting quantities as a function of concentration.

In order to see if this assumption is plausible, an estimate will be made using the values of ρ_A for the crystalline case as guidelines. In Fe Pd, $\rho_A \sim 1.9$ uΩ-cm/at.%. In Co Pd, $\rho_A \sim 1.4$ μ Ω-cm/ /at.%[35]. In the present case, ρ_A will be taken to be $\sim 2\mu$ Ω-cm/ /at.%. Since $\rho_r \sim 90\mu$ Ω-cm, the maximum error (2μ Ω-cm x 4) involved in setting $R \cong \rho_r$ will be less than 10%. Hence, the normalized results are expected to be correct to within 10%. Due to the fluctuations in the quenching rates and the uncertainties in impurity concentrations, this is about the accuracy one may expect from these experiments. All the relevant quantities discussed in connection with the Fe[B] system have been thus normalized. In particular, the normalized values of D_{Fe} are also listed in Table 4 and are plotted as a function of concentration in Fig. 39. They are found to be substantially independent of concentration with the value $\sim 1.55 \times 10^{-8}$ Ω-cm/$^oK^{3/2}$.

3. Linear T Dependence Below T_c

Assuming the molecular field theory to be valid at $T < T_c$, Long and Turner have predicted that ρ should depend linearly on T. This is substantiated by the present experimental results. The linear slopes

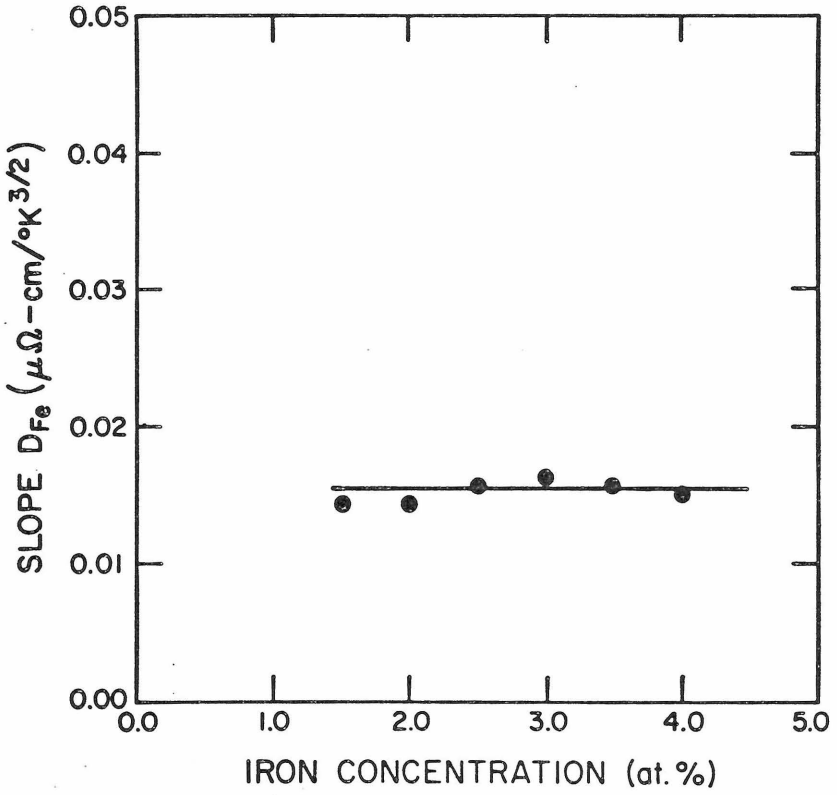

Fig. 39. Slope D_{Fe} vs iron concentration for the $Fe_c[B]_{100-c}$ alloys.

are again normalized and tabulated in Table 4. They are plotted against the Fe concentrations in Fig. 40. It should be noted that they are concentration dependent, being approximately $5 \times 10^{-8}\Omega$-cm/^{o}K for $Fe_{1.5}[B]_{98.5}$, and saturating at approximately $9 \times 10^{-8}\Omega$-cm/^{o}K for the alloys $Fe_{3.0}[B]_{97.0}$ to $Fe_{4.0}[B]_{96.0}$. Although the temperature dependence is correctly predicted by the theory, the more detailed feature of concentration dependence is not confirmed. The theory predicts that the coefficients of the linear temperature dependence should be independent of concentration.

4. Linear T Dependence at High Temperature; Matthiessen's Rule

The ρ vs. T. curves all have a linear temperature dependence at the high temperature end. The slope for each concentration has been normalized by the procedure mentioned in Section (V. B. 2.). These normalized slopes are listed in Table 4 and plotted in Fig. 41, as a function of concentration. The values of these slopes fall in the neighborhood of $1.65 \times 10^{-8}\Omega$-cm/^{o}K. As a comparison, the high temperature slope of [B] (1.59×10^{-8} Ω-cm/^{o}K) is also included. This discrepancy is within the uncertainty involved in the slope determination, and one may say that the high temperature slope is concentration independent. Contrary to the findings in the Cr[B] system, Matthiessen's rule seems to hold in the Fe[B] system.

5. $\Delta\rho$ vs. T

Since Matthiessen's rule seems to hold, an attempt has been made to subtract the normalized $\rho^{N}_{[B]}$ from the normalized $\rho^{N}_{Fe[B]}$.

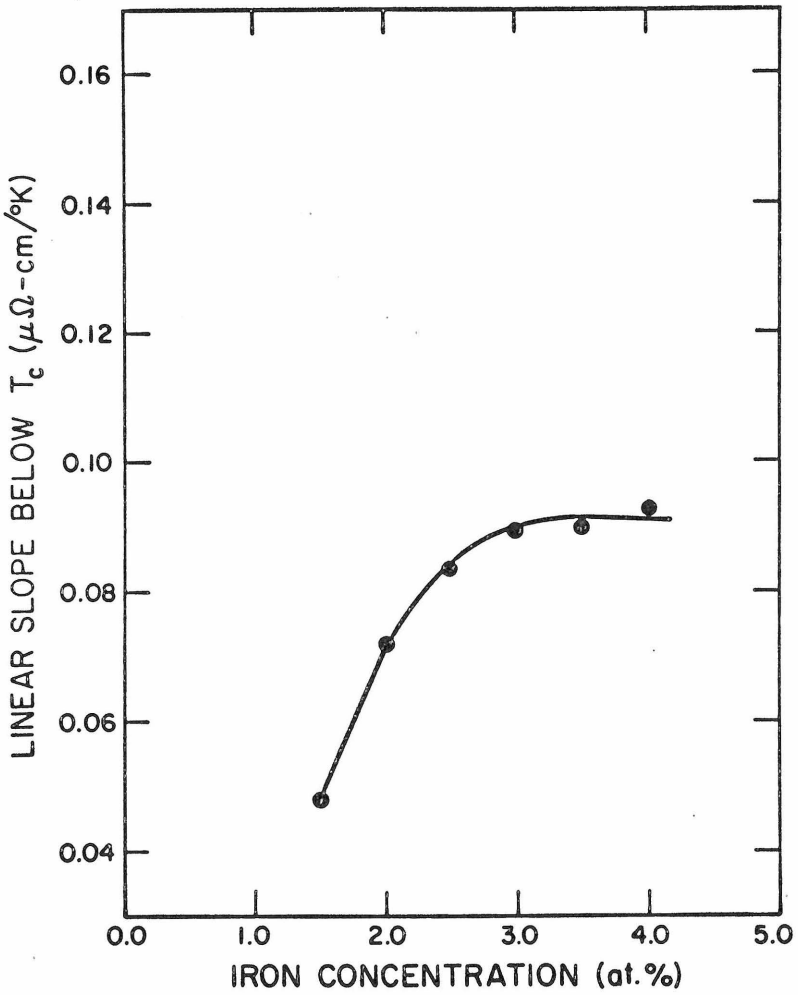

Fig. 40. Linear slope below T_c vs iron concentration curve for the $Fe_c[B]_{100-c}$ alloys.

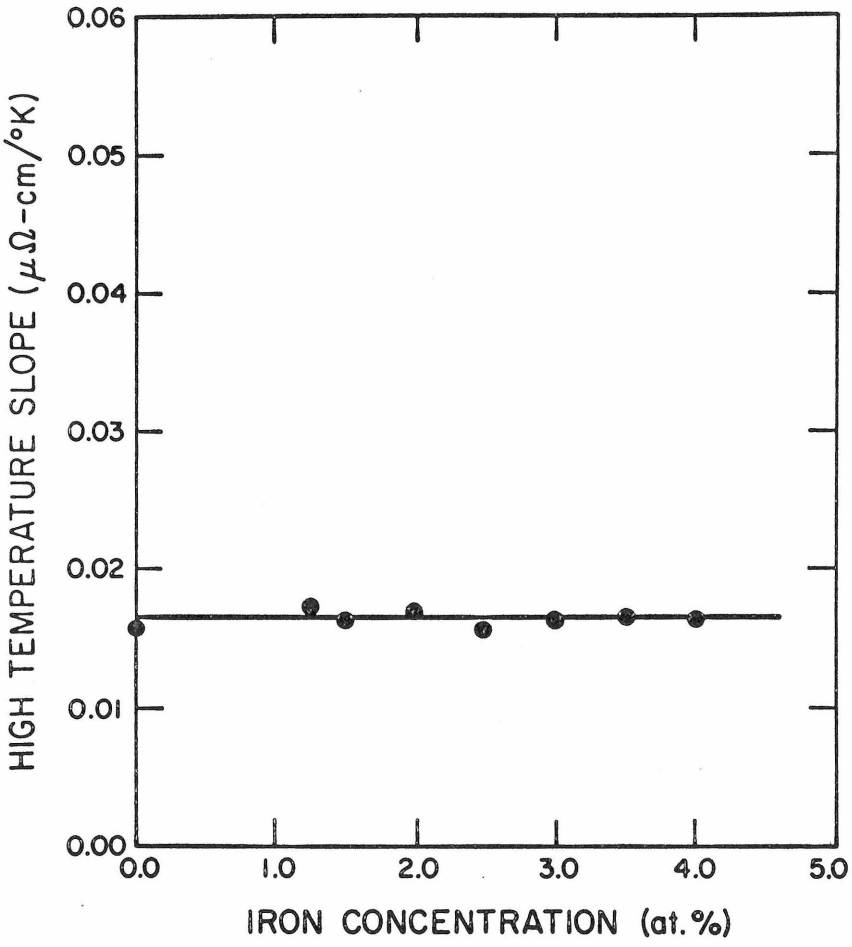

Fig. 41. High temperature slope vs iron concentration for the $Fe_c[B]_{100-c}$ alloys.

The average value of $\rho_{[B]}$ below T = 20°K has been taken to be the R for [B]. The normalized resistivity for the host [B], i.e., $\rho^N_{[B]}$ is just given by $\rho_{[B]} \times (R_{Fe_{2.0}[B]_{98.0}}/R_{[B]})$. The quantity $\rho^N_{Fe[B]}$ is given by $\rho_{Fe[B]} \times (R_{Fe_{2.0}[B]_{98.0}}/R_{Fe[B]})$

The resulting difference $\Delta\rho$ is plotted as a function of temperature for each concentration in Fig. 42. It should be noted that $\Delta\rho$ continues to increase when $T > T_c$. Since T_c is considered to be the temperature below which long range order exists, the increase in $\Delta\rho$ beyond T_c shows the effect of short range order. When T reaches a certain temperature T_s above T_c $\Delta\rho$ increases linearly with temperature with a small slope. It is speculated that T_s is the temperature above which even short range order effects have virtually vanished. The values of T_s are listed as a function of concentration in Table 5 and plotted as a function of c in Fig. 43. It should be kept in mind that the determination of the values of T_s is subject to large deviations. The difference $(T_s - T_c)$ should be an indication of the range in temperature over which short range order is important.

6. Temperature Derivative of the Resistivity $d\rho/dT$

The kink phenomenon in the ρ vs. T curve is quite common for a system undergoing a magnetic transition. Mydosh et al.[41] have studied the Fe_cPd_{100-c} system over the range $0.5 \leq c \leq 12.0$. Their analysis has concentrated on the critical region near the transition temperature. The transition temperature is defined as that at which the $d\rho/dT$ vs. T curve has its maximum, and is expected to be the

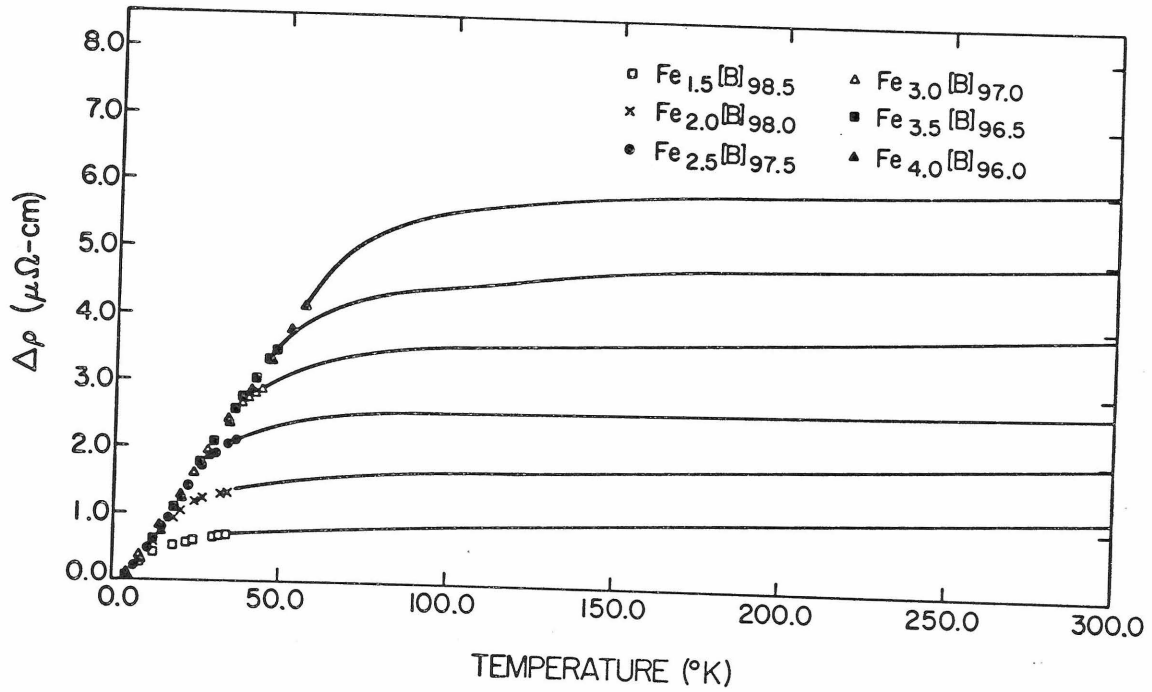

Fig. 42. $\Delta\rho = (\rho^{N}_{Fe_c[B]_{100-c}} - \rho^{N}_{[B]})$ vs temperature curves for the $Fe_c[B]_{100-c}$ alloys.

TABLE 5

Values of the characteristic temperatures T_s, $T_c(R)$ and $T_c(I.B.)$ for the $Fe_c[B]_{100-c}$ alloys.

Concentration (at.%)	T_s (^oK)	$T_c(R)$ (^oK)	$T_c(I.B.)$ (^oK)
$Fe_{1.5}[B]_{98.5}$	40.0	6.5	7.8
$Fe_{2.0}[B]_{98.0}$	56.0	12.0	15.5
$Fe_{2.5}[B]_{97.5}$	70.0	21.5	24.8
$Fe_{3.0}[B]_{97.0}$	100.0	31.0	35.5
$Fe_{3.5}[B]_{96.5}$	130.0	42.0	46.0
$Fe_{4.0}[B]_{96.0}$	150.0	53.5	55.0

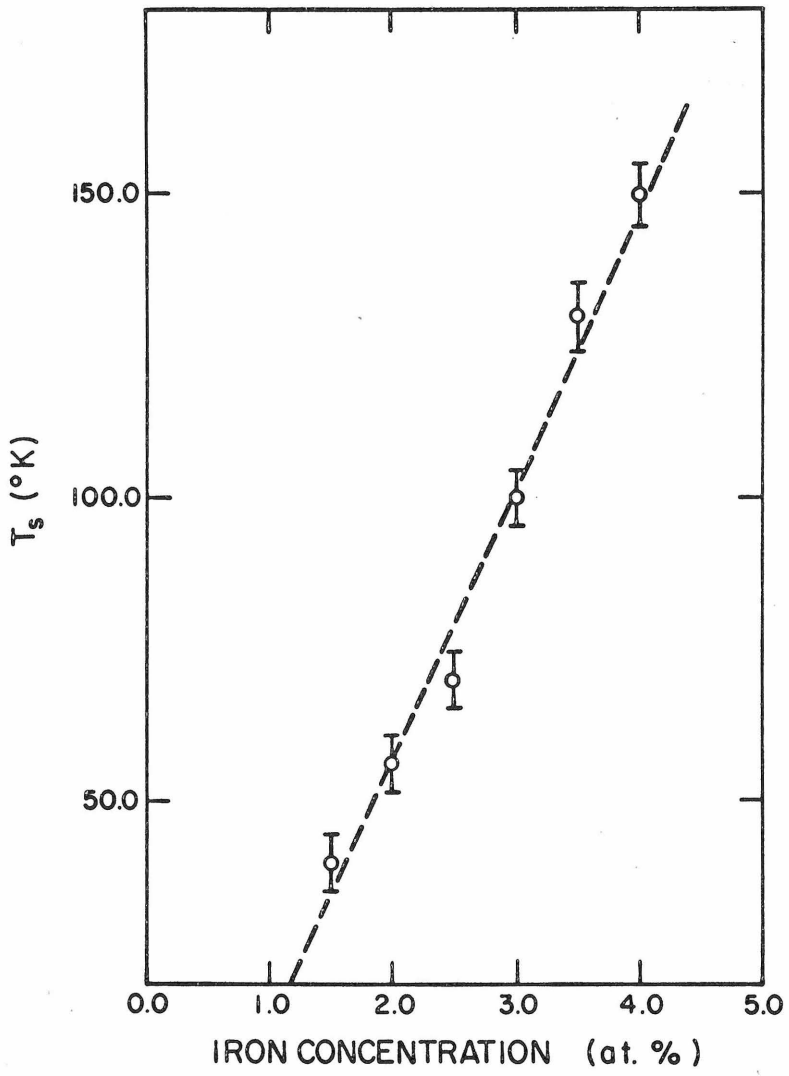

Fig. 43. T_s vs iron concentration for the $Fe_c[B]_{100-c}$ alloys.

temperature at the onset of long range order.[41] The same definition of the transition temperature will be adopted and is designated by $T_c(R)$. The quantity $d\rho/dT$ is obtained by numerical methods: Each set of nine neighboring points is fitted to a quadratic function in temperature T by the least square method. The derivative of the resulting expression is evaluated at the temperature corresponding to the middle point in the set, and is taken to be the derivative $d\rho/dT$ at that point. The scatter in $d\rho/dT$ is expectedly quite large. However, a smooth curve can still be drawn through them. A few examples are shown in Figs. 44 to 47.

At very low temperatures, $d\rho/dT$ rises with temperature with approximately a $T^{\frac{1}{2}}$ dependence. As T increases, $d\rho/dT$ takes on a constant value. This corresponds to the region below T_c where ρ varies linearly with temperature. The values of $d\rho/dT$ over this region are listed as a function of concentration in Table 6. As comparison, the coefficients of the linear temperature dependence in ρ below T_c, obtained by direct measurements, are also listed in Table 6. The general agreement indicates that the numerical differentiation procedure outlined in the above is a reasonable one. The maximum in $d\rho/dT$ is not a sharp peak as predicted theoretically [29] and observed experimentally in crystalline systems[42], where the maximum region has a width of $\sim 1.5^{\circ}K$. Instead, the maximum region in the present case has a width of ~ 5 -$10^{\circ}K$. This is expected to be due to a lack of long range order in amorphous systems. It is also partially due to some artificial averaging involved in the numerical analysis. The width of the region above $T_c(R)$ over which $d\rho/dT$

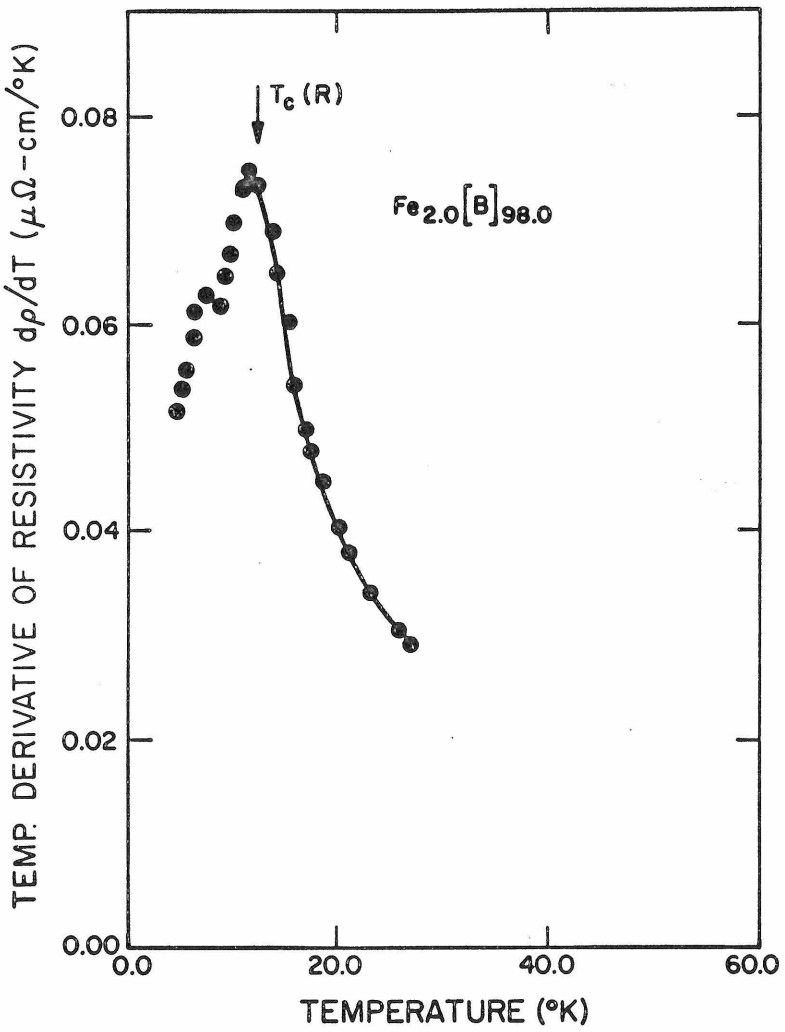

Fig. 44. Temperature derivative of resistivity vs temperature curve for the $Fe_{2.0}[B]_{98.0}$ alloy.

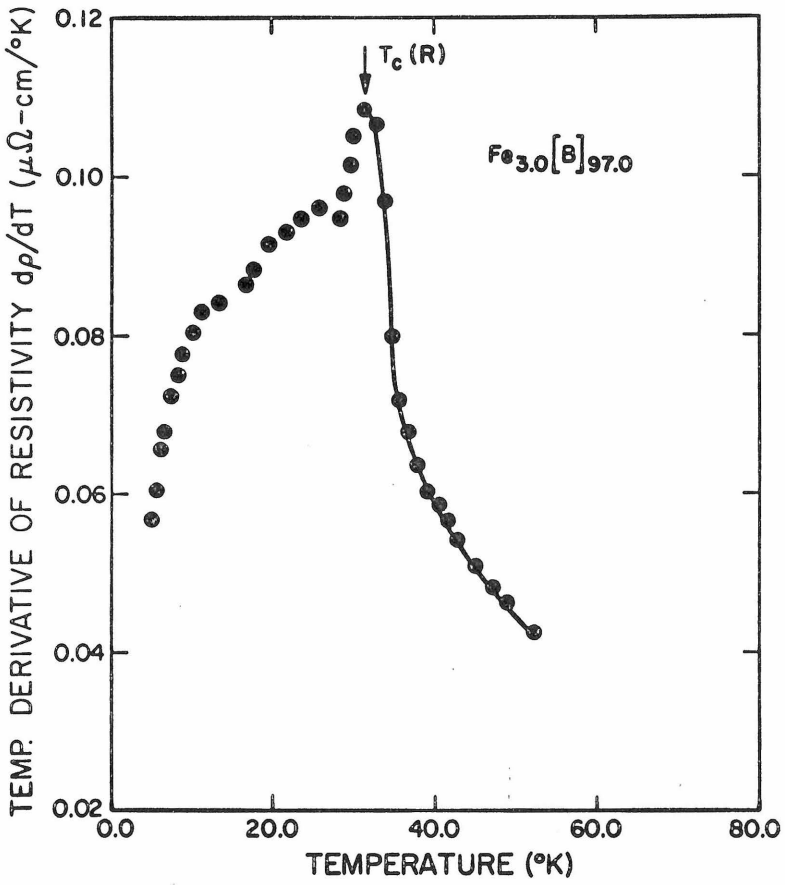

Fig. 45. Temperature derivative of resistivity vs temperature curve for the $Fe_{3.0}[B]_{97.0}$ alloy.

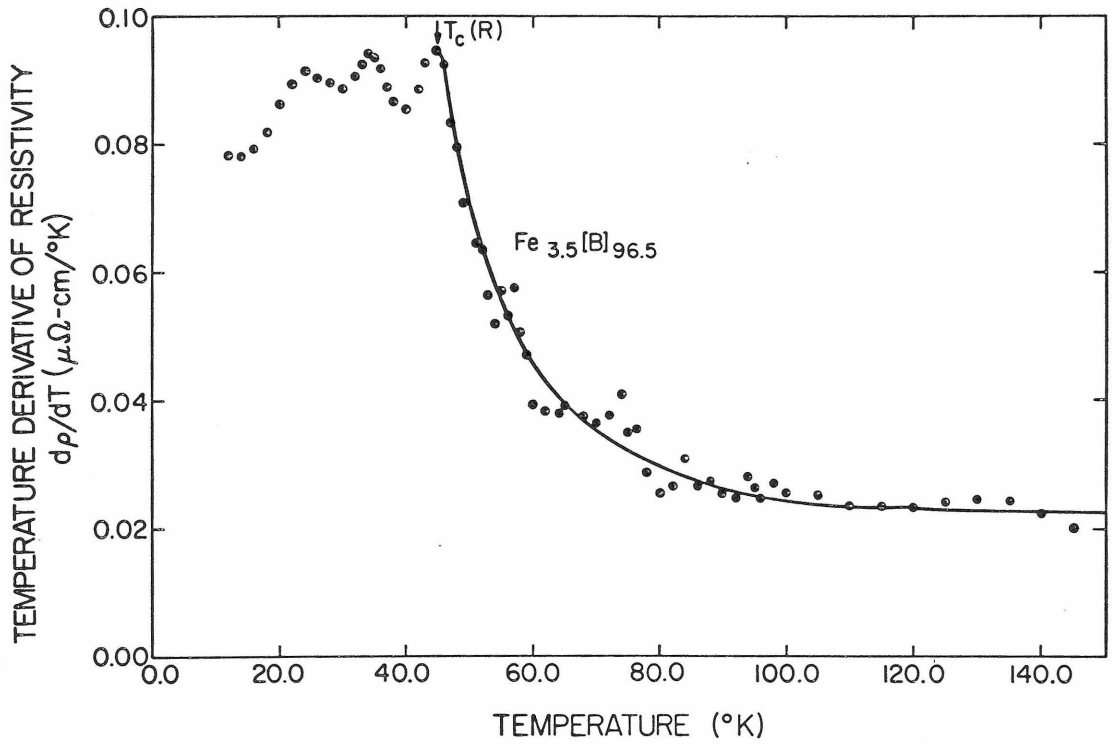

Fig. 46. Temperature derivative of resistivity vs temperature curve for the $Fe_{3.5}[B]_{96.5}$ alloy.

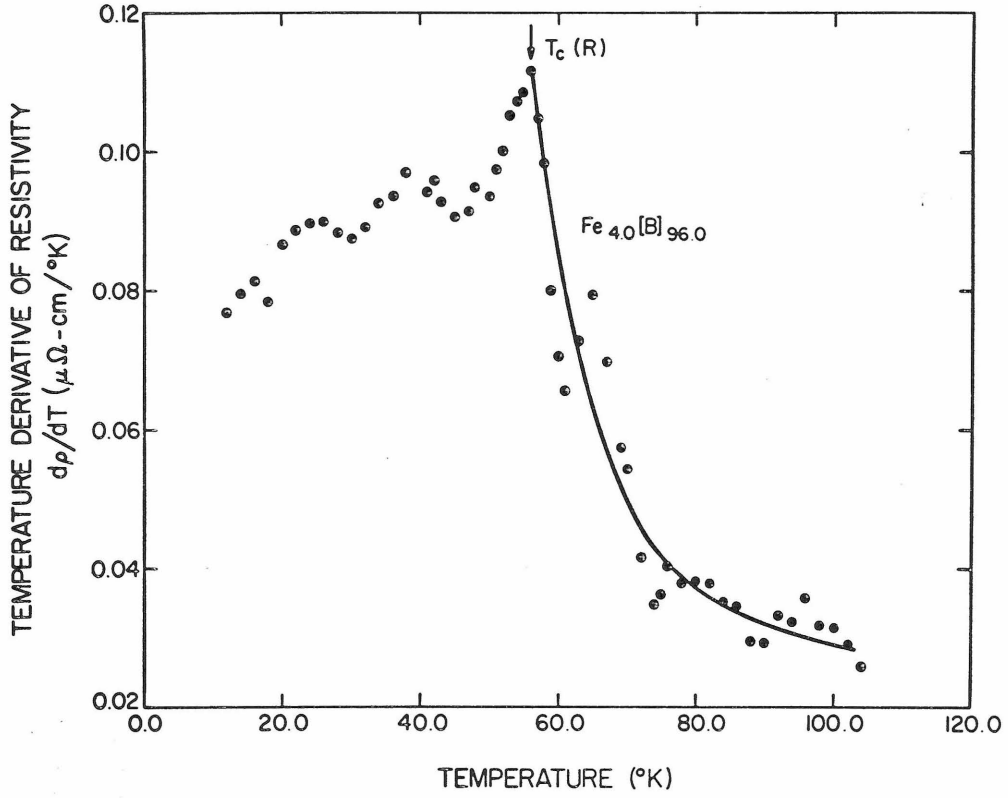

Fig. 47. Temperature derivative of resistivity vs temperature curve for the $Fe_{4.0}[B]_{96.0}$ alloy.

TABLE 6

Results of the $d\rho/dT$ analysis for the $Fe_c[B]_{100-c}$ alloys.

Concentration (at.%)	Linear Slope of ρ Below T_c by direct Measurements ($\mu\Omega$ - cm/^oK)	$d\rho/dT$ over the "flat" region ($\mu\Omega$ - cm/^oK)	Slope C = Normalized Slope of $\log_{10}\lvert T - T_c(R)\rvert$ ($\mu\Omega$ - cm/^oK-$\log_{10}{}^oK$)	λ
$Fe_{1.5}[B]_{98.5}$		0.0474	0.0210	-0.50
$Fe_{2.0}[B]_{98.0}$	0.0717	0.0719	0.0400	-0.50
$Fe_{2.5}[B]_{97.5}$	0.0830	0.0833	0.0492	-0.45
$Fe_{3.0}[B]_{97.0}$	0.0900	0.0896	0.0470	-0.30
$Fe_{3.5}[B]_{96.5}$	0.0890	0.0899	0.0496	-0.25
$Fe_{4.0}[B]_{96.0}$	0.0930	0.0926	0.0700	-0.25

is not a constant, indicates the temperature range in which short range order exists. Several authors have studied this problem, both theoretically and experimentally. As mentioned in the brief review of relevant theories, Mannari has predicted a log $|T - T_c|$ dependence in $d\rho/dT$. Zumsteg and Parks[42] have measured the resistivity of Ni and observed a logarithmic temperature dependence in $d\rho/dT$ for $(T - T_c)/T_c > 3 \times 10^{-4}$. Mydosh et al. [41] in studying the Fe Pd system have failed to confirm the logarithmic $(T - T_c)$ dependence in $d\rho/dT$. Instead they claim a $(T - T_c)^{-\lambda}$ dependence for $(T - T_c)/T_c \geq 0.1$ with $1.2 < \lambda < 1.9$. In this analysis, the data for $d\rho/dT$ have been plotted against $(T-T_c(R))$ on both semi-log and log-log graph papers. The results are shown in Figs. 48 to 50. Due to the large error that one may acquire in a numerical differentiation, whatever conclusion one tends to draw must be tentative. In the present system, from $\sim 2^{\circ}$ to 8°K above $T_c(R)$, $d\rho/dT$ seems to vary as $(T - T_c(R))^{-\lambda}$ $(0.25 < \lambda < 0.5)$. In the range 10°K to 20°K above $T_c(R)$, $d\rho/dT$ seems to follow a $\log_{10} (T - T_c(R))$ dependence. The results seem to be in qualitative agreement with the conclusions of Zumsteg et al., [42] Mydosh et al. [41] and Longworth et al. [43] in different temperature regions.

7. Concentration Dependence of the $\ell n|T-T_c|$ Slope in $d\rho/dT$

On the basis of Mannari's theory, one would expect a logarithmic dependence on $(T - T_c)$ for $d\rho/dT$ at $T > T_c$. The slopes of $\log_{10} (T - T_c(R))$ in the semi-log plots of $d\rho/dT$ for the alloys $Fe_{1.5}[B]_{98.5}$, $Fe_{2.0}[B]_{98.0}$, $Fe_{2.5}[B]_{97.5}$, $Fe_{3.0}[B]_{97.0}$, $Fe_{3.5}[B]_{96.5}$ and $Fe_{4.0}[B]_{96.0}$ have been measured, normalized and listed in Table 6

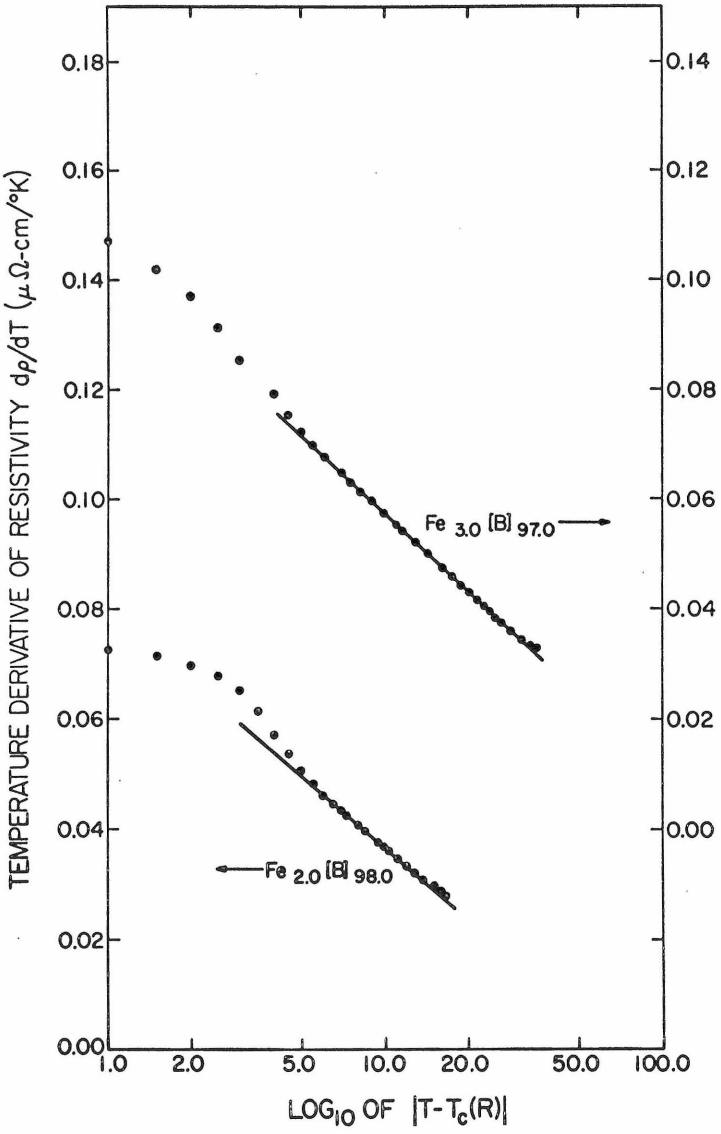

Fig. 48. Temperature derivative of resistivity vs $\log_{10}$ of $|T - T_c(R)|$ curves for the $Fe_{3.0}[B]_{97.0}$ and $Fe_{2.0}[B]_{98.0}$ alloys.

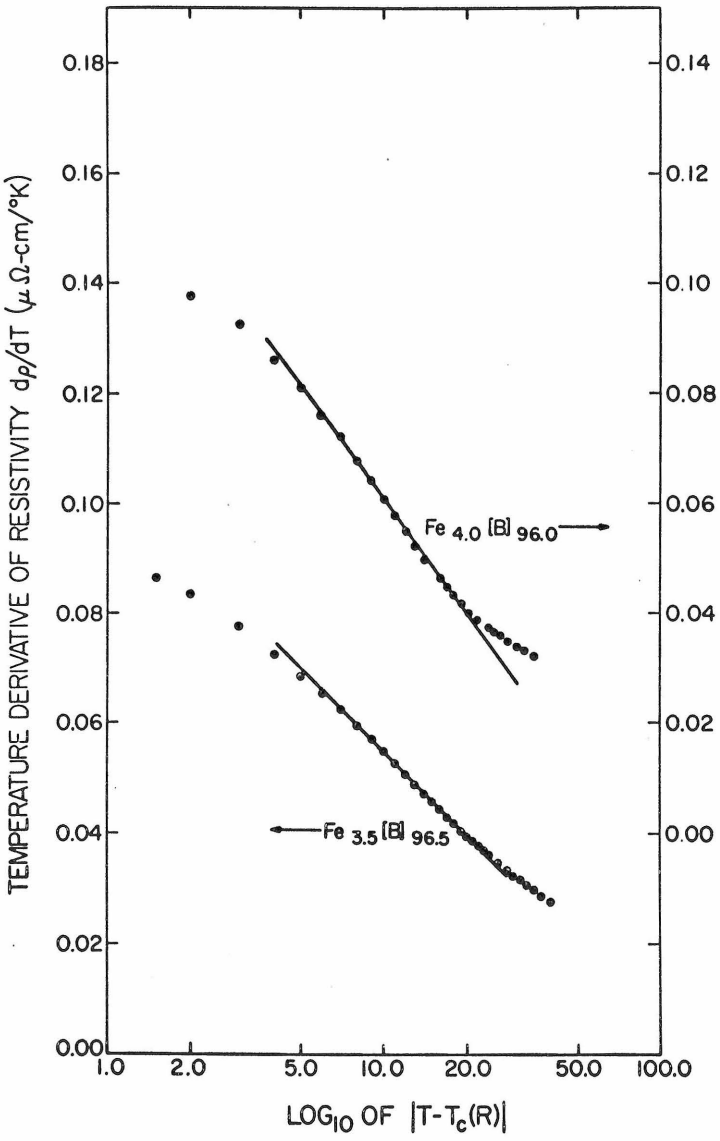

Fig. 49. Temperature derivative of resistivity vs $\log_{10}$ of $|T - T_c(R)|$ curves for the $Fe_{4.0}[B]_{96.0}$ and $Fe_{3.5}[B]_{96.5}$ alloys.

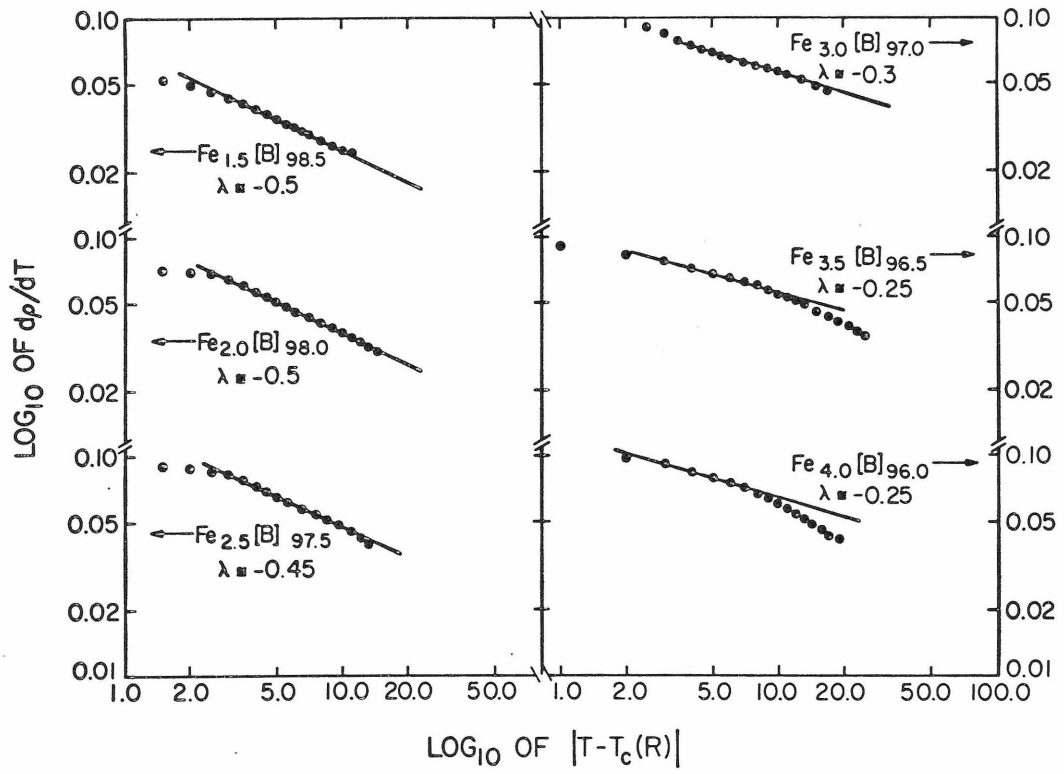

Fig. 50. Log_{10} of $d\rho/dT$ vs $\log_{10}$ of $|T-T_c(R)|$ curve for the $Fe_c[B]_{100-c}$ alloys.

against their corresponding concentrations. These normalized values of the slope, called slope C, are also plotted as a function of concentration c in Fig. 51. The uncertainty is large, reflecting the large error incurred in a numerical differentiation process as noted in Section (V. B. 6.). Bearing in mind the tentative nature of the conclusion, one may suggest that the slopes do lie on a straight line passing through the origin. This concentration dependence is different from the concentration dependence of T_c and $\Delta\rho_{step}$ which lie on straight lines with an intercept at c = ~1.2 at.% Fe on the c- axis (see Figs. 52, 53 and 56). This result suggests that the process, which causes a $\log_{10}(T - T_c)$ term in $d\rho/dT$, is the result of each impurity contributing independently. Probably, no interaction between impurities is involved.

8. Inductance Bridge Measurements and the Concentration Dependence of T_c(I. B.) and T_c(R)

In order to give a cross-check in the determination of the critical temperature, the samples to which the $d\rho/dT$ analysis has been applied were again measured on a standard ac inductance Wheatstone bridge. The temperature at which the deviation of V_{AB} reaches its peak is defined to be the critical temperature of magnetic transition called T_c(I. B.) (see Fig. 22). The values of the transition temperature T_c(I. B.) are listed against their corresponding concentrations in Table 5. For comparison's purpose, the values of T_c(R) are also listed in the same Table. Each set of T_c's is plotted as a function of concentration c separately in Fig. 52 and Fig. 53. The value of T_c(I. B.) is believed to be the Curie temperature.

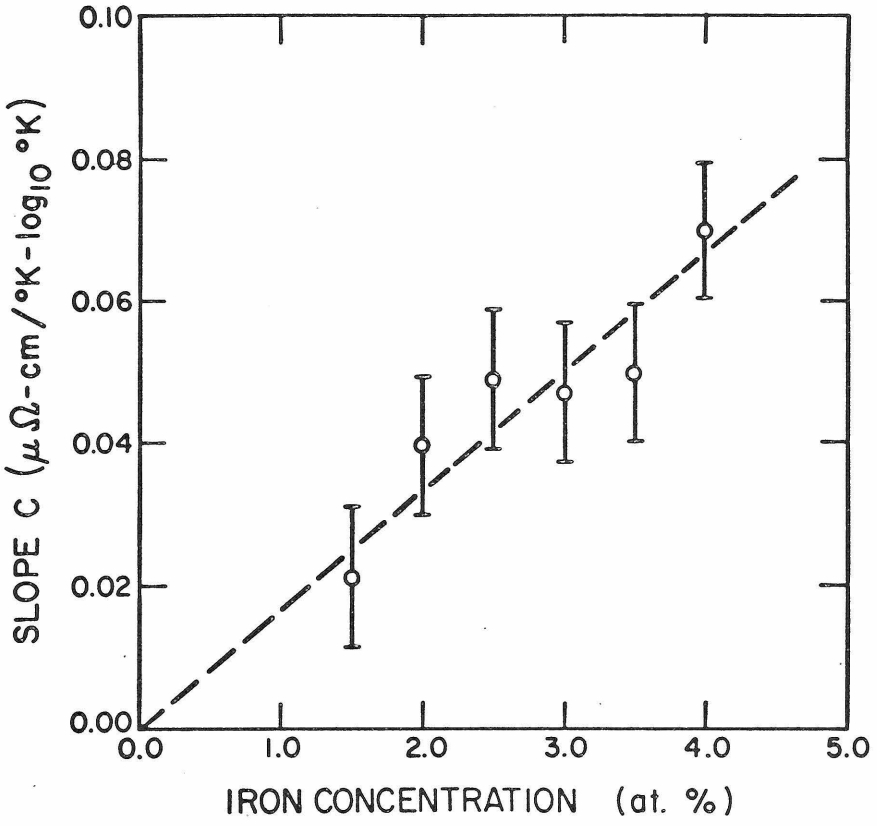

Fig. 51. Slope C (as defined in Section (V.B.7.)) vs iron concentration for the $Fe_c[B]_{100-c}$ alloys.

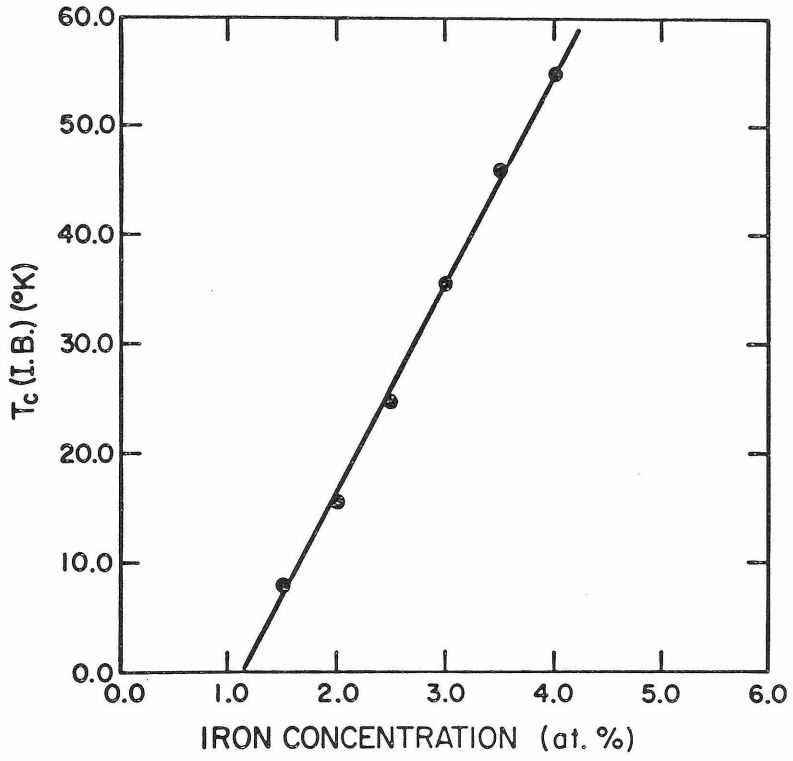

Fig. 52. The Curie temperature T_c(I.B.)(determined from the inductance bridge measurements) vs iron concentration for the $Fe_c[B]_{100-c}$ alloys.

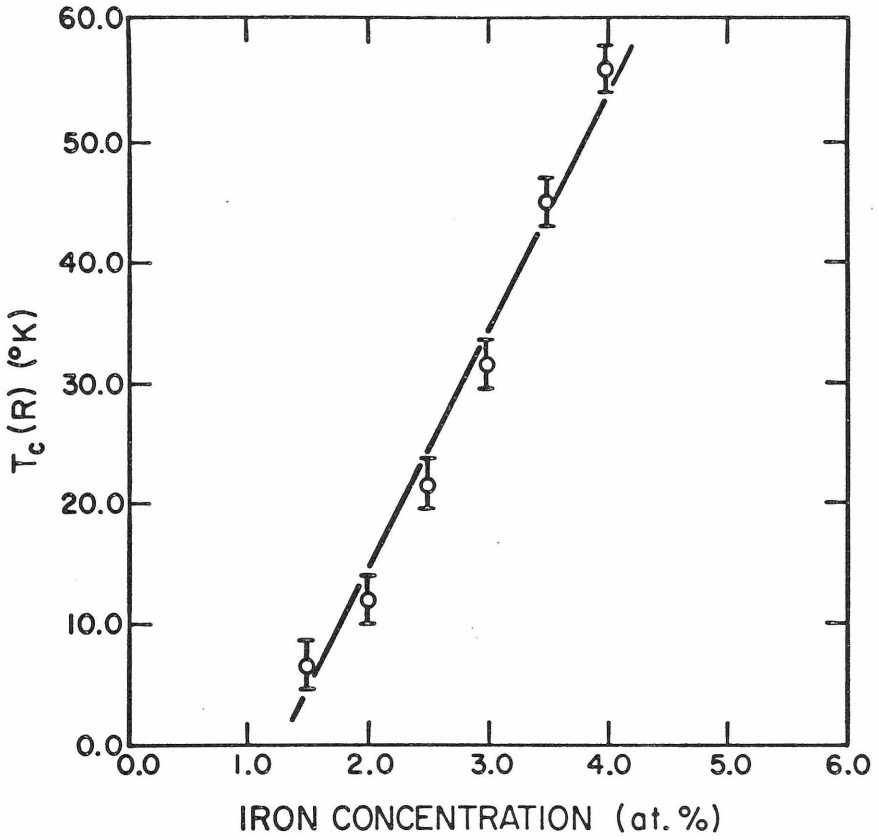

Fig. 53. The Curie temperature $T_c(R)$ (determined from the temperature derivative of resistivity) vs iron concentration for the $Fe_c[B]_{100-c}$ alloys.

It should be noted that the values of T_c(I. B.) lie on a straight line. This indicates that the transition temperatures increase linearly with concentrations, and this behavior is consistent with the concentration dependence derived from the molecular field theory. However, extending the straight line would give an intercept at $c \cong 1.2$ at.% Fe. Hence, it suggests that a minimum Fe impurity concentration is required before a ferromagnetic state can exist. But, beyond this critical concentration, the transition temperature is proportional to the excess impurity concentration.

Fig. 53 shows that the values of T_c(R) possess a similar dependence on concentrations. The fluctuations are larger than those of T_c(I. B.) as expected since numerical differentiation is involved in the determination of T_c(R). The intercept on the c-axis, obtained by extending the straight line, again suggests that the critical concentration is ~ 1.2 at.% Fe. The manifestedly good agreement between the two plots suggests that T_c(I. B.) and T_c(R) arise from the same physical phenomenon. This supports the contention that the maximum in $d\rho/dT$ and hence the 'kink' phenomenon in the resistivity vs. temperature curve is magnetic in origin.

9. Magnetometer Measurement

In order to provide some supporting evidence, the susceptibility of the alloy $Fe_{2.5}[B]_{97.5}$ was measured with the magnetometer. As mentioned earlier, the main interest in the magnetometer measurements is the qualitative temperature dependence. As in the case of FePd[44], the isothermal plots of σ vs. H in the present system is non-linear. Following Hasegawa[45], χ is defined to be the slope of

σ vs. H at the high field end (near 8.4 kilogauss). In the higher temperature range, $1/\chi$ has been plotted as a function of temperature in Fig. 20. At high temperature, $1/\chi$ clearly depends linearly on temperature. According to the operational definition given in the brief review of relevant theories, localized moments exist in this system. By linear extrapolation, one may conclude that at $T = 100^{\circ}K$, $1/\chi$ would vanish. This is the paramagnetic Curie temperature θ_p. It is much higher than T_c(I. B.), which is $25.0^{\circ}K$. However, this discrepancy is expected due to the existence of predominant short range order in the amorphous systems. A similar discrepancy has been observed in the Fe Pd Si system[45]. As the temperature decreases towards the paramagnetic Curie temperature, $1/\chi$ curves away from a linear temperature dependence, just as in Ni[30]. In the low temperature range, the system is expected to be ferromagnetic. The magnetization σ has been plotted as a function of temperature ($4^{\circ}K$ - $77^{\circ}K$) in Fig. 21, for each of the three lowest available H fields. The magnetization σ increases by approximately a factor of a hundred as the ferromagnetic state is approached at low temperature. As the external applied field decreases to 390 gauss, the temperature of the mid-point in the "fall-off" part of the σ vs. T curve moves towards $T = 24^{\circ}K$. As $H_{app} \rightarrow 0$, the corresponding temperature is expected to be slightly lower. This value is consistent with the values of $T_c(R) \sim 21.5^{\circ}K$ and $T_c(I.B.) \sim 25^{\circ}K$ determined for $Fe_{2.5}[B]_{97.5}$. This agreement constitutes a further qualitative confirmation on the correctness of the T_c determinations and of the contention that the system at hand is a ferromagnetic system.

10. $\Delta\rho_{max}[T_c]$ vs. Concentration

One of the interesting results of the present study concerns the concentration dependence of $\Delta\rho_{max}[T_c]$. Following Williams and Loram[35] who have studied the Fe Pd system, $\Delta\rho_{max}[T_c]$ is defined as $\Delta\rho(T=T_c) - \Delta\rho(T=0)$. Yosida and Kasuya have calculated this quantity and have predicted that it should depend linearly on concentration. The quantity $\Delta\rho_{max}[T_c(R)]$ is listed in Table 7 and plotted in Fig. 54 as a function of concentration. That is the values of T_c used are actually the values of $T_c(R)$ defined in Section (V. B. 6.). The plot in Fig. 54 indicates that $\Delta\rho_{max}[T_c(R)]$ is not a linear function of concentration for the lower concentrations. Loram and Williams did not find a linear concentration dependence in $\Delta\rho_{max}[T_c]$ for Fe Pd either. The prediction of a linear concentration dependence for $\Delta\rho_{max}[T_c]$ is based on the assumption that at $T = T_c$, all magnetic ordering ceases to exist, i.e., the transition from the ferromagnetic state to the paramagnetic state is a sharp one. From Fig. 42, where the curves $\Delta\rho$ vs. T are plotted for the various concentrations, it is noticed that the transitions are by no means sharp. Even for 20° to 30° K above T_c, considerable variation in $\Delta\rho$ with temperature is seen implying that considerable short range order persists. As a comparison, the normalized $\delta\rho_{max}[T_c(R)] = \rho[T_c(R)] - \rho[T=0]$ is also plotted as a function of concentration in Fig. 55. It has the same qualitative dependence on concentration as $\Delta\rho_{max}[T_c(R)]$. The concentration dependence of $\Delta\rho_{max}[T_c(I.B.)]$ is similar to that of $\Delta\rho_{max}[T_c(R)]$ and is not presented.

TABLE 7

Values of the resistivity step-heights $\Delta\rho_{max}[T_c(R)]$, $\delta\rho_{max}[T_c(R)]$ and $\Delta\rho_{step}$ for the $Fe_c[B]_{100-c}$ alloys.

Concentration (at.%)	Lower Bound of $\Delta\rho_{step}$ ($\mu\Omega$-cm)	$\Delta\rho_{step}$ ($\mu\Omega$-cm)	Upper Bound of $\Delta\rho_{step}$ ($\mu\Omega$-cm)	$\Delta\rho_{max}[T_c(R)]$ (from $\Delta\rho$) ($\mu\Omega$-cm)	$\delta\rho_{max}[T_c(R)]$ (from ρ) ($\mu\Omega$-cm)
$Fe_{1.5}[B]_{98.5}$	0.73	0.99	1.21	0.21	0.24
$Fe_{2.0}[B]_{98.0}$	1.56	1.79	1.99	0.61	0.59
$Fe_{2.5}[B]_{97.5}$	2.52	2.65	2.74	1.39	1.24
$Fe_{3.0}[B]_{97.0}$	3.56	3.74	3.91	2.18	2.26
$Fe_{3.5}[B]_{96.5}$	4.60	4.83	4.98	3.02	3.22
$Fe_{4.0}[B]_{96.0}$	5.90	5.98	6.05	3.93	4.31

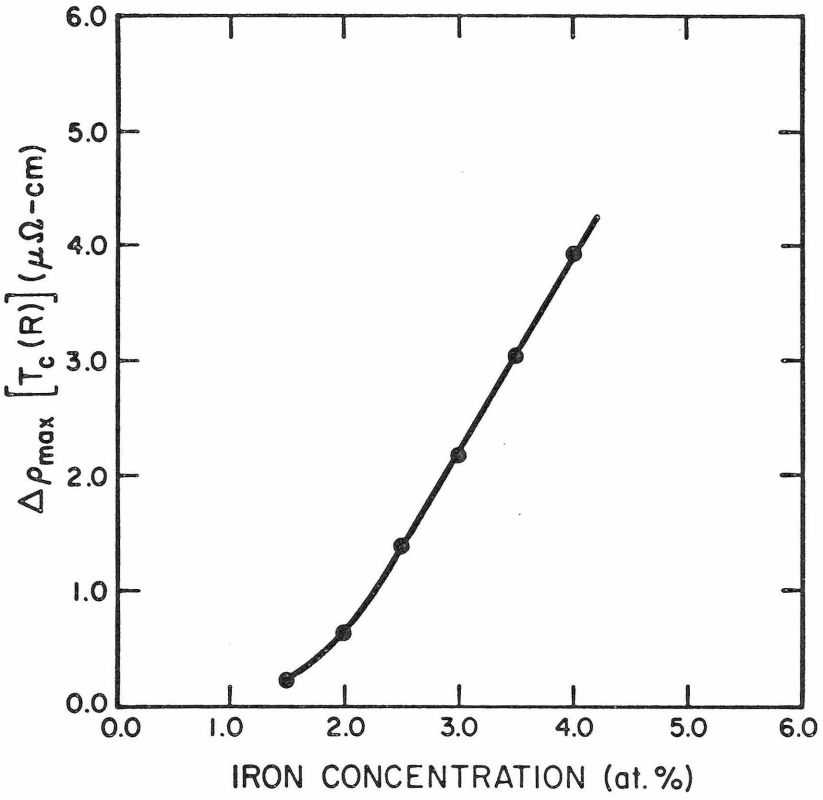

Fig. 54. $\Delta\rho_{max}[T_c(R)] = (\Delta\rho[T_c(R)] - \Delta\rho[T=0])$ vs iron concentration curve for the $Fe_c[B]_{100-c}$ alloys.

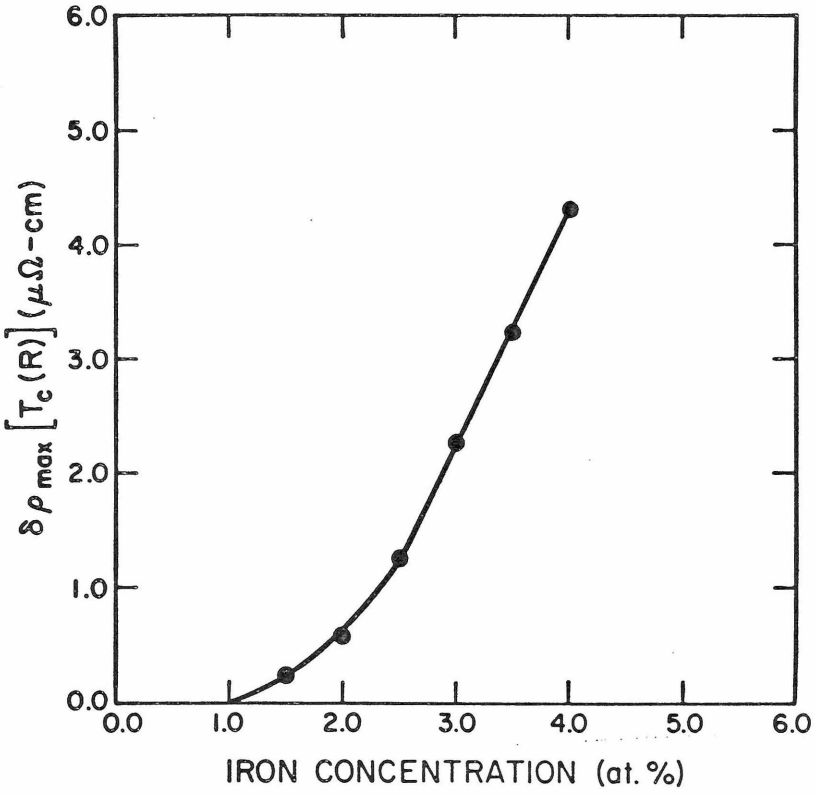

Fig. 55. $\delta\rho_{max}[T_c(R)] = (\rho[T_c(R)] - \rho[T=0])$ vs iron concentration curve for the $Fe_c[B]_{100-c}$ alloys.

11. $\Delta\rho_{step}$ vs. Concentration

A new quantity $\Delta\rho_{step} = \Delta\rho(T >> T_c) - \Delta\rho(T = 0)$ is defined. It is plotted as a function of concentration c in Fig. 56 and is listed vs. concentration in Table 7 together with its upper bound and lower bounds. Based on Yosida and Turner and Long's expressions, one can gain an idea of what this quantity should be. For $T >> 0$ the molecular field approach is assumed valid, and Yosida's expression for the resistivity (c.f. the brief review of relevant theories) will be adopted. For the ferromagnetic case $\langle\ \rangle^+ = \langle\ \rangle^-$ and $H^+ = H^- = B$ and one may write

$$\Delta\rho(T) = \frac{3\pi}{2}\frac{m}{e^2}\frac{1}{\hbar E_F}\left(\frac{V}{N}\right)c\left[V^2 + J_{eff}^2\left\{\langle S_z^2\rangle^+ + \left[S(S+1) - \langle S_z^2\rangle^+ - \langle S_z\rangle^+\right]\left(1+\tanh\frac{g\mu_B}{kT}\right)\right\}\right.$$

$$\left. - \frac{4J_{eff}^2 V^2 (\langle S_z\rangle^+)^2}{2V^2 + J_{eff}^2\left[\langle S_z^2\rangle^+ + (S^2+S-\langle S_z^2\rangle^+ - \langle S_z\rangle^+)\left(1+\tanh\frac{g\mu_B}{kT}\right)\right]}\right] \qquad (37)$$

At $T = T_c$, since it is suspected that the short range order still exists, it is unclear how a simple limiting expression for $\Delta\rho$ can be obtained. This may explain why $\Delta\rho_{max}[T_c(R)]$ vs. c does not obey the predicted concentration dependence, based on the assumption that $\Delta\rho$ has a simple limit at T_c. However, if the expression $\Delta\rho$ is evaluated at $T >> T_c$, the spins are expected to be truly random and $B \to 0$. One may set $\langle S^2\rangle = S(S+1)/3$ and $\langle S^z\rangle = 0$. With these limiting relations, one gets

$$\Delta\rho(T >> T_c) = \frac{3\pi}{2}\frac{m^*}{e^2}\frac{1}{\hbar E_F}\left(\frac{V}{N}\right)c\left[V^2 + J_{eff}^2 S(S+1)\right] \qquad (38)$$

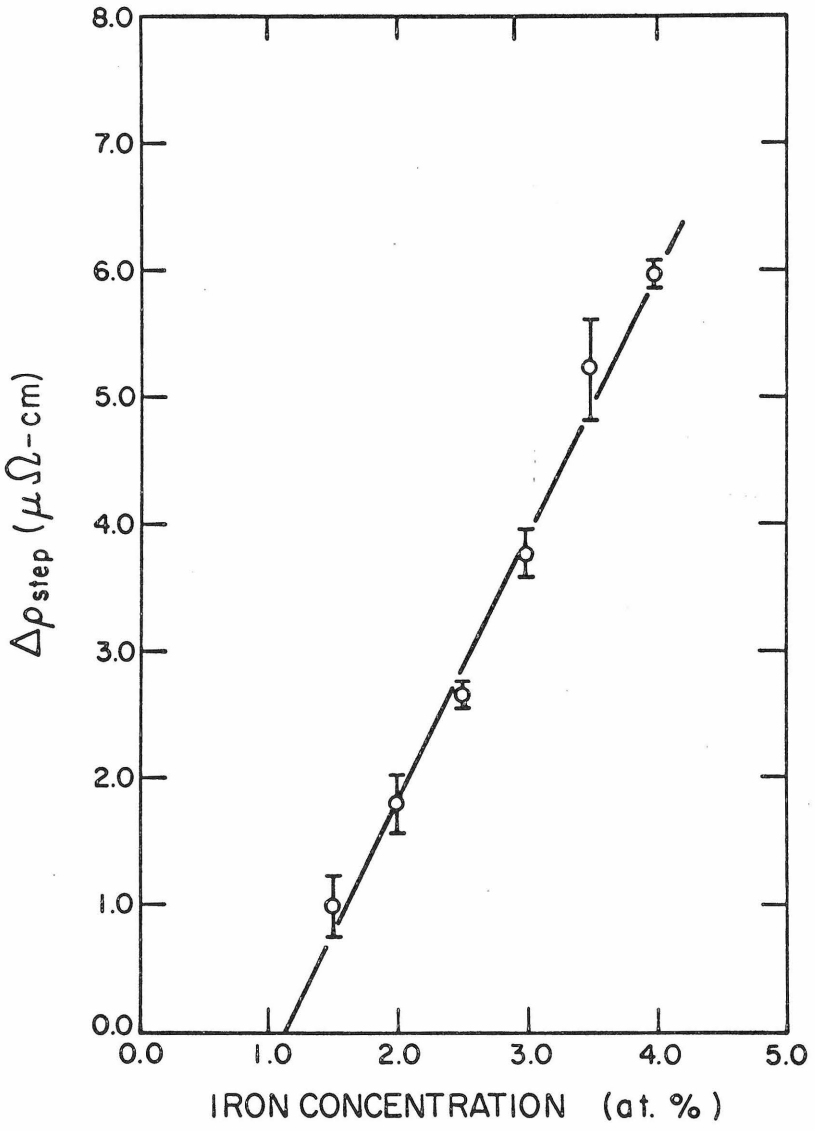

Fig. 56. $\Delta\rho_{step} = [\Delta\rho(T \gg T_c) - \Delta\rho(T=0)]$ vs iron concentration for the $Fe_c[B]_{100-c}$ alloys.

For $T \to 0$

$$\tanh \frac{g\mu B}{kT} = 1 \quad , \langle S^2 \rangle = S(S+1) \text{ and } \langle S \rangle = S$$

With these substitutions, one gets

$$\Delta\rho\,(T \to 0) = \frac{3\pi m}{2\hbar e^2 E_F}\left(\frac{V}{N}\right) c\left[V^2 - 3J_{eff}^2 S^2\right] \tag{39}$$

As $T \to 0$, it is more appropriate to use Turner and Long's expression for $\Delta\rho$ based on spin waves.

$$\Delta\rho\,(T \to 0) = \frac{3\pi m^* c}{2\hbar e^2 E_F}\left(\frac{V}{N}\right)\left\{V^2 + J_{eff}^2 S^2 - \frac{4J_{eff}^2 V^2 S^2}{V^2 + J^2 S^2}\right\}$$

$$= \frac{3\pi m^* c}{2\hbar e^2 E_F}\left(\frac{V}{N}\right)\left\{V^2 - 3J_{eff}^2 S^2\right\} \tag{40}$$

in the limit of strong potential scattering.

It should be noted that this limiting expression is identical to that derived from the molecular field theory for $T = 0$.

With these,

$$\Delta\rho_{step} = \frac{3\pi m^*}{2\hbar e^2 E_F}\left(\frac{V}{N}\right) c\, J_{eff}^2\, S(1+4S) \tag{41}$$

From this expression, one expects $\Delta\rho_{step}$ to depend linearly on concentration c. The fact that the plot of $\Delta\rho_{step}$ vs. c does constitute a straight line is very encouraging. It is noticed that $\Delta\rho_{step} \to 0$ at c = 1.2 at. %. This critical concentration is in agreement with that at which $T_c \to 0$ (see Figs. 52, 53 and 56).

12. An Attempt in Arriving at a Universal Curve for $\Delta\rho/\Delta\rho_{max}[T_c]$ vs. T/T_c

An attempt has been made to correlate the data for the different concentrations. The data for each concentration presented in Fig. 42, are divided by their $\Delta\rho_{max}[T_c]$ evaluated at their critical temperature T_c(I. B.) determined from the inductance bridge measurement. The resulting quantity $\Delta\rho/\Delta\rho_{max}[T_c(\text{I. B.})]$ is plotted as a function of the reduced temperature T/T_c(I. B.). The curve for each concentration has been shifted vertically up or down relative to that of $Fe_{2.5}[B]_{97.5}$ by a different amount ϵ, and the data for all six concentrations ($Fe_{1.5}[B]_{98.5}$, $Fe_{2.0}[B]_{98.0}$, $Fe_{2.5}[B]_{97.5}$, $Fe_{3.0}[B]_{97.0}$, $Fe_{3.5}[B]_{96.5}$ and $Fe_{4.0}[B]_{96.0}$) are then plotted on the same graph in Fig. 57. The values of ϵ are listed as a function of concentration in Table 8. In order to justify this plot, it is recalled that, according to the theories given in Sections (III. C. 1.) and (III. C. 2.)

$$\Delta\rho(T) = \frac{3\pi m^*}{2\hbar e^2 E_f}\left(\frac{V}{N}\right)c\left[V^2 + J_{eff}^2\left\{\langle S_z^2\rangle^+ + (S^2+S-\langle S_z^2\rangle^+ - \langle S_z\rangle)\left(1+\tanh\frac{g\mu B}{kT}\right)\right\} - \frac{4J_{eff}^2V^2(\langle S_z\rangle^{+2})}{2V^2 + J_{eff}^2\left\{\langle S_z^2\rangle^+ + [S(S+1)-\langle S_z^2\rangle^+ - \langle S_z\rangle^+]\left(1+\tanh\frac{g\mu B}{kT}\right)\right\}}\right]$$

$$\Delta\rho_{max}[T_c] = \frac{3\pi m^*}{2\hbar e^2 E_f}\left(\frac{V}{N}\right)c\,J_{eff}^2\,S(1+4S)$$

In the limit of strong potential scattering (i. e. $V \gg J_{eff}$) it can be shown that

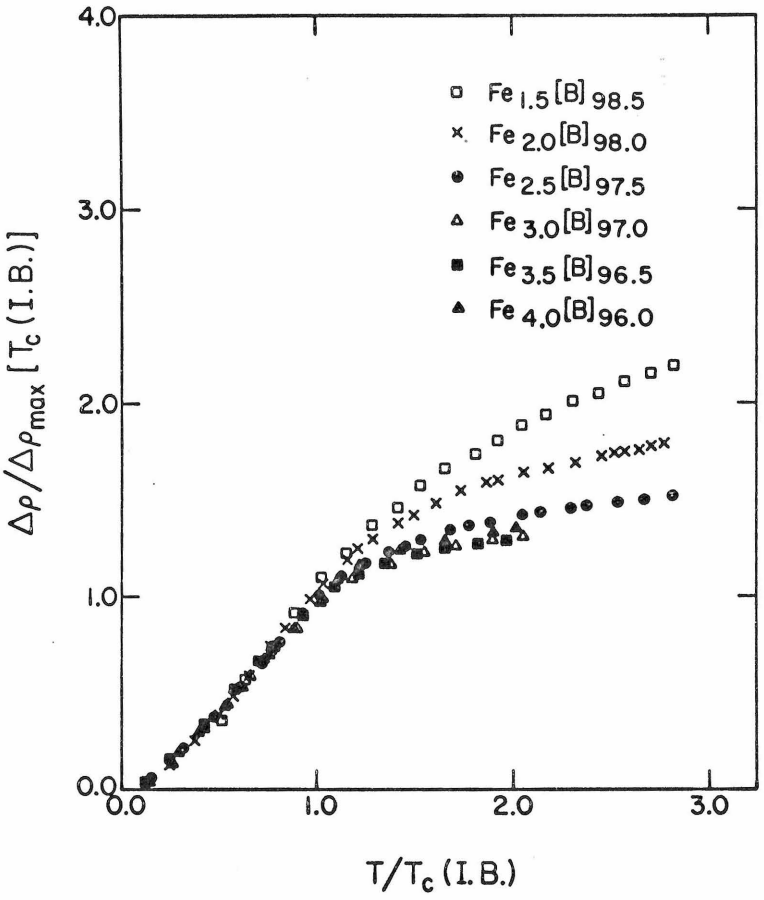

Fig. 57. $\Delta\rho/\Delta\rho_{max}$ vs T/T_c(I.B.) curves for the $Fe_c[B]_{100-c}$ alloys.

TABLE 8

Values of ε used in arriving at the universal curve of resistivity for the $Fe_c[B]_{100-c}$ alloys

Concentration (at.%)	ε (dimensionless)
$Fe_{1.5}[B]_{98.5}$	+0.05
$Fe_{2.0}[B]_{98.0}$	+0.03
$Fe_{2.5}[B]_{97.5}$	0
$Fe_{3.0}[B]_{97.0}$	-0.03
$Fe_{3.5}[B]_{96.5}$	-0.04
$Fe_{4.0}[B]_{96.0}$	-0.04

+ - refer to up or down shifts respectively.

$$\frac{\Delta\rho(T)}{\Delta\rho_{max}[T_c]} = \frac{V^2}{J_{eff}^2 S(1+4S)} + \frac{\{\langle S_i^2\rangle^{\dagger} + [S(S+1) - \langle S_i^2\rangle^{\dagger} - \langle S_i\rangle](1+\tau\tanh\frac{g\mu B}{kT}) - 2\langle S_i\rangle^{\dagger 2}}{S(1+4S)}$$

(42)

Based on this, it is clear that the same temperature dependence is expected for the different concentrations. The temperature independent term $V^2/J_{eff}^2 S(1+4S)$, however, is concentration dependent because V and J_{eff} vary with the concentration c. Hence, if a different constant vertical shift is made for the curve of each concentration in order to give the best fit to the curve of some arbitrarily chosen standard composition ($Fe_{2.5}[B]_{97.5}$ here), a universal curve is expected on the basis of the molecular field theory. From Fig. 57, it is seen that the data for the various concentrations do seem to fall on the same curve for $T/T_c(I.B.) \leq 1$, over which the systems are ferromagnetic. The results indicate that the molecular field theory generally gives satisfactory predictions of the temperature dependence. The curve of the $Fe_{1.5}[B]_{98.5}$ sample does not match that of $Fe_{2.5}[B]_{97.5}$ nearly as well as the others do. For $T/T_c(I.B.) > 1$, the curves deviate from each other. The deviation is particularly pronounced for $Fe_{1.5}[B]_{98.5}$. Ideally, if all magnetic order ceases for $T > T_c$, a flat curve is expected for $T/T_c > 1$. Thus, the deviation from a constant temperature dependence above T_c can be taken to be an indication of the effect of short range order. The temperature range above T_c where $\Delta\rho/\Delta\rho_{max}[T_c(I.B.)]$ is still strongly temperature dependent provides a measure of the size of the region where

short range order is important. The results suggest that short range order is predominant in $Fe_{1.5}[B]_{97.5}$. From $Fe_{3.0}[B]_{97.0}$ on, the $\Delta\rho/\Delta\rho_{max}[T_c(I.B.)]$ curves coincide and approach a constant value (which is also smaller) earlier, suggesting the relative importance of short range order has reached a minimum. This conclusion is reasonable if it is recalled that below 1.2 at.% Fe, none of the effect arising from an ordered magnetic state is observed in the resistivity curves. It is to be expected that short range order still remains to be relatively significant just above the critical concentration above which a magnetically ordered state occurs.

The plot of $\Delta\rho_{max}[T_c(R)]$ vs. c in Fig. 54, and the plot of the linear slope below T_c vs. c in Fig. 40 will be re-examined in the light of the discussion presented in the previous paragraph. Based on the molecular field theory, $\Delta\rho_{max}[T_c]$ is expected to have a linear concentration dependence. Experimentally this is true only for $2.5 \leq c \leq 4.0$. Similarly, based on the molecular field theory, Turner and Long have predicted that the linear slope below T_c should be independent of concentration. Experimentally, this is approximately true only for $4.0 \geq c \geq 3.0$. From these observations, it is suggested that the molecular field theory is applicable only when short range order is not predominant. Alternately, the observed deviations at lower concentrations from the predicted concentration dependence based on the molecular field theory are due to the relative importance of short range order effects in these alloys. From the plot of $\Delta\rho_{step}$ vs. c in Fig. 56 and the related discussion, it is learned that $\Delta\rho_{step}$ is a better measure of the quantity $(3\pi m^* V/2\hbar e^2 E_F N)\, c\, J_{eff}(1+4S)\, S$.

Hence it may be suggested that one should have plotted $\Delta\rho/\Delta\rho_{step}$ vs. T/T_s instead. (The definition of T_s has been given in Section (V.B.5.)). However, the determination of T_s is subject to large uncertainties ($\pm 15^{o}K$) and the resulting curves are subject to such large deviations that the property of a universal curve would be obscured. For similar reasons (uncertainties in the determination of $T_c(R)$), $\Delta\rho/\Delta\rho_{max}[T_c(R)]$ is not plotted against $T/T_c(R)$.

13. Estimation of J_{dd}, $J_{eff\ s\text{-}d}$ and Giant Moment

Based on the molecular field theory, the d-d exchange integral of a ferromagnetic system is related to its Curie temperature as follows:[30]

$$J_{dd} = \frac{3kT_c}{2zS(S+1)} \qquad (43)$$

The estimate of J_{dd} will be made specifically for the alloy $Fe_{3.0}[B]_{97.0}$. This particular alloy ($Fe_{3.0}[B]_{97.0}$) has been chosen because, from the attempt to arrive at a universal curve it is learned that for $c > 3.0$ the molecular field theory gives correct predictions. The formula for J_{dd} is expected to be applicable for this composition. The quantity S is the spin of the Fe impurity in [B]. Based on the discussion related to the Cr [B] system, it is believed that the [B] alloy has a high Fermi energy E_F. This is consistent with the estimation that $S_{Cr} = \frac{1}{2}$ in [B]. Based on the Friedel[8] model and in analogy with the Cr [B] system, it is expected that the Fe impurities will likewise retain a low S value in [B]. Therefore, the value $S_{Fe} = \frac{1}{2}$ will be assumed. The quantity z is the number of nearest magnetic neighbors. Assuming that there

are twelve nearest neighbors out of which 3% are Fe impurities, one finds that $z \cong 0.36$. Taking $T_{c\ experimental} \cong 36^{o}K$ and $S = \frac{1}{2}$, one obtains J_{dd} of $Fe_{3.0}[B]_{97.0} \cong 0.017$ eV. This value will serve as an order of magnitude estimate for the J_{dd} of the other samples.

Based on the value for $\Delta\rho_{step}/c = \frac{3\pi m^{*} V}{2\hbar e^{2} E_{F} N} J_{eff\ sd}^{2} S(1+4S)$ (41')

it is possible to give an estimate of $J_{eff\ s\text{-}d}$ characterizing the interaction between conduction s electrons and the d spins of the host. The following values for the relevant quantities will be used:
m = the free electron mass = 5.11×10^{5} eV/C^{2}; $E_{F} \cong 8.5$ eV;
$(\frac{N}{V})$ = the number of atoms/unit volume = 8.4×10^{22}/cc and $S = \frac{1}{2}$.
From Fig. 56, it is learned that $\Delta\rho/c$ is of the order of 1 $\mu\Omega$cm/at.%. With these estimates, one obtains that $J_{eff\ s\text{-}d} \cong 0.13$ eV.

As it has been mentioned in the brief review of relevant theories, it is possible to estimate μ_{eff} from the slope of the $1/\chi$ vs. T curve. The value of this slope for $Fe_{2.5}[B]_{97.5}$ can be obtained directly from Fig. 20, where $1/\chi$ is plotted as a function of T. Using the expression: slope = $3k/N\mu_{eff}^{2}$ = 0.04 kilogauss/ma, one obtains $\mu_{eff} \cong 6.2\ \mu_{B}$. This would imply $S_{eff} \cong 5/2$. However, this does not mean $S_{Fe} \cong 5/2$ in [B]. As in the case of the Fe Pd system, the giant magnetic moment is considered to be due to the collective effect of the Fe impurity spin and of the surrounding host atoms that are polarized by the impurity. The Fe impurity and its polarized neighbors together act as a unit. The giant moment phenomenon is a characteristic of a polarizable medium.

14. Simple Physical Model and ξ Estimation

The resistivity minima observed at low Fe concentrations suggest that the Kondo effect is the underlying mechanism. Based on the discussion connected with the Cr[B] system, the conceptual model consists of a localized spin surrounded by a cloud of conduction s electrons, as shown schematically in Fig. 58a. As the Fe impurity concentration increases, eventually the conduction electron clouds will come into contact with each other. Accepting the assumption that the Fe atoms tend to couple ferromagnetically, the conduction electron polarization clouds will be in the configuration shown in Fig. 58b. In contrast to the Cr [B] system, where the s electrons in the overlap region (double-shaded region) have no preferred direction of alignment, the conduction electrons in the present overlap region feel an enhanced tendency of alignment coming from both Fe_I and Fe_{II}. When the overlap becomes significant, all the conduction s electrons (participating in the quasi-bound state) will lock into pointing in the same direction. This, in turn, will bring all the d spins into alignment with a strength characterized by J_{sd}. This mutual locking of d spins will greatly suppress the probability for s electrons of having spin-flip intermediate states because the Fe impurity atom is no longer capable of changing the Z-component of its spin to compensate for the change in the Z-component of the s electron spin so as to conserve the Z-component of the total angular momentum of the system. When this happens, the Kondo mechanism is not expected to exist as mentioned in the brief review of relevant theories. Since the d spins are now aligned, a magnetically ordered

s electron polarization cloud about an "Fe-impurity"

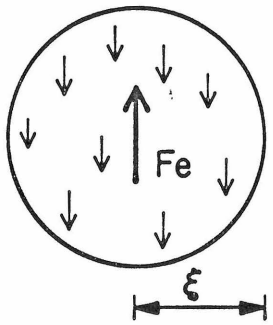

$J_{sd} < 0$

(a)

Enhancement of s electron polarization in the overlap region (double-shaded)

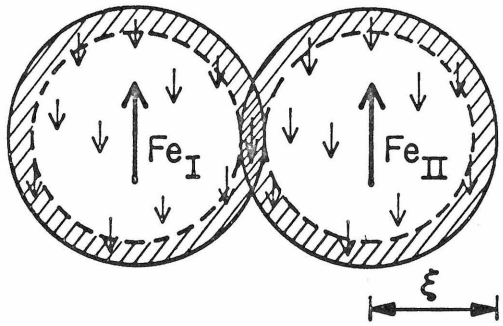

$J_{sd} < 0$

(b)

Enhancement of s electron polarization in the overlap region (double-shaded)

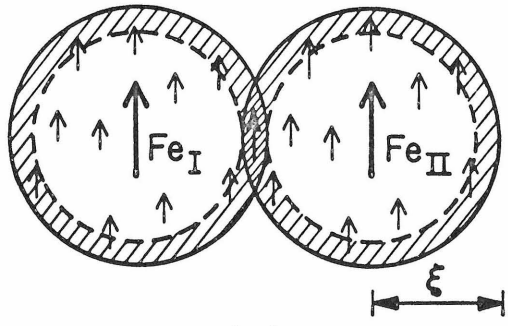

$J_{sd} > 0$

(c)

Fig. 58. The proposed model applied to the $Fe_c[B]_{100-c}$ alloys.

state comes into existence. In fact, it is a ferromagnetic state. It is not an ordinary ferromagnet like iron metal. The basic alloy [B] contains both Pd and Ni and is highly polarizable. It is conceivable that each Fe atom will line up the d holes of a large number of neighboring atoms. This is the origin of giant moments. It is believed that the s electrons will still form polarization clouds surrounding the Fe impurity-d holes composite treating it as a bigger impurity. The resultant ferromagnetic state at higher Fe concentrations is one in the Fe Pd sense made up of the impurity-d band coupled system. Turner and Long have pointed out a main difference between these systems and an ordinary ferromagnet is the lack of translational symmetry. The present system, being amorphous, guarantees this absence of translational symmetry and hence may be an ideal system for substantiating the theory of Turner and Long, since the crystalline order effect is minimized in this case.

In the illustrations of Fig. 58, J_{sd} has been assumed negative, and hence the s electrons are depicted as pointing in a direction opposite to that of the Fe spin. This is suggested by the experimental observation that the resistivity minimum phenomenon (which requires $J_{sd} < 0$) is present at low Fe concentrations. If it is assumed that as the Fe concentration increases the sign of J_{sd} remains unchanged, Fig. 58b. should give a reasonable description of the physical condition. If this physical model is carried further to $T \to 0$, it is expected that the s electron polarization cloud will exactly compensate the Fe impurity spin when the Nagaoka quasi-bound state completes its formation. It should be emphasized that the d spins are still well aligned

and the s spins (those that participate in the quasi-bound state) are similarly well aligned but point in the opposite direction. The conduction s electrons still feel the effect of the ordered spins for all $T < T_c$. This effect is reflected in the ρ vs. T curves. Even though a well ordered magnetic state exists, its effect is not expected to be manifest external to the sample when the spin-compensate-state is complete. This surprising conclusion is tentatively confirmed by some preliminary observation. The inductance of a coil wound around a $Fe_{2.5}[B]_{97.5}$ foil was measured as a function of temperature and is presented in Fig. 59. The inductance increases dramatically as the Curie point is crossed in approaching low temperature. However, as the temperature is further lowered, the inductance drops as if the sample is approaching a non-magnetic state. This effect is understandable in terms of the above mentioned picture. It is expected that the bulk magnetic effect of the sample will appear to decrease as $T \to 0$ when the quasi-bound state approaches completion. However, if an external magnetic field is applied, the spin-compensation is prevented from completion (not destroyed) and the effect of a ferromagnetic state should be seen. This expectation is consistent with the σ vs. T curve for the same sample $Fe_{2.5}[B]_{97.5}$ shown in Fig. 21.

The above assignment of $J_{sd} < 0$ is of course not conclusive. It is possible that J_{sd} may change sign as the Fe concentration is increased. Such a phenomenon has been observed in the system $(Cu_cPd_{100-c})_{99}Fe_1$[46]. In order to explore this possibility further, the resistivities for the samples $Fe_{0.45}[B]_{99.55}$, $Fe_{0.6}[B]_{99.4}$,

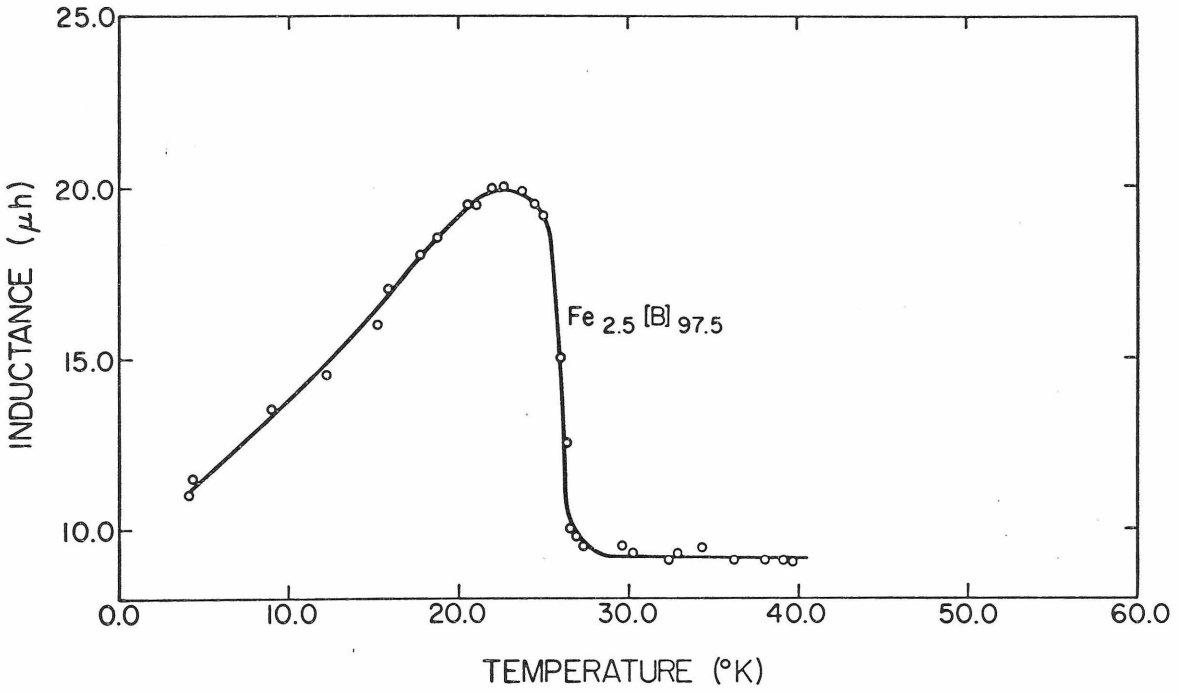

Fig. 59. Inductance vs temperature curve for the $Fe_{2.5}[B]_{97.5}$ alloy.

$Fe_{0.7}[B]_{99.3}$ and $Fe_{0.8}[B]_{99.2}$ are plotted vs. $\log_{10}T$ for $T<15^{o}K$ on an expanded scale in Fig. 60 and Fig. 61. It is noticed that for $Fe_{0.45}[B]_{99.55}$ and $Fe_{0.6}[B]_{99.4}$ a minimum in the resistivity is observed suggesting $J_{sd} < 0$. However, the magnitude of J_{sd} is decreasing as the concentration c is increased. At 0.7 at.% Fe, the resistivity is flat suggesting $J_{sd} \cong 0$. For $Fe_{0.8}[B]_{99.2}$ the resistivity is seen to increase linearly with $\log_{10}T$ for $T < 10^{o}K$. At this temperature range, $\rho_{electron\text{-}phonon}$ is expected to be unimportant. Hence, the experimental data suggest that ρ_{sd} varies linearly with $\log_{10}T$. If it is assumed that this phenomenon is a manifestation of the Kondo effect, the slope of the $\log_{10}T$ term implies $J_{sd} > 0$. It is expected that this trend ($J_{sd} > 0$) will continue as the concentration is further increased. The polarization clouds surrounding the Fe impurity spins should then be in the condition depicted in Fig. 58c. The previous argument that a correlation among s electrons will lead to a coherence in the d spins is still valid. The resistivity and the magnetic susceptibility data for the higher Fe concentrations can be explained equally well by this model. The only difference is that as $T \rightarrow 0$, the Fe spins are not expected to be compensated. The sample as a whole should now show the effect of ferromagnetic order, quite similar to the behavior expected of an ordinary ferromagnet. If this viewpoint is adopted, then the variation in the inductance L must not be considered to be a good indicator of the apparent presence or absence of bulk magnetic moments.

However, it is still assumed that a s electron polarization cloud exists around the Fe impurity for the case $J_{sd} > 0$. It should

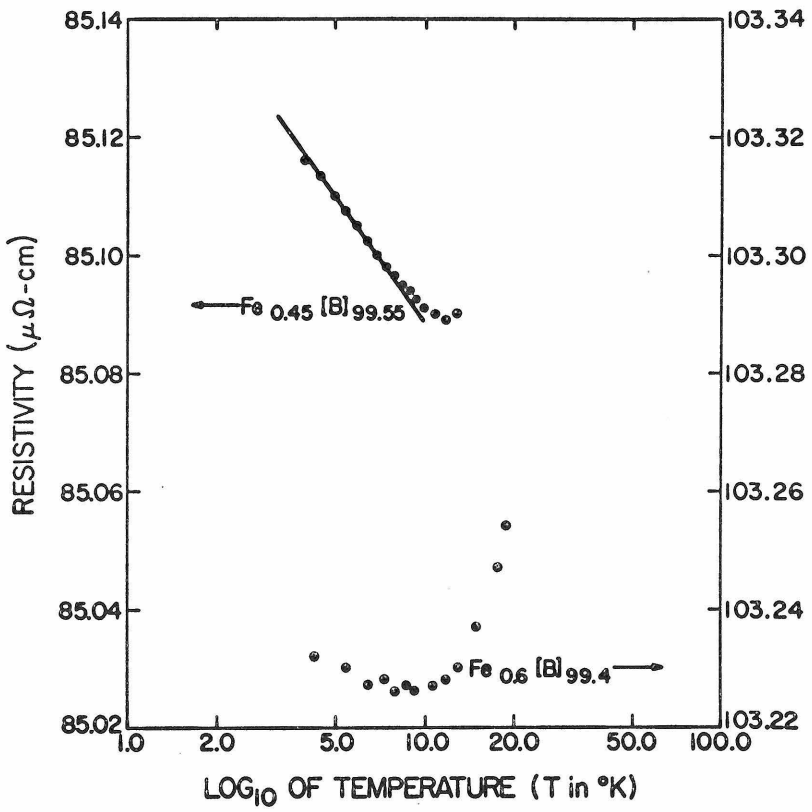

Fig. 60. Resistivity vs $\log_{10}$ of temperature curves for the $Fe_{0.45}[B]_{99.55}$ and $Fe_{0.6}[B]_{99.4}$ alloys.

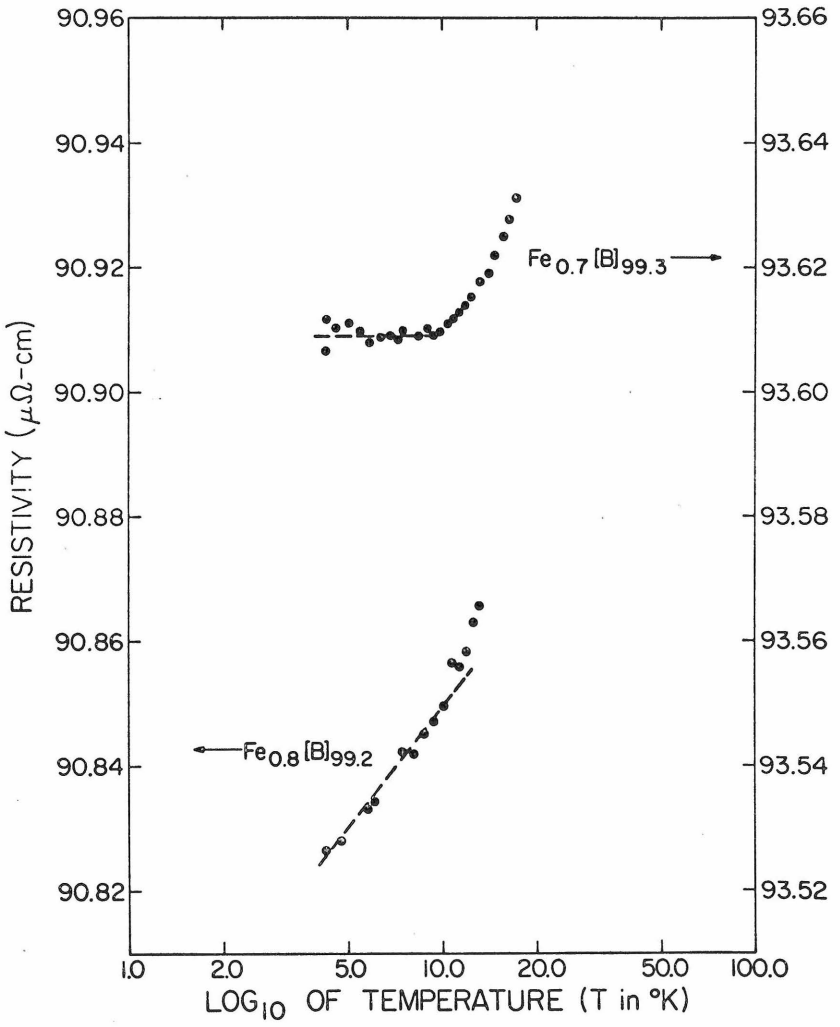

Fig. 61. Resistivity vs $\log_{10}$ of temperature curves for the $Fe_{0.7}[B]_{99.3}$ and $Fe_{0.8}[B]_{99.2}$ alloys.

be recalled that the Kondo theory [12] is applicable for both $J_{sd} > 0$ and $J_{sd} < 0$. Moreover, although Nagaoka[14] has assumed that J_{sd} is negative when the quasi-bound state concept is first proposed, a recent theoretical paper by Maduhkar and Tsuei[47] has shown that a bound state also exists for $J_{sd} > 0$. These considerations are consistent with the above assumption.

It has been noticed that in the Fe[B] system there exists a critical concentration of Fe below which the ferromagnetic state is absent. Similar observations have been reported for the studies of other magnetic systems[48], such as Fe Pd, Ni Pd etc. There have been several theoretical attempts to explain this phenomenon without much success[48]. However based on the present proposed model, the existence of a critical impurity concentration can be explained in a natural way. The central concept in the proposed model is that a s electron polarization cloud exists around each Fe impurity, whether $J_{sd} < 0$ or $J_{sd} > 0$. At low Fe concentrations the polarization clouds do not overlap substantially. The Fe spins behave independently and the phenomenon of resistivity minimum is expected. The Fe impurity concentration must increase to a certain critical value such that there is considerable overlap of the s electron polarization clouds. When this occurs, the d spins are locked and a ferromagnetic state results.

Taking the value of $J_{\text{eff } s\text{-}d} \cong 0.13$ ev determined in Sec. (V.B.12.), one may make an order of magnitude estimate of the effective polarization cloud radius ξ. Using $E_F \cong 8.5$ ev, one obtains $2\xi \geq \frac{E_F}{k_F} \left(\frac{1}{|J_{\text{eff } s\text{-}d}|} \right)$ or $2\xi \geq 30$ Å. From the experimental result that the Kondo effect is partially suppressed at 0.6 at.% of Fe, one

may get an estimate of $2\xi_{exp} \geq 16$ Å. This experimental value is in order of magnitude agreement with the theoretical estimate based on the uncertainty principle argument.

VI. SUMMARY AND CONCLUSIONS

The subject of this thesis is concerned with the temperature dependence of the electrical resistivity of amorphous alloys $[Pd_{41}\ Ni_{41}\ B_{18}]$ (designated by [B] in the following) containing the magnetic elements chromium and iron. Both Cr and Fe in solid solution in a crystalline paramagnetic metal lead to anomalies in the electrical resistivity at low temperature. Such anomalies, however, are present only in dilute solid solutions, of the order of 1 at. % or less. In amorphous alloys they are observed for much higher concentrations, up to about 10 at. %. For simplicity, the term "non-dilute" is used to indicate the order of magnitude of the magnetic impurity concentration. The main characteristic of these magnetic alloys is that the magnetic atoms are close enough in the structure so that some correlation between their spins must be taken into consideration.

The resistivity versus temperature curves for the Cr[B] alloys possess all the characteristic anomalies predicted by the Kondo-Nagaoka theory for a typical dilute magnetic alloy: (1) the presence of a resistivity minimum; (2) the logarithmic increase in the resistivity with decreasing temperature; and (3) the onset of saturation in ρ_{sd} as $T \rightarrow o$. The Hamann theory is considered better in the sense that it is capable of correlating the resistivity data in detail for the temperature range much below the temperature at which the resistivity is minimum. The fact that an agreement of the type shown in Fig. 24 exists between theory and experiment definitely indicates one step forward in the understanding of the magnetic impurity problem. From

this experimental investigation, it is further learned that the theories, which have been developed for the non-interacting impurities problem, apply amazingly well in correlating the data for non-dilute impurity concentrations. This observation is substantiated by the existence of universal resistivity curves (shown in Figs. 32-34) which include data for alloys containing both dilute and non-dilute concentrations of Cr. The fact that one well defined universal curve is achieved using the Hamann theory demonstrates that this theory is superior to the other theories and suggests that as long as the d spins are not locked so that the spin-flip intermediate states are allowed, the resistivities of the alloys containing different Cr concentrations possess the same functional dependence on the reduced temperature, whether or not a correlation exists between the d spins. This is considered a significant extension of the current understanding in the magnetic impurity problem. On the other hand, there are also important changes when the d spins begin to have some correlation: (1) the unitarity limit ρ_o is no longer directly proportional to the concentration c and (2) the Kondo temperature T_K increases with concentration instead of being concentration independent. A simple physical model has been proposed in which the correlation between the d spins is interpreted more specifically as the interaction between the s electron polarization clouds surrounding the d spins. Correlation comes in when the polarization clouds overlap substantially. Contrary to the approach adopted by most investigators, the diameter of the polarization cloud before touching 2ξ, has been correctly expressed as $E_F/(|J_{sd}|k_F)$. The value for 2ξ estimated on this basis is in good agreement with

the present experimental value deduced from the critical concentration at which the effect of correlation between the Cr spins on the unitarity limit ρ_o is observed. Based on the same model, the observed concentration dependence of T_K can be interpreted as an increase in the quasi-bound state binding energy resulting from the cancellation of the s electron polarization in the overlap region.

With the addition of non-dilute concentrations of Fe into [B] alloys a ferromagnetic state results at low temperature. This is a manifestation of spin correlation. The temperature dependence of the ρ vs. T curves, namely $T^{3/2}$ at very low temperature and T just below the Curie temperature, are in excellent agreement with the theory of Turner and Long which was developed for polarizable ferromagnetic alloys like Fe Pd. At high temperatures, ρ is a linear function of T and the Matthiessen's rule seems to hold for the Fe[B] alloys. Based on the theories of Yosida and Turner and Long which employ the molecular field theory, a universal curve of resistivity is obtained at temperatures below T_c for the ferromagnetic Fe[B] alloys. This indicates that the $\Delta\rho$ vs. T curves for the different concentrations possess some identical basic feature in the ferromagnetic temperature range and suggests that the molecular field theory gives a reasonable description of the physical situation. However, in the present study the predicted concentration dependences (based on the molecular field theory) of T_c, ρ_{max} etc. are confirmed only for the alloys containing higher concentrations. The deviations from a linear concentration dependence for the lower concentrations (c near $c_{critical}$ = 1.2 at. %) have been interpreted as being due to the relative

importance of short range order.

At very low Fe concentrations ($c < 0.45$ at. %) the resistivity minimum phenomenon is observed as would be expected of a typical dilute magnetic alloy. The occurrence of the ferromagnetic state at high Fe concentrations has been interpreted in terms of the physical model of an interaction between the s electron polarization clouds surrounding the Fe spins. In particular, the existence of a critical concentration above which a ferromagnetic state can exist for which no conclusive theoretical explanation has been given, finds a natural explanation in the present model. It is suggested that at the critical concentration, the neighboring polarization clouds have just overlapped sufficiently to establish a s electron correlation through a major volume of the sample. Given the tendency for the Fe spins to couple in parallel, a ferromagnetic state will result from the overlap of the s electrons and the induced parallel locking of the d spins. It is proposed that this is one of the mechanisms responsible for the occurrence of ferromagnetism in non-dilute magnetic alloys. This model is expected to be of special relevance in those systems in which the direct interaction between the localized spins is relatively weak as, for example, in the amorphous systems and in the rare earth metals involving unfilled f shells.

It has been recognized for some time that the basic mechanism involved with magnetic impurities in a metallic host is the s-d interaction. It is proposed that the most important aspect in the dilute magnetic problem is the existence of the s electron polarization clouds about the d spins. The proposed physical model suggests that

the important physical phenomena in the non-dilute magnetic problem are: (1) the formation of the s electron polarization clouds about the magnetic spins and (2) the interaction between these s electron polarization spheres. The presence of interaction between the s electron polarization spheres is probably the main difference between the non-dilute magnetic problem and the dilute magnetic problem. The effects predicted by this model is believed to be particularly manifest when $|J_{dd}|$ is small. It should be emphasized that the polarization of the s electrons about the d spins (parameterized by J_{sd}) retains its fundamental importance. However, although the magnitude $|J_{dd}|$ is small, the sign of J_{dd} is of great significance in determining the ultimate magnetic state obtained in the non-dilute magnetic alloys. If $J_{dd} < o$ (i.e., the d spins tend to couple anti-parallel with each other), a condition similar to that in the Cr [B] system is expected. If $J_{dd} > o$ (i.e., the d spins tend to couple parallel), the resulting magnetic state is expected to be similar to that of the Fe[B] system. With this viewpoint, the large amount of theoretical and experimental efforts spent on the dilute magnetic problem in the past few years should be considered justified. The crucial concept of a s electron polarization cloud about a magnetic spin has evolved out of the study of dilute magnetic systems.

Finally, it should be recalled that the [B] alloys are amorphous and are also chemically more complicated than most of the other hosts used in the study of the dilute magnetic problem. It is indeed surprising that the present experimental results can be so simply and adequately correlated by the theories developed for much simpler

alloys. This suggests that the local environment is not fundamentally different. The amorphous environment, however, seems to reduce the correlation between atoms, and in particular, between the d electrons. This is consistent with the observation that relatively high concentrations of Cr (high compared with those in the crystalline hosts) can be added in [B] without quenching the Kondo effect. It is also consistent with the relatively low Curie temperature in the [B] alloys as compared with that in crystalline Fe Pd for the same Fe concentration. Since the correlation between the atoms is reduced in an amorphous alloy, the influence of the conduction s electrons (which is capable of coupling the whole system due to its mobility) in affecting the bulk properties of the system is increased relative to that in a crystalline alloy. Hence, an amorphous alloy should be an ideal system for studying the correlation effects of the s electrons including those of the important s electron polarization clouds around the magnetic d spins.

REFERENCES

1. A. J. Heeger, Solid State Physics 23, 283 (1969)

2. M. D. Daybell and W. A. Steyert, Rev. of Modern Phys. 40, 380 (1968).

3. J. Kondo, Solid State Physics 23, 183 (1969)

4. P. Pietrokowsky, J. Sci. Instr. 34, 445 (1962).

5. N. F. Mott, Adv. Phys. 16, 49 (1967).

6. Pol Duwez, Rapid Quenching Techniques, Chap. 7 in Techniques of Metals Research, edited by R. F. Bunshah (Interscience Publishers, 1968).

7. M. E. Weiner, Ph. D. Thesis, California Institute of Technology (1968).

8. J. Friedel, Can. J. Phys. 34, 1190 (1956); also J. Friedel, Nuovo Cimento (Suppl.) 7, 287 (1958); also J. Friedel, "Metallic Solid Solution," (J. Friedel and A. Guinier, ed.) Benjamin, New York, 1963.

9. P. W. Anderson, Phys. Rev. 124, 41 (1961); also P. W. Anderson and A. M. Clogston, Bull. Am. Phys. Soc. 6, 124 (1961).

10. G. Kemeny, Phys. Rev. 156, 740 (1967).

11. M. Levine and H. Suhl, Phys. Rev. 171, 567 (1968).

12. J. Kondo, Progr. Theoret. Phys. (Kyoto) 32, 37 (1964).

13. M. P. Sarachik, E. Corenzwit and L. D. Longinotti, Phys. Rev. 135, A1041 (1964).

14. Y. Nagaoka, Phys. Rev. 138, A1112 (1965).

15. L. N. Cooper, Phys. Rev. 104, 1189 (1956).

References (Cont'd)

16. D. N. Zubarev, Sov. Phys. Uspekhi 3, 320 (1960).

17. J. Bardeen, L. N. Cooper and J. R. Schrieffer, Phys. Rev. 108, 1175 (1957).

18. M. A. Ruderman and C. Kittel, Phys. Rev. 96, 99 (1954); also K. Yosida, Phys. Rev. 106, 893 (1957); also T. Kasuya, Progr. Theoret. Phys. (Kyoto) 16, 45 (1956).

19. D. R. Hamann, Phys. Rev. 154, 596 (1967).

20. S. D. Silverstein and C. B. Duke, Phys. Rev. 161, 456 (1967); also S. D. Silverstein and C. B. Duke, J. Appl. Phys. 39, 708 (1968).

21. H. Suhl and D. Wong, Physics 3, 17 (1967).

22. Kei Yosida, Phys. Rev. 107, 396 (1957).

23. T. Kasuya, Progr. Theoret. Phys. (Japan) 16, 58 (1956).

24. J. C. Slater, Phys. Rev. 82, 538 (1951).

25. S. Doniach and E. P. Wohlfarth, Proc. Roy. Soc. 295, 442 (1967).

26. H. S. D. Cole and R. E. Turner, J. Phys. C. 2, 124 (1969).

27. R. E. Turner and P. D. Long, (Preprint).

28. T. Izuyama, D. J. Kim and R. Kubo, J. Phys. Soc. (Japan) 18, 1025 (1963).

29. I. Mannari, Rep. of the Res. Lab. for Surf. Sci., 3, 79 (1968). (Faculty of Science, Okayama University.)

30. C. Kittel, Chap. 15 in Introduction to Solid State Physics, 3rd edition (John Wiley and Sons Publishers, 1966).

31. A. Blandin and J. Friedel, J. Physique Rad. 20, 160 (1959).

References (Cont'd)

32. F. Takano and T. Ogawa, Progr. Theoret. Phys. (Japan) 35, 343 (1966).

33. K. Kume, J. Phys. Soc. (Japan) 22, 1116 and 1309 (1967).

34. C. C. Tsuei and R. Hasegawa, Solid State Comm. 7, 1581 (1969).

35. G. Williams and J. W. Loram, J. Phys. Chem. Solids 30, 1827 (1969); also G. Williams, J. Phys. Chem. Solids 31, 529 (1970).

36. J. R. Schrieffer, J. Appl. Phys. 38, 1143 (1967).

37. L. Creveling (unpublished work), c/o M. D. Daybell, W. A. Steyert in Reference (2).

38. M. D. Daybell and W. Steyert, Phys. Rev. Lett. 18, 398 (1967).

39. W. Kohn and S. H. Vosko, Phys. Rev. 119, 912 (1960).

40. D. C. Golibersuch and A. J. Heeger, Solid State Comm. 8, 17 (1970).

41. J. A. Mydosh, J. I. Budnich, M. P. Kawatra and S. Skalski, Phys. Rev. Lett. 21, 1346 (1968).

42. F. C. Zumsteg and R. D. Parks, Phys. Rev. Lett. 24, 520 (1970).

43. G. Longworth and C. C. Tsuei, Phys. Letters 27A, 258 (1968).

44. A. J. Manuel and M. McDougald, J. Phys. C 3, 147 (1970).

45. Rysuke Hasegawa, Ph. D. Thesis, California Institute of Technology (1969).

References (Cont'd)

46. N. V. Volkenshtein, L. A. Ugodnikova and Yu. N. Tsiovkin, Soviet Physics-JETP Lett. 9, 110(1969)

47. A. Maduhkar and C. C. Tsuei, Phys. Letters 32A, 139 (1970).

48. D. J. Kim, Phys. Rev. B, 1, 3725 (1970).